

Movement of K^+ across the Blood-Brain Barrier
of the American Cockroach, *Periplaneta*
americana

Andrea L. Kocmarek, B. Sc.

**MOVEMENT OF K^+ ACROSS THE BLOOD-
BRAIN BARRIER OF THE AMERICAN
COCKROACH, *PERIPLANETA AMERICANA***

by

ANDREA L. KOCMAREK, B.SC.

A Thesis

Submitted to the School of Graduate Studies

in Partial Fulfillment of the Requirements

For the Degree

Master of Science

McMaster University

© Copyright by Andrea L. Kocmarek, September 2009

MASTER OF SCIENCE
(Biology)

McMaster University
Hamilton, Ontario

TITLE: Movement of K^+ across the Blood-Brain
Barrier of the American Cockroach,
Periplaneta americana.

AUTHOR: Andrea L. Kocmarek, B.Sc. (University of
Guelph)

SUPERVISOR: Dr. Michael J. O'Donnell

NUMBER OF PAGES: xi, 125

ABSTRACT

Several previous studies of the blood brain barrier (BBB) of the American cockroach, *Periplaneta americana*, have shown that it is involved in the regulation of K^+ and Na^+ flux across the ventral nerve cord (VNC). Na^+ flux is regulated in part by a Na^+/K^+ -ATPase but few mechanisms involved in the regulation of K^+ flux have been identified. Using the scanning ion-selective electrode technique (SIET) K^+ flux across the VNC can be measured. This technique was used to determine whether K^+ flux is actively regulated and whether the BBB is involved in the regulation of K^+ flux. An uptake of K^+ is seen at the connectives and an efflux is seen at the ganglion under some conditions indicating cycling of K^+ from the ganglion to the connective may be occurring. A Na^+/K^+ -ATPase appears to contribute to an influx of K^+ at the ganglion but not the connective. It is postulated that a K^+/H^+ -exchanger is involved in maintaining K^+ levels at the ganglion. The presence of K^+ -channels (possibly Ca^{2+} -gated) was detected at both the ganglion and the connective, although it appears that K^+ -channels play a greater role in regulating K^+ flux at the connective. These results provide insights into the basic mechanisms regulating ion flux across the cockroach VNC.

ACKNOWLEDGEMENTS

I would like to thank my supervisor, Dr. O'Donnell, for providing me with this opportunity and for his patience and guidance. I would also like to thank the other member of my supervisory committee, Dr. Colin Nurse, for his helpful ideas and advice. I would like to thank Dr. Gary Chiang for the use of his laboratory at Redeemer University College and for teaching me the suction electrode technique.

A special thanks goes to my parents for their support and for encouraging me to pursue my dreams.

Last but not least, I would like to thank all the members of the O'Donnell lab for their help and advice in the lab and for all their proof reading. In particular, I would like to thank Wida Naikhwah for her assistance in the use of ion-selective electrodes to measure the hemolymph K^+ concentration.

THESIS ORGANIZATION AND FORMAT

This thesis is presented as an “open-faced sandwich thesis” with a general introduction and objectives of the research presented in chapter 1 followed by a research paper which is in the format of a manuscript to be submitted for publication in peer-reviewed journals.

Chapter 1: Introduction and project objectives

Chapter 2: Movement of K^+ across the Blood-Brain Barrier of the American Cockroach, *Periplaneta americana*.

Authors: Andrea L. Kocmarek and Michael J. O'Donnell

TABLE OF CONTENTS

Chapter 1:	GENERAL INTRODUCTION	1
	Structural differences between the ganglia and connectives	1
	Previous studies of Na ⁺ and K ⁺ flux across the cockroach BBB	3
	Scanning Ion-selective Electrode Technique (SIET)	6
	Action potentials in sheathed and desheathed VNCs	8
	Extracellular recording of action potentials	9
	Transport of organic cations by the BBB	10
	Thesis Hypotheses	10
Chapter 2:	Movement of K ⁺ across the blood-brain barrier of the American cockroach, <i>Periplaneta americana</i>	20
	Abstract	20
	Introduction	21
	Methods	23
	Insects	23
	Saline Composition	23
	Scanning Ion-selective Electrode Technique (SIET)	23
	K ⁺ flux across the VNC in 3, 15, or 25 mM K ⁺ saline	26
	Effect of changing the permeability of the BBB on K ⁺ flux using amphotericin B and urea	27
	Effect of metabolic inhibition on K ⁺ flux	28
	K ⁺ flux after pre-treatment in K ⁺ -free, 3 mM K ⁺ , and 100 mM K ⁺ saline at 4 °C	28

Effect of low Na ⁺ or changes in saline osmolarity or pH on K ⁺ flux	29
Examination of the effects bafilomycin A ₁ , ouabain, TEA ⁺ , and Ba ²⁺ , and the removal of Ca ²⁺ on K ⁺ flux in control saline	30
The effects of bafilomycin A ₁ , ouabain, and Ba ²⁺ on K ⁺ flux after exposure of the VNC to 100 mM K ⁺ saline for 30 minutes at 4 °C	31
Effect of mechanical stimulation of the cerci on K ⁺ flux	32
H ⁺ flux across the VNC under control conditions and in the presence of the V-type H ⁺ -ATPase inhibitor, bafilomycin A ₁	32
K ⁺ concentration in the hemolymph	33
Extracellular recording of action potentials	34
Statistics	35
Results	37
K ⁺ flux across the VNC in 3, 15, or 25 mM K ⁺ saline	37
Effect of metabolic inhibition on K ⁺ flux	38
K ⁺ flux after incubation in K ⁺ -free, 3 mM K ⁺ , and 100 mM K ⁺ saline at 4 °C	39
Effect of low Na ⁺ on K ⁺ flux	39
Effect of saline osmolarity on K ⁺ flux	40
Effect of pH on K ⁺ flux	40
The effects of bafilomycin A ₁ , ouabain, TEA ⁺ , and Ba ²⁺ and the removal of Ca ²⁺ on K ⁺ flux in 3 mM K ⁺ saline	41
The effects of bafilomycin A ₁ , ouabain, and Ba ²⁺ on K ⁺ flux after exposure of the VNC to 100 mM K ⁺ saline for 30 minutes at 4 °C	42

Effect of mechanical stimulation of the cerci on K^+ flux	42
H^+ flux across the VNC under control conditions and in the presence of the V-type H^+ -ATPase inhibitor, bafilomycin A_1	43
K^+ concentration in the hemolymph	43
Extracellular recording of action potentials	44
Discussion	45
Effect of altering BBB permeability	45
Active transport of K^+ across the VNC	47
A role of K^+ -channels in the regulation of K^+ flux	50
Cycling of K^+	51
Conclusions	52
Appendix A: Saline Composition	118
Appendix B: Organic cation (tetraethylammonium) excretion across the VNC	122

LIST OF FIGURES AND TABLES

Chapter 1

FIGURE 1	Schematic representation of a VNC cross section at the ganglion	19
----------	---	----

Chapter 2

FIGURE 1	Schematic representation of SIET	60
FIGURE 2	Schematic diagram of the experimental set-up for the extracellular recording	63
FIGURE 3	K ⁺ flux after dissection and scanning of the VNC in 3, 15, or 25 mM K ⁺ saline	65
FIGURE 4	K ⁺ flux after exposure to amphotericin B or urea	67
FIGURE 5	The effect of amphotericin B or urea on K ⁺ flux over time	69
FIGURE 6	The effect of CN ⁻ on K ⁺ flux	71
FIGURE 7.0	Schematic of incubation in 4 °C K ⁺ -free, 3 mM K ⁺ , or 100 mM K ⁺ saline	73
FIGURE 7.1	Effect of incubation in 4 °C K ⁺ -free, 3 mM K ⁺ , or 100 mM K ⁺ saline for 30 or 60 minutes	75
FIGURE 8.0	Schematic of removal of Na ⁺ from the saline	78
FIGURE 8.1	K ⁺ flux in Na ⁺ -free and 10% Na ⁺ -saline	80
FIGURE 9.0	Schematic of exposure to high and low osmolarity saline	82
FIGURE 9.1	K ⁺ flux after exposure to saline where the osmolarity had been increased or decreased by ~25%	84
FIGURE 10.0	Schematic of changing saline pH	86
FIGURE 10.1	K ⁺ flux after exposure to salines with pH ranging from 6.2 to 8.2	88
FIGURE 11.0	Schematic for exposure to ouabain, Baf A ₁ , TEA ⁺ , BA ²⁺ , or Ca ²⁺ -free saline	90
FIGURE 11.1	K ⁺ flux after the addition of ouabain, Baf A ₁ , TEA ⁺ , BA ²⁺ , or Ca ²⁺ -free saline	92

FIGURE 12.0	Schematic for exposure to ouabain, Baf A ₁ , or Ba ²⁺ after incubation in 100 mM K ⁺ saline	95
FIGURE 12.1	The effects of Baf A ₁ , ouabain, and Ba ²⁺ on K ⁺ flux after incubation in 100 mM K ⁺ saline at 4 °C for 30 minutes	97
FIGURE 13	Effect of mechanical stimulation of the cerci on K ⁺ flux	99
FIGURE 14.0	Schematic of H ⁺ scans after exposure to control saline and Baf A ₁	101
FIGURE 14.1	H ⁺ flux after exposure to control saline and Baf A ₁	103
FIGURE 14.2	Schematic of H ⁺ scan over time in control saline or Baf A ₁	105
FIGURE 14.3	H ⁺ flux over time in control saline or Baf A ₁	107
FIGURE 15	An example of spontaneous nerve firing	109
FIGURE 16	An example of elicited firing	111
FIGURE 17	Working hypothesis for the effects of ouabain	113
FIGURE 18	Working hypothesis for the effects of K ⁺ channel blockers	115
FIGURE 20	Cycling of K ⁺ in 15 and 25 mM K ⁺ saline	117

Appendix A

TABLE 1	Composition of 3, 15, and 25 mM K ⁺ Salines	118
TABLE 2	Composition of Salines Containing Amphotericin B, Urea, or CN ⁻	118
TABLE 3	Composition of K ⁺ -free, 3 mM K ⁺ , and 100 mM K ⁺ Salines	119
TABLE 4	Composition of Reduced Na ⁺ Salines	119
TABLE 5	Composition of Salines used in Osmolarity Experiments	120
TABLE 6	Composition of Salines used in pH Experiments	120
TABLE 7	Composition of 3 mM K ⁺ Salines Containing Ba ²⁺ , Baf A ₁ , 1221Ouabain, or TEA ⁺ and Ca ²⁺ -free Saline	
TABLE 8	Composition of 100 mM K ⁺ saline containing Baf A ₁ , ouabain, or Ba ²⁺	121

APPENDIX B

- FIGURE 1 Schematic for the of incubation in 4 °C 100 mM TEA⁺ saline 124
and scanning in 0.1 mM TEA⁺ saline
- FIGURE 2 TEA⁺ efflux in 0.1 mM TEA⁺ saline after incubation in 100 mM 125
TEA⁺ saline

CHAPTER 1:

General Introduction

The insect central nervous system is composed of the brain, the subesophageal ganglion, and the ventral nerve cord (VNC). The sheath surrounding the VNC was identified as a blood brain barrier (BBB) that inhibited the movement of ions, including Na^+ and K^+ (Bennett *et al.*, 1975; Schofield *et al.*, 1984a,b; Schofield and Treherne, 1978, 1984; Thomas and Treherne, 1975; Treherne, 1966, Treherne *et al.*, 1970, 1973). Several studies have examined the flux of Na^+ across the VNC but few mechanisms responsible for regulating K^+ flux across the BBB of the cockroach have been identified. Since K^+ and Na^+ are involved in depolarization and repolarization of the axons, protecting the VNC from changes in ion concentrations in the fluid bathing the nerve cells/neurons is important (Schofield *et al.*, 1984a). Previous studies used the cockroach *Periplaneta americana* as it is a model insect typically used in physiology studies. In addition, colonies of the insect are easy and inexpensive to maintain and the VNC is large enough to be easily dissected.

A better understanding of how ion transport across the VNC occurs may be useful in developing new insecticides. Many insecticides act as neurotoxins and some, including pyrethroids and fipronil, act by interfering with the transport of Na^+ and Cl^- at the nerve (Coats, 1990; Narahashi *et al.*, 2007).

Structural differences between the ganglia and connectives

Several studies have reported regional differences in the cellular composition of the blood brain barrier (BBB) surrounding the ganglia and the connectives. These differences may play a role in regulating ion flux. The BBB of the ganglia is composed of three parts; a layer of connective tissue called the neural lamella, a perilemma consisting of cuboidal cells with a high density of

mitochondria, and a continuous layer of glial cells called the perineurium (Hess, 1958; Treherne *et al.*, 1970, 1982). It has been suggested that the perineurium is the primary barrier to diffusion in the cockroach based on the high level of electrical resistance (Schofield *et al.* 1984a; Schofield and Treherne, 1984).

Additional glial cells are found under the perineurium, with nerve soma within the ganglia reported to be ensheathed by two to twenty overlapping layers of glial cells (Hess, 1958; Schofield *et al.* 1984a; Schofield and Treherne, 1984; Treherne *et al.*, 1970). Bundles of one to ten nerve fibres are also surrounded by glial cells. The glia surrounding the giant axons (these glia are also called mesaxons) are separated from one another and from the axons by a network of narrow intercellular channels (mesaxon channels) with occasional larger spaces (Treherne *et al.*, 1970). The mesaxon channels largely control the rate of movement of K^+ from the medium within the VNC to the axon surface.

The BBB of the connectives lacks the perilemmal layer and has a thinner neural lamella (Hess, 1958). Nerve fibres have a greater diameter and glial cell layers are thicker within the connectives than those of the ganglia. The peripheral nerves are similar in structure to the connectives. In addition, a layer of fat typically adheres to the surface of the BBB where the connectives join the ganglia (Smith and Shipley, 1990).

Treherne *et al.* (1982) suggested there were two extracellular fractions in the cockroach central nervous system (CNS). The first is contained in the neural lamella above the perineurium. The second fraction is found in the immediate vicinity of the axon surface and is connected to the general extracellular system by mesaxon channels (Treherne *et al.* 1970, 1982). This fraction is believed to contain a reservoir of unevenly distributed Na^+ , K^+ , and Ca^{2+} and it may aid in the quick

recovery of ion concentrations after axon firing (Schofield and Treherne, 1978; Treherne *et al.*, 1982).

Regional differences in current flow across the cockroach BBB have also been reported (Smith and Shipley, 1990). Outward current flow was reported at the ganglion, while an inward flow was reported at the connectives and peripheral nerves. This inward flow of current is greatest at the areas of the connectives and peripheral nerves adjacent to the ganglia. The ions responsible for carrying these currents were not identified by Smith and Shipley (1990). In this study, the role that K^+ plays in these currents is examined.

Previous studies of Na^+ and K^+ flux across the cockroach BBB

Several studies have examined Na^+ and K^+ flux across the BBB of the cockroach and the crayfish. In intact cockroach VNC preparations, an efflux of Na^+ was observed from the connectives (Tucker and Pichon, 1972). Removal of the BBB increases the rate of efflux, indicating that the BBB is a barrier to Na^+ movement. Na^+ levels within the BBB are mediated, at least in part, by membrane transport mechanisms (Schofield and Treherne, 1978). A Na^+/K^+ -ATPase, which can be inhibited by ouabain, was shown to be present in the *Periplaneta americana* VNC and inhibition of the Na^+/K^+ -ATPase reduces the efflux of Na^+ (Grasso, 1967; Schofield and Treherne, 1978; Treherne, 1966). In addition, voltage-dependent sodium channels allowing an influx of Na^+ were reported in desheathed cockroach neurons (Treherne, 1966).

The movement of K^+ from a high K^+ bathing medium to the extra-axonal fluid surrounding cockroach giant axons involves a high degree of electrical resistance (Treherne *et al.*, 1970). This resistance is decreased by stretching the preparation and can be further decreased by removal of the neural lamella (a procedure which also damages the perineurium) indicating that the BBB presents a barrier to the diffusion of K^+ .

The cockroach BBB can also be disrupted using a hypertonic urea solution which reduces the barrier to movement of Na^+ and K^+ as measured by extraneuronal potentials and action potentials (Treherne *et al.*, 1973). In addition, exposure to urea decreased electrical resistance and the potential difference across the perineurium (Schofield *et al.*, 1984b). Schofield *et al.*, (1984b) reported that the urea-induced increase in the leak of cations across the BBB is chiefly caused by changes in cell-cell junctions. These changes lead to an increase in the permeability of the paracellular pathway. After exposure to urea or alternatively desheathing of the nerve cord, immersion in 10, 12.5, or 25 mM K^+ saline caused a decrease in action potential amplitude suggesting elimination of axonal function (Thomas and Treherne, 1975). Replacement of the 25 mM K^+ saline with 3 mM K^+ saline restored the amplitude of the action potentials to the levels observed prior to urea exposure or desheathing.

Few of the transporters responsible for regulating K^+ flux across the arthropod BBB have been identified. Ca^{2+} -dependent and Ca^{2+} -independent K^+ -channels have been reported in desheathed cockroach neurons (Grolleau and Lapied, 1995). Similarly, Butt *et al.* (1990) and Butt (1991) reported that the highly K^+ -selective permeability of the crayfish perineurium is due to a Ca^{2+} -dependent increase in K^+ -uptake by the perineurial glia. In addition to Ca^{2+} -activated K^+ -channels, the presence of voltage activated K^+ -channels is suggested. Additional studies of the crayfish BBB reveal that K^+ -flux is also regulated by a Na^+/K^+ -ATPase and by a $\text{Na}^+:\text{K}^+:2\text{Cl}^-$ -co-transporter found in the glial cells (Hargittai *et al.*, 1990; Hassan and Lieberman, 1988; Lieberman and Hassan, 1988).

Several studies have also examined the ability of the BBB to protect the underlying nerves from changes in saline pH or osmolarity. When the crayfish VNC was put in high K^+ saline with a pH of 9 the rate of K^+ entry across the BBB was reduced relative to the controls (Butt, 1991). The

opposite effects were seen when the VNC was put in acidic saline. However, a change in pH had no effect on glial K^+ -selective permeability. The author suggests that changes in pH primarily affect cation-binding properties of the extracellular matrix. In low pH, H^+ may displace K^+ from binding sites in the matrix and in high pH more sites may become available to bind K^+ .

In sheathed cockroach nerve cords increasing or decreasing saline osmolarity by 10% did not result in cellular swelling or shrinkage and did not affect nervous conduction (Twarog and Roeder, 1956). Desheathing resulted in cellular swelling and loss of nerve function in the hypotonic saline but no immediate structural or functional effects were observed in the hypertonic saline. In the crayfish, increasing bathing solution osmolarity by approximately 20% did not affect perineurial permeability to K^+ ; however increasing osmolarity by 40 or 60% resulted in a concentration dependent increase in permeability (Butt, 1991). Increasing osmolarity did not directly affect perineurial glial K^+ selectivity. Butt suggests these effects are due to disruption of intercellular junctions as the result of cell shrinkage.

When exposed to hyposmotic solutions crayfish glial cells were reported to expand resulting in a decrease of intercellular volume and in hyperosmotic saline the opposite effects were seen (Lieberman and Hassan, 1988). Lieberman and Hassan (1988) reported a Na^+/K^+ -ATPase was involved in inhibiting cellular swelling and a $Na^+:K^+:2Cl^-$ cotransporter was involved in the regulation of cellular shrinkage. The systems acted additively with respect to K^+ uptake.

Sensory neurons innervate the filiform hairs found on the cerci of the cockroach and these nerves synapse with the terminal giant interneurons of the VNC (Blagburn, 1989; Stern *et al.*, 1997). Stimulation of these filiform hairs by wind has been shown to result in action potentials and escape behaviour, while damage to the nerves prevented the action potentials and escape behaviour (Stern *et*

al., 1997). This thesis examines the possibility that physical stimulation of the cerci would result in changes in K^+ flux across the BBB.

Scanning Ion-Selective Electrode Technique (SIET)

The scanning ion-selective electrode technique (SIET) uses ion-selective microelectrodes to measure the extracellular ion concentration at two points within the unstirred layer adjacent to the surface of a tissue. The concentration difference between the two points can then be used to calculate the corresponding ion flux using Fick's law of diffusion (Donini and O'Donnell, 2005; Rheault and O'Donnell, 2004). SIET allows for direct measurement of net ion-transport in near real-time without physically touching (and possibly damaging) the tissue. In addition, the technique has a rapid response time (typically a few seconds) and continuous measurements may be taken over several hours.

The construction of an ion-selective microelectrode involves several steps. Borosilicate glass micropipettes are first made hydrophobic by exposure to silane vapour at approximately 200 °C (Deyhimi and Coles, 1982; Munoz *et al.*, 1983). Silanization permits retention of the liquid ionophore cocktail when the tip is placed in aqueous solutions and prevents short circuiting of the electrical potential across the liquid membrane. Without silanization, electrical shunting occurs along the inner surface of the micropipette as the glass provides a low resistance electrical pathway.

The micropipettes are then backfilled with an appropriate electrolyte (i.e. 500 mM KCl for K^+ -selective electrodes). Lastly, an organic cocktail containing an ion-selective ionophore is applied to the tip. In neutral carrier ionophores the carrier acts as a shuttle, carrying ions across the interface between the liquid membrane and the external solution (Ammann, 1986).

Selectivity coefficients for ion-selective microelectrodes are often measured using the separate solution method. The potential of the ion-selective electrode (compared to its reference) is measured in a solution of the test ion “X” and then in the solution of the interfering ion “Y”. The selectivity coefficient (K_Y) is then calculated using:

$$K_y = a_x/a_y \times [10^{-(E_y/E_x)}]/S \quad \text{Equation 1}$$

where E_y is potential measured in a solution containing an activity of the interfering ion (a_y), E_x is the potential measured in a solution containing an activity of the test ion (a_x), S is the slope of the electrode, defined as the change in electrode potential during a 10-fold change in a_x . For the valinomycin based ionophore used in the K^+ -selective microelectrodes in this thesis selectivity coefficients ($\text{Log}K_y$) for K^+ relative to Na^+ and Ca^{2+} are -3.89 and -4.9, respectively, indicating that the electrode is 8000 and 80 000 times, respectively, more selective for K^+ .

Although ion-selective electrodes measure ion activity and not concentration, data can be expressed in terms of concentrations if it is assumed that the ion activity coefficient is the same in calibration and experimental solutions. Expression of data in terms of concentrations simplifies comparisons with previous studies in which ion concentrations were measured by techniques such as atomic absorption spectroscopy and/or ion fluxes were measured with radioisotopes.

SIET uses ion-selective electrodes to measure ionic concentration gradients in the unstirred layers next to tissues. The microelectrode is moved between two points (the first point ~5 to 10 μm from the tissue surface and the second a further 30 to 100 μm away) by computer controlled stepper motors at each measurement site. The voltage difference (ΔV) recorded at the two points can be converted to a corresponding concentration difference (ΔC) using the electrode calibration curve. The concentration difference can be converted to net flux (J) using Fick’s law:

$$J = D(\Delta C/\Delta X) \quad \text{Equation 2}$$

where D is the diffusion coefficient of the ion of interest and ΔX is the excursion difference.

Multiple points on a tissue can be scanned making SIET useful for determining spatial differences in ion transport. Alternatively, a single point can be repeatedly scanned at intervals of as little as 10 s to provide a temporal analysis of ion transport. One caveat for the use of SIET in the study of a multilayered preparation such as the VNC is that it can be difficult to identify whether changes in flux are the result of actions at the BBB, the underlying nerves, the extracellular fluid, or a combination of these.

Action potentials in sheathed and desheathed VNCs

Na^+ and K^+ are particularly important in generating action potentials and interference with the mechanisms that regulate their levels will impair nerve firing. Loss of action potential firing in response to a particular treatment may indicate that ions are lost or gained by the axons, and this gain or loss may influence the flux of ions across the BBB.

Previous studies have suggested that the BBB plays a role in maintaining nerve firing by modulating the movement of ions, including K^+ . Voltage-activated, Ca^{2+} -dependent K^+ channels were reported to be involved in the repolarization and the early after-hyperpolarization of action potentials in *P. americana* (Derst *et al.*, 2003). In the crayfish, during axon stimulation K^+ accumulates extracellularly (Smith, 1983). The extent of this accumulation is reduced by active transport mechanisms, including a Na^+/K^+ -ATPase, and possibly by mesaxon channels which may allow K^+ to diffuse away from the periaxonal space.

Immersion in high K^+ salines was reported to lead to the blockage of nerve conduction in a concentration dependent manner (Twarog and Roeder, 1956). Desheathing the nerve cord changed the time it took to obtain blockage from minutes to seconds. Once the nerve cords were placed back

in control saline nerve conduction recovered, with desheathed preparations recovering more quickly than intact preparations. The results suggested that the blockage of nerve conduction observed in high K^+ saline was due to the high K^+ concentration and indicated that an intact BBB slows K^+ movement.

Drugs are commonly used in studies of action potential generation in invertebrates. For example, the presence of CN^- , a metabolic inhibitor, was reported to cause a progressive decline in the amplitude of evoked action potentials in the squid giant axon (Adams *et al.*, 1985). Ten minutes after the addition of CN^- no action potentials were observed; however, these effects were reversible. In desheathed cockroach nerve cords the K^+ channel blockers, tetraethylammonium (TEA^+) and 3,4-diaminopyridine, were shown to decrease the intensity of the depolarizing currents necessary for eliciting action potentials (Yawo *et al.*, 1985).

Extracellular recording of action potentials

The suction electrode technique is often used to measure axon firing. It has the advantage of allowing measurements to be made from the outside of the tissue. Insertion into the actual cell is not required, limiting damage to the cell. Measurements can be made in real time.

Glass microelectrodes are pulled using a micropipetter puller and the tips were broken to a diameter of approximately 40 to 80 μm . The microelectrodes were filled with saline and attached via suction to the connectives. Stimulating and recording electrodes are attached through Ag/Ag-Cl wires to a stimulator or an amplifier, respectively. The circuits are completed by second Ag/Ag-Cl wire.

Transport of organic cations by the BBB

The BBB of the cockroach may also be involved in protecting the underlying axons from toxins. Murray *et al.*, (1994) reported that the BBB of the tobacco hornworm protects the central nervous system from the build up of the cation, nicotine. ATP-dependent pumps, known as *P*-glycoproteins are found in the BBB and remove nicotine from around the axons allowing the tobacco hornworm to tolerate high levels of nicotine in its hemolymph. Studies of vertebrates indicate that *P*-glycoproteins in the BBB also transport other potentially toxic organic cations (Bendayan *et al.*, 2002; Miller *et al.*, 2002). Transport of the prototypical organic cation, tetraethylammonium (TEA^+) is often used to study organic cation transport mechanisms. TEA^+ fluxes can be measured using TEA^+ -selective microelectrodes and SIET (Rheault and O'Donnell, 2004). Appendix B in this thesis reports preliminary SIET measurements to characterize the transport of TEA^+ across the BBB and determine regional differences in transport.

Thesis Hypotheses

This thesis will test several hypotheses 1) Disruption of the BBB by altering the osmolarity, pH, or ion concentration of saline or through the addition of drugs that interfere with active transport, block ion channels, or disrupt membrane integrity should result in changes in ion flux across the VNC. These changes can be measured using SIET, which is non-invasive and measures in near real-time. The technique can be useful in determining how ion flux is regulated within the VNC. 2) I also hypothesize that there will be regional differences in K^+ flux, based on previous research indicating current efflux from the ganglion and influx at the connective (Smith and Shipley, 1990). The ion carrying this current was not identified. My studies examine the contribution of K^+

to this current. 3) K^+ flux may be linked to movement of other ions, e.g. H^+ or Na^+ . 4) In addition, the ability of stimulation of the cerci to affect K^+ flux was also examined.

References

- Adams, D.J., Takeda, K., and Umbach, J.A. 1985. Inhibitors of calcium buffering depress evoked transmitter release at the squid giant synapse. *J Physiol.* 369:145-159.
- Ammann, D. 1986. Ion-selective microelectrodes: principles, design, and application. Springer-Verlag, Berlin.
- Bendayan, R., Lee, G., and Bendayan, M. 2002. Functional expression and localization of P-glycoprotein at the blood brain barrier. *Microsc Res Tech.* 57(5):365-380.
- Bennett, R.R., Buchan, P.B., Treherne, J.E. 1975. Sodium and lithium movements and axonal function in cockroach nerve cords. *J Exp Biol* 62(1):231-241.
- Blagburn, J.M. 1989. Synaptic specificity in the first instar cockroach: patterns of monosynaptic input from filiform hair afferents to giant interneurons. *J Comp Physiol [A]*. 169:607-614.
- Butt, A.M. 1991. Modulation of a glial blood-brain barrier. *Ann NY Acad Sci.* 633:363-377.
- Butt, A.M., Hargittai, P.T., and Lieberman, E.M. 1990. Calcium-dependent regulation of potassium permeability in the glial perineurium (blood-brain barrier) of the crayfish. *Neurosci.* 38(1):175-185.

Coats, J.R. 1990. Mechanisms of toxic action and structure-activity relationships for organochlorine and synthetic pyrethroid insecticides. *Environ Health Perspect.* 87:255-262.

Cohen, M.W. 1970. The contribution by glial cells to surface recordings from the optic nerve of an amphibian. *J Physiol.* 210:565-580.

Derst, C., Messutat, S., Walther, C., Eckert, M., Heinemann, S.H., and Wicher, D. 2003. The large conductance Ca^{2+} -activated potassium channel (pSlo) of the cockroach *Periplaneta americana*: structure, localization in neurons and electrophysiology. *Euro J Neurosci.* 17:1197:1212.

Deyhimi, F. and Coles, J.A. 1982. Rapid silylation of a glass surface: choice of reagent and effect of experimental parameters on hydrophobicity. *Helv Chim Acta.* 65:1752-1759.

Donini, A. and O'Donnell, M.J. 2005. Analysis of Na^+ , Cl^- , K^+ , H^+ and NH_4^+ concentration gradients adjacent to the surface of anal papillae of the mosquito *Aedes aegypti*: application of self-referencing ion-selective microelectrodes. *J Exp Biol.* 208(Pt 4):603-10.

Grasso, A. 1967. A sodium and potassium stimulated adenosine triphosphatease in the cockroach nerve cord. *Life Sci.* 6:1911-1918.

Grolleau, F. and Lapied, B. 1995. Separation and identification of multiple potassium currents regulating the pacemaker activity of insect neurosecretory cells (DUM neurons). *J Neurophysio* 73(1):160-171.

Hargittai, P.T., Butt, A.M., and Lieberman, E.M. 1990. High potassium selective permeability and extracellular ion regulation in the glial perineurium (blood-brain barrier) of the crayfish. *Neurosci.* 35(1):163-177.

Hassan, S. and Lieberman, E.M. 1988. Studies of axon-glial cell interactions and periaxonal K^+ homeostasis--II. The effect of axonal stimulation, cholinergic agents and transport inhibitors on the resistance in series with the axon membrane. *Neurosci.* 25(3):961-969.

Hess, A. 1958. The fine structure of nerve cells and fibers, neuroglia, and sheaths of the ganglion chain in the cockroach (*Periplaneta americana*). *J Biophys Biochem Cytol* 4(6):731-742.

Lieberman, E.M. and Hassan, S. 1988. Studies of axon-glial cell interactions and periaxonal K^+ homeostasis--III. The effect of anisosmotic media and potassium on the relationship between the resistance in series with the axon membrane and glial cell volume. *Neurosci.* 25(3):971-981.

Miller, D.S., Graeff, C., Droulle, L., Fricker, S., and Fricker, G. 2002. Xenobiotic efflux pumps in isolated fish brain capillaries. *Am J Physiol Regul Integr Comp Physiol.* 282(1):R191-198.

- Munoz, J.L., Deyhimi, F., and Coles, J.A. 1983. Silanization of glass in the making of ion-sensitive microelectrodes. *J Neurosc Meth.* 8(3):231-247.
- Murray, C.L., Quaglia, M., Arnason, J.T., and Morris, C.E. 1994. A putative nicotine pump at the metabolic blood-brain barrier of the tobacco hornworm. *J Neurobiol.* 25(1):23-34.
- Narahashi, T., Zhao, X., Ikeda, T., Nagata, K., and Yeh, J.Z. 2007. Differential actions of insecticides on target sites: basis for selective toxicity. *Hum Exp Toxicol.* 26(4):361-366.
- Rheault, M.R. and O'Donnell, M.J. 2004. Organic cation transport by Malpighian tubules of *Drosophila melanogaster*: application of two novel electrophysiological methods. *J Exp Bio* 207:2173-2184.
- Schofield, P.K. and Treherne, J.E. 1978. Kinetics of sodium and lithium movement across the blood-brain barrier of an insect. *J Exp Biol.* 74:239-251.
- Schofield, P.K., Swales, L.S., and Treherne, J.E. 1984a. Potentials associated with the blood-brain barrier of an insect: recordings from identified neuroglia. *J Exp Biol* 109:307-318.
- Schofield, P.K., Swales, L.S., and Treherne, J.E. 1984b. Quantitative analysis of cellular and paracellular effects involved in disruption of blood-brain barrier of an insect by hypertonic urea. *J Exp Biol.* 74:239-251.

Schofield, P.K. and Treherne, J.E. 1978. Kinetics of sodium and lithium movement across the blood-brain barrier of an insect. *J Exp Biol.* 74:239-251.

Schofield, P.K. and Treherne, J.E. 1984. Localization of the blood-brain barrier of an insect: electrical model and analysis. *J Exp Biol.* 74:239-251.

Smith, D.O. 1983. Extracellular potassium levels and axon excitability during repetitive action potentials in crayfish. *J Physiol.* 336:143-157.

Smith, P.J.S. and Shipley, A. 1990. Regional variation in the current flow across an insect blood-brain barrier. *J Exp Biol.* 154:371-382.

Stern, M., Ediger, V.L., Gibbon, C.R., Blagburn, J.M., and Bacon, J.P. 1997. Regeneration of cercal filiform hair sensory neurons in the first-instar cockroach restores escape behavior. *J Neurobiol.* 33(4):439-458.

Thomas, M.V. and Treherne, J.E. 1975. An electrophysiological analysis of extra-axonal sodium and potassium concentrations in the central nervous system of the cockroach (*Periplaneta americana* L. *J Exp Biol.* 63:801-811.

Treherne, J.E. 1966. The effects of ouabain on the efflux of sodium ions in the nerve cords of two insect species (*Periplaneta americana* and *Carausius morosus*). *J Exp Biol.* 44:355-362.

Treherne, J.E., Lane, N.J., Moreton, R.B., and Pichon, Y. 1970. A quantitative study of the potassium movements in the central nervous system of *Periplaneta americana*. *J Exp Biol.* 53:109-136.

Treherne, J.E., Schofield, P.K., and Lane, N.J. 1982. Physiological and ultrastructural evidence for an extracellular anion matrix in the central nervous system of an insect (*Periplaneta americana*). *Brain Res* 247:255-267.

Treherne, J.E., Schofield, P.K., and Lane, N.J. 1973. Experimental disruption of the blood-brain barrier system in an insect (*Periplaneta americana*). *J Exp Biol* 59:711-723.

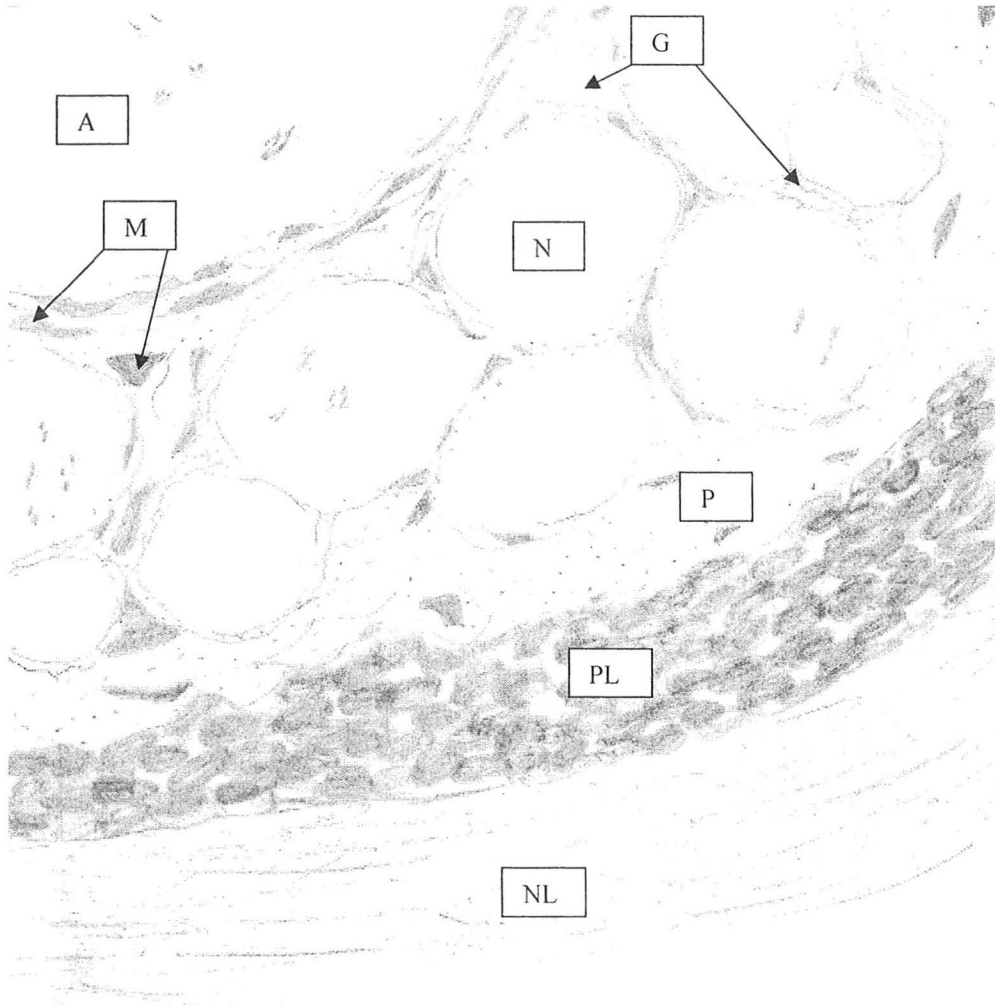
Tucker, L.E. and Pichon, Y. 1972. Sodium efflux from the central nervous connectives of the cockroach. *J Exp Biol.* 56:441-457.

Twarog, B.M. and Roeder, K.D. 1956. Properties of the connective tissue sheath of the cockroach abdominal nerve cord. *Bio Bull Mar Bio.* 111: 278-286.

Yawo, H., Kojima, H., and Kuno, M. 1985. Low-threshold, slow-inactivating Na⁺ potentials in the cockroach giant axon. *J Neurophys.* 54(5):1087-1099.

Fig. 1. Schematic representation of a VNC cross section at the ganglion. A = axons, G = glial cell, M = mesaxon channel, N = nerve soma, P = perineurium, PL = perilemma, and NL = neural lamella.

Note that at the connectives the nerve fibres have a larger diameter and glial cell layers are thicker than at the ganglion and the neural lamella is thinner. There is no perilemma at the connectives.



Based on studies by Hess (1958), Schofield *et al.*, (1984a), Schofield and Treherne, (1984), Smith and Shipley (1990), and Treherne *et al.* (1970, 1982).

CHAPTER 2:

Abstract

Several previous studies of the blood brain barrier (BBB) of the American cockroach, *Periplaneta americana*, have shown that it is involved in the regulation of K^+ and Na^+ flux across the ventral nerve cord (VNC). Na^+ flux is regulated in part by a Na^+/K^+ -ATPase but few mechanisms involved in the regulation of K^+ flux have been identified. Using the scanning ion-selective electrode technique (SIET) K^+ flux across the VNC can be measured. This technique was used to determine whether K^+ flux is actively regulated and whether the BBB is involved in the regulation of K^+ flux. An uptake of K^+ is seen at the connectives and an efflux is seen at the ganglion under some conditions indicating cycling of K^+ from the ganglion to the connective may be occurring. A Na^+/K^+ -ATPase appears to contribute to an influx of K^+ at the ganglion but not the connective. It is postulated that a K^+/H^+ -exchanger is involved in maintaining K^+ levels at the ganglion. The presence of K^+ -channels (possibly Ca^{2+} -gated) was detected at both the ganglion and the connective, although it appears that K^+ -channels play a greater role in regulating K^+ flux at the connective. These results provide insights into the basic mechanisms regulating ion flux across the cockroach VNC.

Introduction

Several studies focusing on the transport of Na^+ and K^+ have shown the existence of a blood brain barrier (BBB) surrounding the ventral nerve cord (VNC) of the cockroach, *Periplaneta americana* (Bennett *et al.*, 1975; Schofield *et al.*, 1984a,b; Schofield and Treherne, 1978, 1984; Thomas and Treherne, 1975; Treherne, 1966, Treherne *et al.*, 1970, 1973). Protection of the VNC from changes in K^+ and Na^+ concentrations is particularly important since these ions are involved in depolarization and repolarization of the axons (Schofield *et al.*, 1984a).

Voltage sensing microelectrodes and radioisotope fluxes have been used to demonstrate that the BBB protects the underlying nerves from changes in ion concentration, pH, or osmolarity within the hemolymph by regulating the ability of Na^+ and K^+ to cross the BBB (Butt, 1991; Schofield and Treherne, 1978; Treherne, 1966; Twarog and Roeder, 1956).

Na^+/K^+ -ATPases have been implicated in the transport of Na^+ across the BBB of the cockroach (Schofield and Treherne, 1978; Treherne, 1966). In the crayfish, K^+ flux is regulated by a Na^+/K^+ -ATPase and a $\text{Na}^+:\text{K}^+:2\text{Cl}^-$ -co-transporter (Hargittai *et al.*, 1990) and K^+ flux has been reported to be regulated across the cockroach BBB, although most studies did not identify specific transporters (Schofield *et al.*, 1984a,b; Thomas and Treherne, 1975). Ca^{2+} -dependent and Ca^{2+} -independent K^+ channels have been reported in desheathed *P. americana* neurons (Grolleau and Lapied, 1995) and they were also reported to be involved in the regulation of K^+ across the crayfish BBB (Butt, 1991). Ca^{2+} -dependent channels were reported to be blocked by the removal of Ca^{2+} and by the addition of Ca^{2+} -blockers, including Ba^{2+} .

Many of the previous studies inferred Na^+ and K^+ movements from voltage changes or measurements of radioisotope fluxes (Butt, 1991; Schofield *et al.*, 1984b; Schofield and Treherne, 1978; Treherne *et al.*, 1973). The scanning ion-selective electrode technique (SIET) used in this

study to examine K^+ transport has the benefit of allowing net ion-transport to be directly measured in near real-time without physically touching (and possibly damaging) the tissue (Donini and O'Donnell, 2005; Rheault and O'Donnell, 2004). An ion-selective electrode measures ion concentration at two positions within the unstirred layer next to the VNC and the difference in the concentrations is used to calculate ion flux. This method is useful in determining whether there are regional differences in the transport of K^+ across the BBB.

In this study, the ability of the BBB to regulate K^+ flux when exposed to increased or decreased saline K^+ levels, low Na^+ saline, or to changes in saline pH or osmolarity have been studied. The involvement of Na^+/K^+ -ATPases and V-type H^+ -ATPases in the BBB's regulation of K^+ flux were examined using the transport inhibitors ouabain, and bafilomycin A_1 . The presence of K^+ channels and their role in regulating K^+ flux across the cockroach BBB were examined using Ca^{2+} -free saline and the K^+ channel blockers, TEA^+ and Ba^{2+} . This study will also examine whether K^+ flux was altered by the electron transport inhibitor, CN^- , or amphotericin B, which creates pores in membranes, or by exposure to urea, which opens gaps in the perinerium.

Methods

2.1 Insects

Periplaneta americana were obtained from Ward's of Canada Inc. and a colony was maintained in the insect room of the McMaster Life Sciences building at a temperature of 21 to 23°C. Water, sugar, and commercial dog food were available *ad libitum*. Adults, both male and female, were used in all experiments.

2.2 Saline Composition

Control cockroach saline (Pichon and Boistel, 1967a and b; Schofield and Treherne, 1978; Thomas and Treherne, 1975; Treherne *et al.*, 1973) was composed of (mM) glucose (20), L-glutamine (10), Trehalose (5), HEPES (8.6), NaCl (139), KCl (3), CaCl₂ (2), MgCl₂ (2), NaHCO₃ (10.2), and NaH₂PO₄ (4.3). The compositions of the other saline solutions used are reported in Tables 5.1 to 5.8 in Appendix A. All salines were maintained at pH 7.2 unless otherwise reported.

2.3 Scanning Ion-selective Electrode Technique (SIET)

Transport of ions into or out of the VNC produces gradients in ion concentration in the unstirred layer adjacent to the surface of the tissue. The gradient for the ion of interest can be calculated from the voltages recorded by an ion-selective microelectrode moved between two points within the unstirred layer. Ion flux can then be calculated from the concentration gradients using Fick's law, as described below. Measurements of fluxes in this way is the basis of the scanning ion electrode technique (SIET), which allows fluxes to be repeatedly measured in near real time at sites along the length of the VNC. Extensive description of the use of SIET are reported in Rheault and

O'Donnell (2001, 2004) and Donini and O'Donnell (2005). SIET measurements were made using hardware from Applicable Electronics (Forestdale, MA, USA) and automated scanning electrode technique (ASET) software (version 2.0) from Science Wares Inc. (East Falmouth, MA, USA).

Procedures for microelectrode construction and ion flux measurement were similar to those described in Rheault and O'Donnell (2004). Micropipettes were prepared by pulling unfilamented borosilicate glass capillaries on a P97 Flaming Brown puller (Sutter, Novato, CA) to a tip diameter of 3 μm to 5 μm . To ensure uptake of the ionophore the micropipettes were silanized by exposure to *N,N*-dimethyltrimethylsilylamine vapour under a glass Pyrex dish on a hot plate at 200 °C for 20 to 60 minutes. Silanized micropipettes were stored in a desiccator.

K^+ -selective and H^+ -selective microelectrodes were based on K^+ ionophore I, cocktail B (60398) or H^+ ionophore I, cocktail B (95293), respectively (Fluka, Buchs, Switzerland). The microelectrodes were first backfilled with 500 mM KCl or 100 mM NaCl and 100 mM NaCitrate, depending on whether the microelectrodes were to be used for K^+ or H^+ , respectively, until approximately 2/3 of the barrel was filled. The ionophore cocktail was then applied to the tip of the microelectrode until a column of approximately 50 to 100 μm was taken up. Once the ionophore had been applied the microelectrodes were stored in 150 mM KCl (for K^+ electrodes) or control saline (for H^+ electrodes).

K^+ electrodes were calibrated in solutions containing 150 mM KCl and 15 mM KCl/135 mM NaCl. H^+ electrodes were calibrated in control saline with pH between 6.5 and 8.5. K^+ and H^+ electrodes had slopes of 50-54 mV or 58-66 mV, respectively, for a ten-fold change in K^+ concentration or a 1-unit change in pH.

Reference electrodes were made from 10 cm length of borosilicate capillary glass (Kwik-Fil™, TW150-4, WPI, Sarasota, FL) that were bent at approximately 45° 1 to 2 cm from the end to

facilitate placement in the sample dish. The capillaries were filled with boiling control saline containing 3% to 5% agar, allowed to cool, and were stored at 4 °C in control saline.

During SIET scans, the ion-selective microelectrode was moved by a system of computer-controlled stepper motors, controlled through ASET software. From a position approximately 10 µm (position A) from the tissue the microelectrode was moved 100 µm perpendicular to the tissue surface to position B (Fig. 1A). At each position, the microelectrode remained stationary during the 3 or 4.5 s waiting period (for K⁺ and H⁺, respectively) and microelectrode voltage was recorded and averaged for 0.5 s during the sample period. The apparatus is depicted schematically in Fig. 1B.

The voltage difference (ΔV) across the 100 µm excursion distance was converted into a concentration difference ($\mu\text{mol}/\text{cm}^3$) using slopes from calibration solutions. The following equation was used:

$$\Delta C_B = C_B \times [10^{\Delta V/S}] - C_B \quad \text{Equation 1}$$

where C_B is the background ion concentration and S is the slope of the electrode in mV.

K⁺ and TEA⁺ flux (J_I) were calculated using Fick's equation:

$$J_I = D_I(\Delta C_B/\Delta X), \quad \text{Equation 2}$$

where D_I is the diffusion coefficient, ΔC_B is the change in background ion concentration, and ΔX is the electrode excursion distance. The diffusion coefficients for K⁺ was $1.92 \times 10^{-5} \text{ cm}^2/\text{s}$ (Donini and O'Donnell, 2005; Rheault and O'Donnell, 2004).

The salines contained the buffer, HEPES, and calculated H⁺-fluxes needed to be corrected for the buffer capacity of the solution using the equation (Donini and O'Donnell, 2005):

$$J_I = [(D_H + D_I)B_H] \times (\Delta C/\Delta X), \quad \text{Equation 3}$$

where D_H is the diffusion coefficient of HEPES ($6.2 \times 10^{-6} \text{ cm}^2/\text{s}$), D_I is the diffusion co-efficient of H⁺ ($9.4 \times 10^{-5} \text{ cm}^2/\text{s}$) and B_H is the buffer capacity of HEPES which is calculated from the equation:

$$B_H = (C_H/C_B) \times [F/(1+F)^2] \quad \text{Equation 4}$$

where C_H is the concentration of the HEPES and F is calculated from:

$$F = \log_{10}(pK_{aH})/C_B \quad \text{Equation 5}$$

where $\log_{10}(pK_{aH})$ is the dissociation constant of HEPES ($pK_{aH} = 7.55$).

2.4 Experimental Design

2.4.1 K^+ flux across the VNC in 3, 15, or 25 mM K^+ saline

After the removal of the head, legs, and wings, the cockroach was pinned dorsal side up in a 60 x 15 mm disposable Petri dish with a layer of Sylgard on the bottom containing control (3 mM K^+), 15, or 25 mM K^+ saline. The dorsal exoskeleton was removed, as were the gut, fat body, and reproductive organs. The ventral nerve cord (VNC) from the last thoracic ganglion to the last (6th) abdominal ganglion was then detached from the ventral exoskeleton. The ends of the VNC were pinned with minuten pins in a second dish and covered with fresh 3, 15, or 25 mM K^+ saline. The VNC was stretched slightly to reduce movement during scanning.

SIET scans of a ganglion or connective were begun within 5 minutes. To avoid changes in ion flow caused by damage to the BBB due to the cut ends or by pin placement, at least one connective and ganglion separated the scanned area from the pins holding the tissue in place. The first to fifth abdominal ganglia and the connectives between these ganglia were considered acceptable for scanning. Only areas of the VNC free of fatty tissue were scanned. For all SIET experiments, the mean of 3 replicates per point was taken at 4 to 6 points along the ganglion or the connective. The mean of the individual 4 to 6 points was calculated to provide the flux for one ganglion or connective preparation. Each SIET scan took approximately 5 minutes.

2.4.2 Effect of changing the permeability of the BBB on K^+ flux, using amphotericin B and

urea

The antibiotic amphotericin B has been reported to form pores in membranes, making them permeable to small monovalent ions (Schirmanns and Zeiske, 1994a and b). After the VNC was scanned in control saline (to provide a control value), amphotericin B in the vehicle dimethyl sulfoxide (DMSO) was added to provide a final concentration of 5 μ M amphotericin B and 0.09% DMSO in control saline. Preliminary experiments showed that DMSO does not affect the response of the microelectrode or K^+ flux at levels up to 0.1% (Fig. 11.1A and B). The same area of the VNC as previously scanned was then scanned twice at intervals of 5 minutes.

To measure the effects of amphotericin B over time, a control scan was performed as described above; however, after the addition of amphotericin B scans at a single point on the same section of tissue as scanned for the control were performed for 20 to 30 minutes.

Urea opens gaps in the perineurial cells of the cockroach BBB (Schofield *et al.*, 1984b). Using a protocol based on the studies by Schofield *et al.* (1984b), Thomas and Treherne (1975), and Treherne *et al.* (1973), the VNC was scanned in control saline, the control saline was then replaced with saline containing 3 M urea, and after 15 seconds the VNC was rinsed 4 times with control saline to ensure all the urea was removed. The same area of the VNC as previously scanned was scanned twice more in control saline. The effects of urea were examined over time by scanning a single point for 20 to 30 minutes after the VNC was scanned in control saline and immersed in 3 M urea for 15 seconds.

A series of scans where control saline was added instead of amphotericin served as controls.

2.4.3 Effect of metabolic inhibition on K^+ flux

The cockroaches were dissected as described in Section 2.4.1 and the tissue was scanned once (control). The tissue was then rinsed 4 times with room temperature saline containing the electron transport inhibitor, CN^- (1 mM). The same section of tissue as previously scanned was scanned twice more (5 minutes/scan) while exposed to CN^- .

2.4.4 K^+ flux after incubation in K^+ -free, 3 mM K^+ , and 100 mM K^+ saline at 4 °C

Several experiments were designed to perturb the level of K^+ within the VNC so that mechanisms involved in K^+ homeostasis could be studied. The VNCs were put in K^+ -free, 3 mM K^+ , or 100 mM K^+ saline and incubated at 4 °C in a refrigerator for 30 or 60 minutes prior to scanning. The temperature was lowered in an attempt to inhibit active transport mechanisms, allowing K^+ to diffuse out of or into the BBB in the cases of the K^+ -free and 100 mM K^+ saline, respectively. To remove any ions adhering to the surface of the BBB, the VNCs were washed 4 times with 4 °C control saline following incubation.

Preliminary analysis showed occasional significant differences between first and second and first and third scans when the VNC was scanned 3 consecutive times after removal from the refrigerator. During this time the preparation warmed to room temperature. As the result of these differences, only the third scan beginning 20 to 25 minutes after removal from the refrigerator is presented in the results of K^+ experiments involving incubation at 4 °C. Saline temperature was 18 °C 20 minutes after removal from the refrigerator.

2.4.5 Effect of low Na^+ , or changes in saline osmolarity or pH on K^+ flux

Based on Butt's (1991) study of electrical potentials across the perineurial sheath and the giant axon membrane in crayfish in response to changes in the extracellular environment, the effects of low Na^+ or changes in pH or osmolarity on K^+ flux were examined. Saline containing 10% of the Na^+ concentration of control saline and Na^+ -free saline were tested. Any Na^+ removed was replaced with *N*-methyl-D-glucamine to maintain Cl^- levels and saline osmolarity. *N*-methyl-D-glucamine increased K^+ activity so K^+ levels were decreased in low Na^+ salines until a K^+ activity equivalent to that of 3 mM K^+ in control saline was obtained. In the Na^+ -free saline, NaH_2PO_4 and KCl were removed and 10.2 mM NaHCO_3 was replaced with 3 mM KHCO_3 in order to remove all the Na^+ while maintaining K^+ levels. A PO_4 -free, HCO_3^- -reduced saline, that controlled for those changes but left Na^+ levels the same as those in control saline, was also tested.

The effects of high and low saline osmolarity on K^+ flux were also examined. Sucrose (88.75 mM) was added to control saline to increase osmolarity by approximately 25% (high osmolarity saline). Low osmolarity saline was produced by removing 44 mM NaCl to produce a saline with 75% of the control saline's osmolarity. As a control for the removal of the Na^+ and Cl^- ions a saline with the same osmolarity as control saline was made by removing 44 mM NaCl and replacing it with 88.75 mM sucrose.

Salines with pH ranging from 6.2 to 8.2 were used to study the effect of changes in pH on K^+ flux. Control saline (pH of 7.2) was buffered with HEPES. For salines with a pH less than 7.2 PIPES buffer was used instead of HEPES. PIPES and HEPES have effective buffering ranges of 6.1 to 7.5 and 6.8 to 8.2, respectively.

In all cases, cockroaches were dissected in control saline as described in Section 2.4.1 and the VNC was scanned once in control saline to establish baseline K^+ flux. The saline was then

replaced with fresh control saline or one of the experimental salines and scanned twice more. The total time for each scan was 5 minutes.

2.4.6 Examination of the effects bafilomycin A₁, ouabain, TEA⁺, and Ba²⁺, and the removal of Ca²⁺ on K⁺ flux in control saline

In view of several studies indicating the presence of a Na⁺/K⁺-ATPase in the VNC (Grasso, 1967; Schofield and Treherne, 1978; Treherne, 1966), I examined the effects of ouabain, a Na⁺/K⁺-ATPase inhibitor on K⁺ transport in control saline at room temperature. The effects of bafilomycin A₁ (Baf A₁), a V-type H⁺-ATPase inhibitor were examined in light of a report of Baf A₁-sensitive K⁺ transport and a H⁺/K⁺-ATPase in mammalian glial cells (Shirihai *et al.*, 1998). DMSO (final concentration ≤0.1%) was used as a vehicle for Baf A₁ and ouabain.

A VNC was pinned into a 200 μL well cut into the Sylgard layer of a 35 x 10 mm disposable Petri dish, 180 μL of control saline was added, and the VNC was scanned once to establish a control value. The 200 μL volume was chosen to limit the amount of drug required to achieve the correct concentration. Following the addition of 20 μL of control saline (in the control scans), or 20 μL saline containing vehicle with 0.1 mM Baf A₁ or 1 mM ouabain, the VNCs were scanned twice more. This addition provided final concentrations of 0.01 mM Baf A₁ and 0.1 mM ouabain, respectively, in control saline.

The effects of the K⁺ channel blockers, TEA⁺ and Ba²⁺, and the removal of Ca²⁺ were also examined. The cockroaches were dissected as described in Section 2.4.1 and the tissue was scanned once. The tissue was then rinsed 4 times with room temperature saline containing either 20 mM TEA⁺ or 5 mM Ba²⁺ or Ca²⁺-free saline. The same section of tissue as previously scanned was scanned twice more (scan time 5 minutes) in the experimental saline.

2.4.7 The effects of bafilomycin A₁, ouabain, and Ba²⁺ on K⁺ flux after exposure of the VNC to 100 mM K⁺ saline for 30 minutes at 4 °C

The effects of Baf A₁ and ouabain on K⁺ transport were also determined after K⁺ flux had been perturbed by incubation in 100 mM K⁺ saline for 30 minutes at 4 °C. Since the preparation warmed from 4 to 22 °C after removal from the refrigerator the tissue could not serve as its own control. The results obtained by incubation of the VNC in 100 mM K⁺ saline for 30 minutes at 4 °C without any of the inhibitors or vehicle (as described in Section 2.4.4) were used as the control.

The VNCs were pinned into a well in the Sylgard layer of a 35 x 10 mm disposable petri dish. One hundred eighty μL of 110.78 mM K⁺ saline and 20 μL of 3 mM K⁺ saline containing vehicle alone (0.1% DMSO), 0.1 mM Baf A₁, or 1 mM ouabain were pipetted into the well. This provided final concentrations of 0.01 mM Baf A₁, and 0.1 mM ouabain, respectively, in 100 mM K⁺ saline. The tissue was then incubated at 4 °C for 30 minutes. After washing the VNC with 3 mM K⁺ saline (4 times), the preparations were scanned in 3 mM K⁺ saline containing vehicle, 0.01 mM Baf A₁, or 0.1 mM ouabain.

The effects of the K⁺ channel blocker, Ba²⁺, on K⁺ flux were also examined. Preparations exposed to Ba²⁺ were prepared as described in Section 2.4.4 for the VNCs incubated in 100 mM K⁺ saline for 30 minutes except saline containing 5 mM Ba²⁺ and 100 mM K⁺ replaced the 100 mM K⁺ saline. The 3 mM K⁺ saline was replaced with saline containing 5 mM Ba²⁺ and 3 mM K⁺ for the washing and scanning.

Scans begun 20 to 25 minutes after the removal of the preparation from the refrigerator are reported in the results section.

2.4.8 Effect of mechanical stimulation of the cerci on K^+ flux

The cockroaches were dissected as described in Section 2.4.1 except the terminal ganglion of the VNC was not entirely detached from the ventral exoskeleton. The nerves emanating from the terminal ganglion were left attached to the cerci. The preparations were pinned into the Sylgard layer of a Petri dish containing fresh 3 mM K^+ saline. Flux was measured at a single point beginning every 30 seconds for 2.5 to 3 minutes. The cerci were stimulated by touching them repeatedly with forceps for 1 minute (approximately 120 times). Flux was measured at the same area of the VNC again (10 repetitions at a single point twice). The mean of the first and second groups of 5 repetitions was calculated.

2.4.9 H^+ flux across the VNC under control conditions and in the presence of the V-type H^+ -ATPase inhibitor Bafilomycin A_1

The effects of the V-type H^+ -ATPase inhibitor, Baf A_1 , on H^+ flux were also examined. DMSO was used as the vehicle for Baf A_1 at a concentration of 1%, based on preliminary studies (Spaic, unpublished) and the observation that this level did not affect H^+ flux. The cockroaches were dissected as described in Section 2.4.1 and the VNC was put in control saline. A ganglion or connective was scanned once to establish baseline H^+ flux. Control saline, DMSO, or Baf A_1 (to provide a final concentration of 10 μ M Baf A_1) was added and the same area of tissue as previously scanned was scanned once again. Each scan took 5 minutes to complete.

As a significant decrease in H^+ flux was observed over time at the ganglion the experimental design was modified. The preparations were dissected in control saline and immediately before beginning the scan 50 μ L of either control saline or saline containing Baf A_1 (final concentration 10 μ M in 1% DMSO) was added. Then a single point was scanned 35 times at 40 second intervals.

2.5 K^+ concentration in the hemolymph

Previous studies had reported hemolymph K^+ concentrations between 28 and 8 mM in adult cockroaches (Pichon, 1970; Treherne *et al.*, 1975; Thomas and Treherne, 1975; Weidler and Sieck, 1977). These studies showed high variability between individual insect and that hemolymph K^+ levels were dependent on diet, access to water, and sampling location. The hemolymph K^+ concentration of the insects used in the preceding and following experiments was determined using an ion selective microelectrode. A reference microelectrode was made by backfilling a micropipette with 150 mM KCl solution. A K^+ -selective microelectrode was fabricated as described in Section 2.3 and calibrated in solutions containing 150 mM KCl or 15 mM KCl/135 mM NaCl. Electrode slope was between 50 and 56 mV/decade change in K^+ concentration.

A live cockroach was immersed in paraffin oil and hemolymph was collected from a leg and from the abdomen. In 50% of the samples the hemolymph was collected from the leg followed by the abdomen and for the other 50% it was collected from the abdomen then the leg. To collect hemolymph from the leg the femur was removed with dissection scissors, the coxa was squeezed with forceps and the hemolymph that came out of the incision was collected with a 2 μ L pipette. To collect hemolymph from the abdomen an incision was made with dissection scissors between the first pair of segments after the last set of legs, the abdomen was gently squeezed with forceps and the hemolymph was collected with the pipette.

The hemolymph samples were transferred into small wells in a Sylgard lined Petri dish filled with paraffin oil. Ion selective and reference microelectrodes were placed in the hemolymph droplet and voltage was recorded with a high impedance electrometer (pH/ion AMP, A-Asystems, Carlsberg, WA) connected to a PC-based data acquisition system (PowerLab, ADInstruments, CO) and analyzed using CHART software (ADInstruments).

The concentration of K^+ in the hemolymph was calculated using the equation:

$$[K^+]_{\text{hemo}} = [K^+]_{\text{cal}} \times 10^{(\Delta V/S)}, \quad \text{Equation 6}$$

where $[K^+]_{\text{hemo}}$ is the concentration of K^+ in the hemolymph, $[K^+]_{\text{cal}}$ is the concentration of K^+ within one of the calibration solutions, ΔV is the change in voltage between the hemolymph and some calibration solution and S is the slope of the electrode.

2.6 Extracellular recording of action potentials

The cockroaches were dissected in control saline as described in section 2.4.1. The VNCs were placed in control saline. Glass microelectrodes were pulled using a PUL-1 micropipetter puller (WPI) and the tips were broken to a diameter of approximately 40 to 80 μm . The microelectrodes were filled with saline and attached via suction to the connectives. The stimulating electrodes were attached to an Anapulse Stimulator 301-T (WPI) and the recording electrode was connected to a DAM50 amplifier (WPI). The circuits are completed by second Ag/Ag-Cl wires. In the case of the stimulating electrode this wire is wrapped around the barrel of the electrode and in the case of the recording electrode it is placed in the saline surround the preparation. A schematic of this set-up is depicted in Fig. 2. Only VNCs in which nerve firing was elicited after electrical stimulation were used for experimentation.

To determine if the nerves were firing spontaneously, recordings were taken using Data-Trax Data Acquisition Software (WPI), for 10 to 15 seconds without electrical stimulation. The tissue was then stimulated once every second for 1 to 1.4 ms with a voltage between 10 and 40 V to evoke nerve firing. Elicited action potentials were recorded for 10 to 30 seconds. The control saline was replaced with saline containing 0.1 mM ouabain, 1 mM CN^- , or 5 mM Ba^{2+} . Saline containing 0.1% DMSO served as a control since the ouabain saline contained 0.1% DMSO as a vehicle.

Spontaneous and evoked activity was recorded again. To determine if the drug effects were reversible the experimental saline was replaced with control saline and spontaneous and evoked activity were recorded as described above.

Data were analyzed using DataTrax2 Data Acquisition Software (WPI). The number of samples showing spontaneous and evoked activity, the number of action potentials observed after electrical stimulation, and the duration and magnitude of the action potentials were recorded. Averages were calculated using the 3 largest action potentials in a group of action potentials, since these actions potentials were the most easily and consistently identified in subsequent groups of action potentials. To select a group of action potentials a time was selected at random and the first group of action potentials observed after that time was measured. The mean of 4 different groups of action potentials were calculated to provide the values for 1 treatment.

2.7 Statistics

All values are expressed as means (\pm standard error of the means). For the K^+ SIET experiments a paired Student's t-test was used to determine significant changes in mean flux over time from one set of VNCs by comparing the first scan (control) with following scans in all experiments except for the comparison of the effects of 3, 15, and 25 mM K^+ saline. For the studies where the effects of the 3, 15 and 25 mM K^+ salines were compared, a two-sample t-test, which assumed equal or unequal variance based on the results of an F-test, was used.

Since there was a significant decrease in H^+ flux over time (as determined by a paired Student's t-test) at the ganglion a two-sample t-test, which assumed equal or unequal variance based on the results of an F-test, was used to compare the Baf A_1 -treated scans with the control saline-treated scans.

The paired Student's t-test was also used to determine whether a significant difference existed in the K^+ concentrations of hemolymph taken from the leg or the abdomen. In addition, it was used to determine if ouabain, Ba^{2+} , or CN^- had significant effects on action potentials amplitude, duration, and frequency.

Differences were considered significant if $p < 0.05$. All statistical calculations were performed using Microsoft Office Excel.

Results

3.1 K^+ flux across the VNC in 3, 15, or 25 mM K^+ saline

Control (3 mM K^+), 15 and 25 mM K^+ saline were used to determine the conditions under which an efflux or influx of K^+ could be seen and if there were regional variations in K^+ flux. Control saline containing 3 mM K^+ was used because this level of K^+ had been used in previous studies (Pichon and Boistel, 1967a and b; Schofield and Treherne, 1978; Thomas and Treherne, 1975; Treherne *et al.*, 1973). In 3 mM K^+ saline a significantly greater efflux (~18-fold) was observed from the ganglion compared to the connective. When 15 or 25 mM K^+ saline was used instead of 3 mM K^+ saline, K^+ flux was observed to change from a small efflux to a large influx (Fig. 3B) at the connective. No significant changes in K^+ flux were observed at the ganglion when 15 or 25 mM K^+ saline was used instead of 3 mM K^+ saline (Fig. 3A).

3.2 Effect of changing the permeability of the BBB on K^+ flux using amphotericin B and urea

Amphotericin B and urea were used to examine the effects of alteration of BBB permeability on K^+ flux. Addition of 20 μ L control saline did not significantly alter K^+ flux (Fig. 4A and B). The addition of amphotericin B, which creates pores in membranes, initially increased K^+ efflux from the ganglion 17-fold relative to the control scan (Fig. 4C). However, by the second scan in amphotericin B (5 to 10 minutes after the addition of amphotericin B) the efflux was only 13-fold the control efflux. Similar results were seen at the connective with 26-fold and 11-fold increases in K^+ efflux observed at Scans 1 and 2, respectively, compared to the control scan (Figure 4D). The efflux from the ganglion was greater than that from the connective in control saline and with the addition of amphotericin B.

Conversely, the addition of urea resulted in a greater efflux from the connective than the ganglion. Exposure to urea resulted in a decrease to approximately 15% of the control K^+ efflux during Scan 1 and an influx during Scan 2 at the ganglion (Fig. 4E). At the connective a decrease to 6% of the control efflux was seen during Scan 2 (Fig. 4F).

Due to the rapid nature of the increase and decrease in K^+ flux after the addition of amphotericin B averaging 4 points in one scan (as in Fig. 4) may result in a loss of detail. Fig. 5 shows the changes in K^+ flux over time at a single point after the addition of amphotericin B or control saline or after exposure to 3 M urea for 15 s. After the addition of amphotericin B there was a steep increase in K^+ efflux at both the ganglion and the connective followed by a gradual decrease to approximately 0 pmol/s/cm² (Fig. 5C and D). In the control ganglion and connectives there were much smaller effluxes that gradually decrease to negligible levels (Fig. 5A and B). After exposure to urea a higher efflux of K^+ is seen at the connectives compared to the controls; however there appears to be no differences in the efflux from the control ganglia and the ganglia exposed to urea (Fig. 5E and F).

3.3 Effect of metabolic inhibition on K^+ flux

The electron transport inhibitor, CN^- was used to determine whether active transport played a role in the regulation of K^+ flux across the VNC. Inhibition of metabolism with CN^- , caused significant increases in K^+ efflux at both the ganglion and the connective compared to the control scans (Fig. 6A and B). At the ganglion, a 2-fold increase in efflux was observed during Scans 1 and 2. At the connective a 2-fold increase was observed after Scan 1 and a 3-fold increase was observed after Scan 2.

3.4 K^+ flux after incubation in K^+ -free, 3 mM K^+ , and 100 mM K^+ saline at 4 °C

In order to decrease or increase levels of K^+ within the VNC and to examine the effect the changes in K^+ levels would have on K^+ flux the preparations were exposed to K^+ -free, 3 mM K^+ , or 100 mM K^+ saline at 4 °C for 30 or 60 minutes. These preparations were compared with preparations scanned in 3 mM K^+ saline at 22 °C without incubation at the lower temperature (Fig 7.0). At the ganglion, immersion in 4 °C K^+ -free saline for 30 or 60 minutes caused the K^+ efflux to be reduced to approximately 20% and 12%, respectively, of the efflux from controls maintained at 22 °C (Fig. 7.1A). Incubation in K^+ -free saline for 60 minutes at 4 °C changed the K^+ efflux at the connective to an influx but no significant effects on flux were seen after 30 minutes of incubation (Fig. 7.1D).

Incubation in 3 mM K^+ saline at 4 °C for 60 minutes reduced K^+ efflux from the ganglion to 25% of the efflux observed from ganglia in 22 °C 3 mM K^+ saline (Fig. 7.1B). No significant effects were seen at the ganglion after 30 minutes of incubation (Fig. 7.1B) or at the connective after 30 or 60 minutes (Fig. 7.1E).

Incubation in 100 mM K^+ for 60 minutes increased the K^+ efflux at the ganglion and the connective to approximately 200% and 500% of the respective 22 °C 3 mM K^+ control fluxes (Fig. 7.1C and F). No significant changes were seen at either the ganglion or the connective after 30 minutes of incubation in 100 mM K^+ saline.

3.5 Effect of low Na^+ on K^+ flux

Based on several studies indicating the presence of a Na^+/K^+ -ATPase the effects of low Na^+ on K^+ flux were examined (Grasso, 1967; Schofield and Treherne, 1978; Treherne, 1966). After a control scan the preparations were immersed in reduced Na^+ saline (Fig 8.0). Na^+ -free saline caused

a significant change from a K^+ efflux to an influx at the connective; however, these effects were not seen when 90% of the Na^+ was removed (Fig. 8.1B). Na^+ -free saline did not affect K^+ flux at the ganglion (Fig. 8.1A). The removal of PO_4^- and the reduction of HCO_3^- from 10 mM to 3mM (to control for these changes in Na^+ -free saline) did not affect K^+ flux (Fig. 8.1A and B).

3.6 Effect of saline osmolarity on K^+ flux

After a control scan the preparations were immersed in hyper- or hyposmotic saline (Fig. 9.0) based on previous studies by Twarog and Roeder (1956) and Butt (1991) that showed the BBB played a role in regulating cell volume and K^+ permeability. An increase in saline osmolarity caused a time dependent decrease to 27% of the control K^+ efflux at the ganglion (Fig. 9.1A) and a change from K^+ efflux to influx at the connective (Fig. 9.1B). No significant effects were observed when the VNC was immersed in saline if reduced osmolarity; however, a significant increase (~50%) in efflux was observed at the ganglion when the VNC was immersed in saline with a normal osmolarity in which approximately 30% of the NaCl had been replaced with sucrose.

3.7 Effect of pH on K^+ flux

After a control scan in pH 7.2 saline the preparations were immersed in saline with a pH of 6.2 to 8.2 (Fig 10.0) based on the effects changes in saline pH had on K^+ movement at the crayfish BBB (Butt, 1991). When PIPES was used as a buffer instead of HEPES at pH 7.2, there were no significant effects on K^+ flux at either the ganglion or the connective (Figures 10.1A and B). Increasing pH to 8.2 had no effects on K^+ flux at the ganglion or connective. A significant decrease in K^+ efflux was observed at the ganglion only at pH 6.2 (Figure 10.1A). An influx was seen during the first experimental scan in salines with pH of 7.0, 6.7, and 6.2 compared to the initial control

efflux; however, during the second experimental scan only saline with a pH of 7.0 remained significantly different. Since these influxes show recovery to control values and do not increase proportionally to decreasing pH this suggests these changes from efflux to influx were not the result of changes in pH.

3.8 The effects of bafilomycin A₁, ouabain, TEA⁺, and Ba²⁺ and the removal of Ca²⁺ on K⁺ flux in 3 mM K⁺ saline

The inhibitors, bafilomycin A₁ and ouabain were used to investigate the role a V-type H⁺-ATPase and a Na⁺/K⁺-ATPase played in K⁺ flux, respectively. After a scan in control saline the preparations were scanned after the addition of Baf A₁, ouabain, or DMSO (Fig 11.0A) or the control saline was replaced with saline containing Ba²⁺ or TEA⁺ or in saline with PO₄⁻ or Ca²⁺ had been removed (Fig. 11.0B). Baf A₁, an inhibitor of V-type H⁺-ATPases, caused a 23% reduction in K⁺ efflux during the 2nd scan at the ganglion but had no effect at the connective (Fig. 11.1A and B). Conversely, ouabain, an Na⁺/K⁺-ATPase inhibitor caused significant increases in efflux at the ganglion during Scans 1 and 2 compared to the Control scan (55 and 64%, respectively) (Fig. 11.1A). There were no significant effects of ouabain at the connective (Fig. 11.1B).

The presence of K⁺-channels and their role in the regulation of K⁺ flux was investigated using the K⁺-channel blockers, Ba²⁺ and TEA⁺. Ca²⁺-free saline was used to determine whether these channels were Ca²⁺-dependent. Efflux at the ganglion was reduced by ~50% by the K⁺ channel blocker Ba²⁺ (Figure 11.1C). At the connective, a K⁺ influx was observed after the addition of Ba²⁺ where an efflux had previously been observed (Figure 11.1D). At the connective, the addition of TEA⁺, another K⁺ channel blocker, or the removal of Ca²⁺ were observed to decrease K⁺ efflux compared to the control scans at both the 1st (to 26 and 8% of the control, respectively) and 2nd scans

(to 46 and 31% of the control, respectively) (Figure 11.1D). The addition of TEA⁺ and the removal of Ca²⁺ did not have significant effects at the ganglion (Figure 11.1C).

3.9 The effects of bafilomycin A₁, ouabain, and Ba²⁺ on K⁺ flux after exposure of the VNC to 100 mM K⁺ saline for 30 minutes at 4 °C

To further investigate the effects of Baf A₁, ouabain, and Ba²⁺ on K⁺ flux, K⁺ levels within the VNC were increased by immersion of the VNC in 100 mM K⁺ saline for 30 minutes at 4 °C. A schematic representation of the procedure is presented in Fig 12.0. After the addition of ouabain and Ba²⁺, ~2.5-fold increases in K⁺ efflux were observed at the ganglion compared to the efflux of K⁺ after incubation in 100 mM K⁺ saline for 30 minutes without drug (Control). See Figure 12.1A. The addition of Ba²⁺ produced a 4.5-fold increase in the K⁺ efflux from the connective compared to the Control (Figure 12.1B). The addition of Baf A₁ produced a decreased efflux from the ganglia and an influx at the connectives; however, these effects were not significant. The use of 0.1% DMSO as a vehicle had no effect on K⁺ flux.

3.10 Effect of mechanical stimulation of the cerci on K⁺ flux

In order to investigate whether action potentials induced by physical stimulation of the cerci resulted in changes in K⁺ flux the cerci were lightly touched approximately 120 times by forceps. Stimulation of the cerci had no significant effects on the efflux of K⁺ from either the ganglion or the connective (Fig. 13A and B, respectively).

3.11 H^+ flux across the VNC under control conditions and in the presence of the V-type H^+ -ATPase inhibitor, bafilomycin A_1

To further investigate the role a V-type H^+ -ATPase might play in the regulation of K^+ flux proton fluxes were measured before and after the addition of bafilomycin (Fig. 14.0). In control saline the efflux of H^+ from the ganglion was significantly greater than that from the connective for both the Control and Experimental scans.

Due to significant changes in H^+ flux over time the Control and Experimental scans from the Baf A_1 and DMSO treated preparations were compared to the Control and Experimental scans from the preparations treated with control saline only. At the ganglion both the Control scan and the Experimental scan in the preparations treated with Baf A_1 were significantly lower than the respective control saline treated scans (Fig. 14.1A). No significant effects were observed at the connective (Fig. 14.1B).

Since a significant decrease in H^+ occurred over time at the ganglion the method was modified to a single point was scanned in either control saline or saline containing Baf A_1 . Fig. 14.2 depicts the method. There were no significant differences between the efflux from the control or Baf A_1 treated preparations (Fig. 14.3). A significant decrease in flux occurred after 4 minutes of scanning for preparation in both treatments.

3.12 K^+ concentration in the hemolymph

The average K^+ concentrations were found to be $20.5 (\pm 2.1)$ and $16.0 (\pm 1.9)$ mM in the hemolymph from the abdomen and leg, respectively. These concentrations were not significantly different ($n = 8$).

3.13 Extracellular recording of action potentials

Extracellular recordings of action potential were made to investigate whether CN^- , ouabain, or Ba^{2+} had an effect on nerve firing, as inhibition of nerve firing would be the result of affects at the neurons. The addition of CN^- stopped all spontaneous and evoked nerve firing in a time dependent manner ($n = 8$). The duration and the magnitude of the spontaneous action potentials observed were the same as those from the controls (1.33 ± 0.15 vs. 1.30 ± 0.16 ms and 11 ± 1 vs. 14 ± 3 mV, respectively). The effects of CN^- were not reversed by the replacement of CN^- saline with control saline.

The addition of Ba^{2+} increased the number of samples showing spontaneous firing from 4 of 10 to 7 of 10 but all samples showed evoked firing before, during, and after the Ba^{2+} treatment. Ouabain and its vehicle (0.1% DMSO) had no significant effects on the number of samples showing spontaneous nerve firing (4 of 8 and 5 of 8, respectively) and all of samples showed evoked nerve firing. Neither Ba^{2+} nor ouabain had an effect on the duration (1.00 ± 0.11 vs. 1.40 ± 0.15 ms and 1.58 ± 0.07 vs 1.82 ± 0.11 ms, respectively) or amplitude (12 ± 1 vs. 11 ± 1 mV and 8 ± 1 vs. 10 ± 1 mV) of the spontaneous action potential compared to their controls. Ba^{2+} did not effect the duration or amplitude of the elicited action potentials (1.21 ± 0.08 vs. 1.26 ± 0.11 ms and 25 ± 3 vs. 37 ± 5 mV). Ouabain did also not effect the duration or amplitude of the elicited action potentials (1.02 ± 0.04 vs. 1.06 ± 0.05 ms and 35 ± 4 vs. 27 ± 3 mV).

Examples of spontaneous and elicited action potentials are shown in Fig. 15 and 16, respectively.

Discussion

The results suggest that active transporters, including a Na^+/K^+ -ATPase and a V-type H^+ -ATPase, as well as K^+ -channels contribute to ion flux across the ganglion and the connective of the VNC. Although SIET does have the benefit of leaving multilayer preparations like the VNC undamaged, it does not identify in which layer specific transporters are found. The described treatments may have affected the nerves, the extracellular matrix, the BBB, or some combination of the above.

4.1 Effect of altering BBB permeability

The addition of amphotericin B, which alters BBB permeability by creating pores in membranes, resulted in a large and rapid increase in K^+ efflux. As the levels of K^+ within the VNC decreased the rate of efflux decreased. This suggests levels of K^+ within the VNC are above the level of electrochemical equilibrium, as indicated by Pichon and Boistel (1967b), and also indicate that an intact BBB reduced the efflux of K^+ from the VNC.

Urea was reported to reduce barriers to K^+ and Na^+ flux by increasing gaps between perineural cells (Treherne *et al.*, 1973). It is possible that the effects of urea are due to damage to the cells within the BBB in addition to the opening of the intracellular junctions; however, Treherne *et al.*, considered this unlikely as urea treatment did not result in ultrastructural changes to the cells, did not disrupt the barrier to ionic lanthanum, and as action potentials returned to control values once placed into control saline after urea treatment. Scans of single sites revealed an increase in K^+ flux from the connectives in the first few minutes after urea treatment followed by a decrease in efflux. This finding suggests that K^+ gradients across the BBB run down quickly when the permeability of the paracellular pathway is increased by disrupting cell-cell junctions with urea. Indeed, a decrease

in K^+ flux was detected in the first and/or second scans of multiple sites after urea treatment, these decreases may have been due to the length of time (~ 5 min) required to rinse the preparation and set up the scan.

Another explanation of the differences seen after the urea and amphotericin B treatments may be due to the fact that the urea opens gaps between cells and the amphotericin B puts pores in cell membranes. A large amount of K^+ may be released from the cells, whereas the levels of K^+ available in the extracellular fluid may be relatively low. This would result in the greater efflux of K^+ seen after the addition amphotericin B relative to the efflux observed after the addition of urea.

A previous study has shown that if the BBB was damaged exposure to hypotonic saline resulted in cellular swelling of the nerve cord but no swelling was observed if the BBB was intact (Twarog and Roeder, 1956). Conversely, Butt (1991) reported that hyperosmolarity induced increased BBB cell permeability in the crayfish as measured by transperineurial resistance. However, effects were only seen when osmolarity was increased by 40% or more.

In the present study, decreasing saline osmolarity by ~25% did not have significant effects on K^+ flux at either the ganglion or the connective suggesting the BBB protects against decreases in hemolymph osmolarity. However, in saline of normal osmolarity with a portion of the NaCl replaced by sucrose a significant increase in efflux was observed at the ganglion. The change in efflux may be due to the removal of Cl^- since removal of 100% of saline Na^+ has been shown not to affect K^+ flux at the ganglion. This suggests the possible involvement of a Cl^- -dependent transporter (e.g. a $K^+:Cl^-$ or a $Na^+:K^+:2Cl^-$ cotransporter) in K^+ flux across the VNC.

The addition of sucrose to increase saline osmolarity (~125% of the osmolarity of control saline) caused a decrease to 27% of the control K^+ efflux at the ganglion and a significant change from an efflux to an influx at the connective. High extracellular osmolarity typically leads to cell

shrinkage and compensatory mechanisms attempt to increase intracellular osmolarity in order to regulate cell volume (Baumgarten and Feher, 1998). A decrease in K^+ efflux may reflect cellular K^+ uptake during cell volume regulation.

In addition, the lack of change in K^+ flux observed when the cerci were stimulated with forceps may indicate the BBB is involved in regulating the K^+ released by the axons during an action potential.

Taken together the results indicate that the BBB restricts exchange of K^+ between the VNC and the hemolymph and that disruption of the BBB can alter K^+ flux.

4.2 Active transport of K^+ across the VNC

The role that active transporters play in the regulation of K^+ flux is indicated by the increase in K^+ efflux that occurs after the addition of CN^- , an inhibitor of ATP production. The study of nerve action potentials in preparations exposed to CN^- also supports this hypothesis. K^+ levels within the nerves must be higher than those of the surrounding extracellular fluid in order for the nerves to repolarize after action potentials. When the active transport mechanisms responsible for restoring high K^+ levels or removing Na^+ are inhibited it will lead to the cessation of the observed action potential. Immersion of the VNC in saline containing 1 mM CN^- initially resulted in normal nerve firing but this nerve firing typically stopped within a minute. Given that CN^- inhibits nerve firing, the increased K^+ efflux may reflect loss of K^+ from the nerves.

This thesis investigated the involvement of two types of active transporters, a Na^+/K^+ -ATPase and a V-type H^+ -ATPase, in the transport of K^+ into and out of the VNC. Fig. 17 presents the working hypothesis for the effects of ouabain, a Na^+/K^+ -ATPase inhibitor. The VNC has been simplified in the figure by showing the BBB as composed of only one layer, instead of multiple cell

types. The glial cells surrounding the neurons are not depicted. The transporters are shown in the BBB but may also be in the neuronal membranes as SIET measures the net flux outside the VNC.

Net K^+ flux as measured by SIET reflects the sum of the action of transporters moving K^+ into and out of the VNC. If the number of K^+ ions moving out of the VNC is greater than the number of K^+ ions moving into the VNC an efflux will be measured.

The addition of ouabain resulted in an increased K^+ efflux at the ganglion in 3 mM K^+ saline. A similar efflux was seen when the VNC was incubated in 100 mM K^+ saline for 30 minutes at 4°C to raise VNC K^+ levels and then scanned in 3 mM K^+ saline, all in the presence of ouabain. These results suggest the presence of a Na^+/K^+ -ATPase at the ganglion responsible for pumping K^+ into (and Na^+ out of) the ganglion (Fig. 17). The addition of ouabain did not have a significant effect at the connective suggesting that either a Na^+/K^+ -ATPase does not play a significant role in the short-term regulation of K^+ across the connective or that the ganglion is a “leakier” tissue than the connective, making changes in flux immediately obvious. Treherne (1966) also reported that the addition of ouabain resulted in a reduced Na^+ efflux across the BBB but did not specify the location of the pump.

Ouabain did not have significant effects on the number or magnitude of action potentials recorded from the cockroach VNC. This suggests the Na^+ and K^+ levels within the neurons are not affected in the short-term by inhibition of Na^+/K^+ -ATPases. This could be due to the presence of other regulatory mechanisms or it may indicate that the BBB limits the access of ouabain to the neurons within the VNC.

The results of this study indicate that changes in hemolymph Na^+ levels have little effect on K^+ flux across the VNC. At the connectives, removal of 100% of the Na^+ caused a small but significant change from K^+ efflux to influx; however, no change was seen when 90% of the Na^+ was

removed. At the ganglion, removal of 100% of the Na^+ did not have a significant effect on K^+ flux. This supports the findings of Treherne *et al.* (1975) who stated that fluctuations in the cation content of the connectives could not be related to Na^+ activity in the hemolymph. It may be that reserves of Na^+ within the VNC, possibly within the extracellular space immediately surrounding the nerve as suggested by Schofield and Treherne (1978) and Treherne *et al.* (1982), allow the function of Na^+/K^+ -ATPases in saline containing reduced levels of Na^+ .

At the ganglion, a significant decrease in K^+ efflux was observed after the addition Baf A_1 to 3 mM K^+ saline. However, there was no decrease in efflux from the ganglion after incubation of the VNC in 100 mM K^+ saline containing Baf A_1 and scanning in 3 mM K^+ saline containing Baf A_1 . An efflux of H^+ was measured at both the ganglion and the connective, with a significantly greater efflux at the ganglion. The addition of Baf A_1 at the connective had no effect on H^+ flux which is consistent with Baf A_1 's lack of effect on K^+ flux at the connective. However, due to a decrease in H^+ efflux at the ganglion over time the H^+ efflux after the addition of Baf A_1 could not be compared to previous control scans from the same preparation. When a single point was scanned in either control saline or in the presence of Baf A_1 there was no significant differences in the initial efflux, nor did the rate of the decrease in efflux differ between the two treatments. When all of the results are considered together it is unlikely that a V-type H^+ -ATPase contributes significantly to K^+ flux.

Alterations in hemolymph pH appear to have little effect on K^+ flux across the VNC. No sustained changes in K^+ flux were observed in response to a change in saline pH from 7.2 to either 6.2 or 8.2 at the connectives. Changing pH from 7.2 to 6.2 caused a significant decrease in efflux at the ganglion but no change was seen in saline with a pH of 6.7. This effect could be due to the presence of TWIK-related acid-sensitive K^+ channels or pH may affect other regulatory mechanisms such as cell-cell junctions. Increasing pH to 8.2 did not cause significant effects at the ganglion.

4.3 A role of K^+ -channels in the regulation of K^+ flux

The results also indicate a role for K^+ channels in mediating K^+ fluxes into or out of the VNC. Fig. 18 presents the working hypothesis for the effects of K^+ -channel blockers on K^+ flux.

The addition of the K^+ channel blocker Ba^{2+} decreased K^+ efflux at the ganglion and resulted in a K^+ influx at the connective in 3 mM K^+ control saline. Similarly, the addition of TEA^+ , an alternate K^+ channel blocker caused a reduction in K^+ efflux at the connective. TEA^+ blocks voltage sensitive K^+ -channels (Armstrong, 1975) while Ba^{2+} affects a wide variety of channels including voltage insensitive Ca^{2+} -sensitive channels (Butt, 1991). These results indicate part of the K^+ efflux observed in control saline is through K^+ channels and that these channels are more important in the regulation of K^+ flux at the connective than the ganglion. When K^+ leakage is reduced by the blockade of K^+ channels, the reduction in efflux or the change to an influx is consistent with the presence of mechanisms for the uptake of K^+ , such as the Na^+/K^+ -ATPase.

The removal of Ca^{2+} also resulted in a significant decrease in K^+ flux at the connective. In combination with previous studies that have indicated the presence of Ca^{2+} -dependent K^+ channels in cockroach nerves (Grolleau and Lapied, 1995; Sun *et al.*, 1999), this information suggests Ca^{2+} -dependent K^+ channels play a role in regulating K^+ flux. Removal of Ca^{2+} may also induce paracellular leakage; however, it would be expected that this would cause an increase in K^+ flux rather than a decrease based on the effects of urea.

Paradoxically, a significant increase in K^+ efflux from both the ganglion and the connectives after incubation of the VNC in 100 mM K^+ saline containing 5 mM Ba^{2+} at 4°C was observed. It is proposed that Ba^{2+} 's action on the BBB occurs more quickly than the inhibition of active transport by cooling or that paracellular leakage occurs. Paracellular leakage may allow the diffusion of K^+ into the VNC and/or active transport mechanisms may continue to transport K^+ while the tissue

cools, while K^+ is prevented from leaving the VNC because Ba^{2+} blocks K^+ -channels (Fig. 18). This results in higher K^+ levels within the VNC than those seen after incubation with 100 mM K^+ alone. During the portion of the experiment in 3 mM K^+ saline Ba^{2+} continues to block K^+ efflux via K^+ -channels but other transport mechanisms, such as a $K^+ : Cl^-$ cotransporter, a K^+ / H^+ -exchanger, or paracellular leakage, contribute to K^+ efflux.

4.4 Cycling of K^+

Previous studies of hemolymph K^+ concentrations have reported concentrations between 28 and 8 mM; however, variation in K^+ levels between individual cockroaches is high (Pichon, 1970; Treherne *et al.*, 1975; Thomas and Treherne, 1975; Weidler and Sieck, 1977). Hemolymph K^+ concentration was also reported to be dependent on the sampling location and diet. The K^+ concentration of the hemolymph surrounding the VNC of insects used in these experiments was found to be 20.5 mM.

In saline with K^+ concentrations closer to physiological values than 3 mM (15 or 25 mM) an efflux of K^+ is observed at the ganglion and an influx is observed at the connectives. These findings raise the possibility of K^+ cycling from the connectives to the ganglion (Fig. 19).

In the hemolymph K^+ may be pumped out of the ganglion via active transport mechanisms such as the Na^+ / K^+ -ATPase. At the connectives K^+ may diffuse into the VNC via K^+ -channels or paracellularly. When the VNC is in 3 mM K^+ saline the level of K^+ outside the BBB may be so low compared to the level within the VNC that an efflux of K^+ is seen from both the ganglion and the connective suggesting the cycling in K^+ is inhibited. When the level of K^+ within the VNC is reduced by exposure to K^+ -free saline for 60 minutes an efflux at the ganglion and an influx at the

connective is observed. This indicates that K^+ levels within the VNC have decreased sufficiently to allow K^+ cycling between the connective and the ganglion to resume.

Smith and Shipley (1990) identified an outward flow of electrical current across the BBB at the ganglion and an inward flow of current at the connective from cockroach VNCs in 3 mM K^+ saline. It is possible that at least a portion of this current is the result of K^+ flux.

4.5 Conclusions

The results suggest several avenues for further exploration of ion transport into and out of the VNC. H^+ flux should be measured over a shorter time frame in order to determine whether Baf A_1 reduces H^+ efflux at the ganglion. These experiments would allow further testing of the hypothesis that a V-type H^+ -ATPase removing H^+ from the VNC is paired with a K^+/H^+ -exchanger that causes an influx of H^+ and an efflux of K^+ . The involvement of other transporters, including a Na^+/H^+ exchanger or $K^+:Cl^-$ or $Na^+:K^+:2Cl^-$ cotransporters, in the regulation of K^+ flux could be investigated with the inhibitors [(dihydroindenyl)oxy]alkanoic acid (DIOA), 5-(N-ethyl-N-isopropyl)-amiloride (EIPA), and bumetanide, respectively. Indeed a $Na^+:K^+:2Cl^-$ cotransporter was found to be expressed in the nerve cord of *Manduca sexta* (Gillen *et al.*, 2006)

The effects of low Cl^- saline could also be used to investigate the presence of $K^+:Cl^-$ or $Na^+:K^+:2Cl^-$ cotransporters, as removal of Cl^- should inhibit the transporters. Experimenting with low Cl^- saline is also necessary to determine the cause of the significant increase in efflux from the ganglion seen in saline with normal osmolarity where NaCl had been replaced with sucrose.

All of these results point to the idea that multiple mechanisms are responsible for regulating ion flux across the BBB at the ganglia and connectives. A smaller efflux or an influx is typically seen at the connective compared to the efflux from the ganglion. It appears that active transport

mechanisms are responsible for maintaining K^+ levels within the BBB and that the BBB offers the underlying neurons some protection from changes in saline ion concentrations and pH. A Na^+/K^+ -ATPase appears to contribute to an influx of K^+ at the ganglion but not the connective. The presence of K^+ -channels (possibly Ca^{2+} -gated) was detected at both the ganglion and the connective, although it appears that K^+ -channels play a greater role in regulating K^+ flux at the connective. These results provide insights into the basic mechanisms regulating ion flux across the cockroach VNC and will be useful in designing future studies. Preliminary experiments have also shown that TEA^+ flux can be resolved and indicate that it is possible to study the transport of organic cations across the VNC (Section 6.0 - Appendix B).

References

- Armstrong, C.M. 1975. Evidence for ionic pores in excitable membranes. *Biophys J.* 15(9):932-933.
- Baumgarten, C.M. and Feher, J.J. 1998. Osmosis and the Regulation of Cell Volume. In Sperelakis, N. (2nd ed.), *Cell Physiology Source Book*. Toronto, Academic Press. pp 278-279.
- Bennett, R.R., Buchan, P.B., Treherne, J.E. 1975. Sodium and lithium movements and axonal function in cockroach nerve cords. *J Exp Biol* 62(1):231-241.
- Butt, A.M. 1991. Modulation of a glial blood-brain barrier. *Ann NY Acad Sci* 633:363-377.
- Donini, A. and O'Donnell, M.J. 2005. Analysis of Na⁺, Cl⁻, K⁺, H⁺ and NH₄⁺ concentration gradients adjacent to the surface of anal papillae of the mosquito *Aedes aegypti*: application of self-referencing ion-selective microelectrodes. *J Exp Biol.* 208(Pt 4):603-10.
- Gillen, C.M., Blair, C.R., Heilman, N.R., Somple, M., Stulberg, M., Thombre, R., Watson, N., Gillen, K.M., and Itagaki, H. 2006. The cation-chloride cotransporter, masBSC, is widely expressed in *Manduca sexta* tissues. *J Insect Physiol.* 52(7):661-8.
- Grolleau, F. and Lapied, B. 1995. Separation and identification of multiple potassium currents regulating the pacemaker activity of insect neurosecretory cells (DUM neurons). *J Neurophysio* 73(1):160-171.

Hargittai, P.T., Butt, A.M., and Lieberman, E.M. 1990. High potassium selective permeability and extracellular ion regulation in the glial perineurium (blood-brain barrier) of the crayfish. *Neurosci.* 35(1):163-177.

Ianowski J.P., Christensen R.J., and O'Donnell M.J. 2002. Intracellular ion activities in Malpighian tubule cells of *Rhodnius prolixus*: evaluation of $\text{Na}^+ - \text{K}^+ - 2\text{Cl}^-$ cotransport across the basolateral membrane. *J Exp Biol.* 205(Pt 11):1645-55.

Ianowski J.P., and O'Donnell M.J. 2004. Basolateral ion transport mechanisms during fluid secretion by *Drosophila* Malpighian tubules: Na^+ recycling, $\text{Na}^+ : \text{K}^+ : 2\text{Cl}^-$ cotransport and Cl^- conductance. *J Exp Biol.* 207(Pt 15):2599-2609.

Leonard, E.M. 2008. Investigations into Cadmium Tolerance In *Chironomus Riparius*: Spatial Patterns of Transport and Sequestration. Hamilton, ON: McMaster University. pp 24-25.

Pichon, Y. 1970. Ionic content of haemolymph in the cockroach, *Periplaneta americana*. A critical analysis. *J Exp Biol.* 53(1):195-209.

Pichon, Y. and Boistel, J. 1967a. Current-voltage relations in the isolated giant axon of the cockroach under voltage-clamp conditions. *J Exp Biol.* 47(2):343-55.

Pichon, Y. and Boistel, J. 1967b. Microelectrode study of the resting and action potentials of the cockroach giant axon with special reference to the role played by the nerve sheath. *J Exp Biol.* 47:357-373.

Rheault, M.R. and O'Donnell, M.J. 2001. Analysis of epithelial K⁺ transport in Malpighian tubules of *Drosophila melanogaster*: evidence for spatial and temporal heterogeneity. *J Exp Biol.* 204(Pt 13):2289-2299.

Rheault, M.R. and O'Donnell, M.J. 2004. Organic cation transport by Malpighian tubules of *Drosophila melanogaster*: application of two novel electrophysiological methods. *J Exp Bio* 207:2173-2184.

Schofield, P.K., Swales, L.S., and Treherne, J.E. 1984a. Potentials associated with the blood-brain barrier of an insect: recordings from identified neuroglia. *J Exp Biol* 109:307-318.

Schofield, P.K., Swales, L.S., and Treherne, J.E. 1984b. Quantitative analysis of cellular and paracellular effects involved in disruption of blood-brain barrier of an insect by hypertonic urea. *J Exp Biol.* 74:239-251.

Schofield, P.K. and Treherne, J.E. 1978. Kinetics of sodium and lithium movement across the blood-brain barrier of an insect. *J Exp Biol* 74:239-251.

Schofield, P.K. and Treherne, J.E. 1984. Localization of the blood-brain barrier of an insect: electrical model and analysis *J Exp Biol* 74:239-251.

Schirmanns, K. and Zeiske, W. 1994a. An investigation of the midgut K^+ pump of the tobacco hornworm (*Manduca sexta*) using specific inhibitors and amphotericin B. *J Exp Biol.* 188(1):191-204.

Schirmanns, K. and Zeiske, W. 1994b. K^+ channel permeation and block in the midgut epithelium of the tobacco hornworm *Manduca sexta*. *J Exp Biol.* 197(1):179-200.

Shirihai, O., Smith, P.J.S., Hammar, K. and Dagan, D. 1998. H^+ and K^+ gradient generated by microglia H/K ATPase. *Glia.* 23, 339-348.

Smith, P.J.S. and Shipley, A. 1990. Regional variation in the current flow across an insect blood-brain barrier. *J Exp Biol.* 154:371-382.

Sun, X.P., Schlichter, L.C., and Stanley, E.F. 1999. Single-channel properties of BK-type calcium-activated potassium channels at a cholinergic presynaptic nerve terminal. *J Physiol.* 518 (3):639-651.

Thomas, M.V. and Treherne, J.E. 1975. An electrophysiological analysis of extra-axonal sodium and potassium concentrations in the central nervous system of the cockroach (*Periplaneta americana* L.) *J Exp Biol* 63:801-811.

Treherne, J.E. 1966. The effects of ouabain on the efflux of sodium ions in the nerve cords of two insect species (*Periplaneta americana* and *Carausius morosus*). *J. Exp Biol.* 44:355-362.

Treherne, J.E., Buchan, P.B., and Bennett, R.R. 1975. Sodium activity of insect blood: physiological significance and relevance to the design of physiological saline. *J Exp Biol* 62(3):721-732.

Treherne, J.E., Lane, N.J., Moreton, R.B., and Pichon, Y. 1970. A quantitative study of the potassium movements in the central nervous system of *Periplaneta americana*. *J Exp Biol.* 53:109-136.

Treherne, J.E., Schofield, P.K., and Lane, N.J. 1973. Experimental disruption of the blood-brain barrier system in an insect (*Periplaneta americana*). *J Exp Biol* 59:71-723.

Twarog, B.M. and Roeder, K.D. 1956. Properties of the connective tissue sheath of the cockroach abdominal nerve cord. *Bio Bull Mar Bio.* 111:278-286.

Weidler, D.J. and Sieck, G.C. 1977. A study of ion binding in the hemolymph of *Periplaneta americana*. *Comp Biochem Physiol A Comp Physiol.* 56(1A):11-4.

Fig 1. (A) Non-invasive measurement by the scanning ion-selective electrode technique of ion flux across the cockroach ventral nerve cord (VNC). The technique exploits gradients in ion activity within the unstirred layer next to the VNC by ion transport. In this example, K^+ is measured approximately $10\ \mu\text{m}$ from the tissue and then a second measurement is taken $110\ \mu\text{m}$ from the tissue. An efflux of K^+ across the VNC results in a higher concentration of K^+ at next to the tissue relative to further away. The size of the labels and the density of the shading correspond to K^+ concentration. (B) Schematic diagram of the equipment used during SIET measurement. The VNC and the ion-selective microelectrode are observed through a microscope equipped with a charge coupled device (CCD) camera. An orthogonal (XYZ) array of stepper-motors, controlled by the computer motion control system, move the amplifier headstage and the attached ion-selective microelectrodes to sites along the VNC and then at two points perpendicular to the tissue surface (see Fig. 1A). The data acquisition system records the voltage differences between the two points. Voltage gradients at different sites can be overlaid as vectors on an image of the tissue captured by the frame grabber connected to the CCD camera.

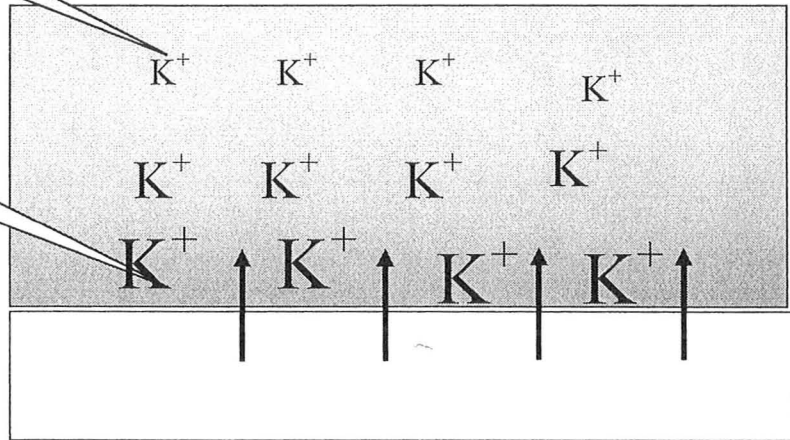
A

110 μm
from VNC
(Position
B)

10 μm
from VNC
(Position
A)

Unstirred layer

VNC



B

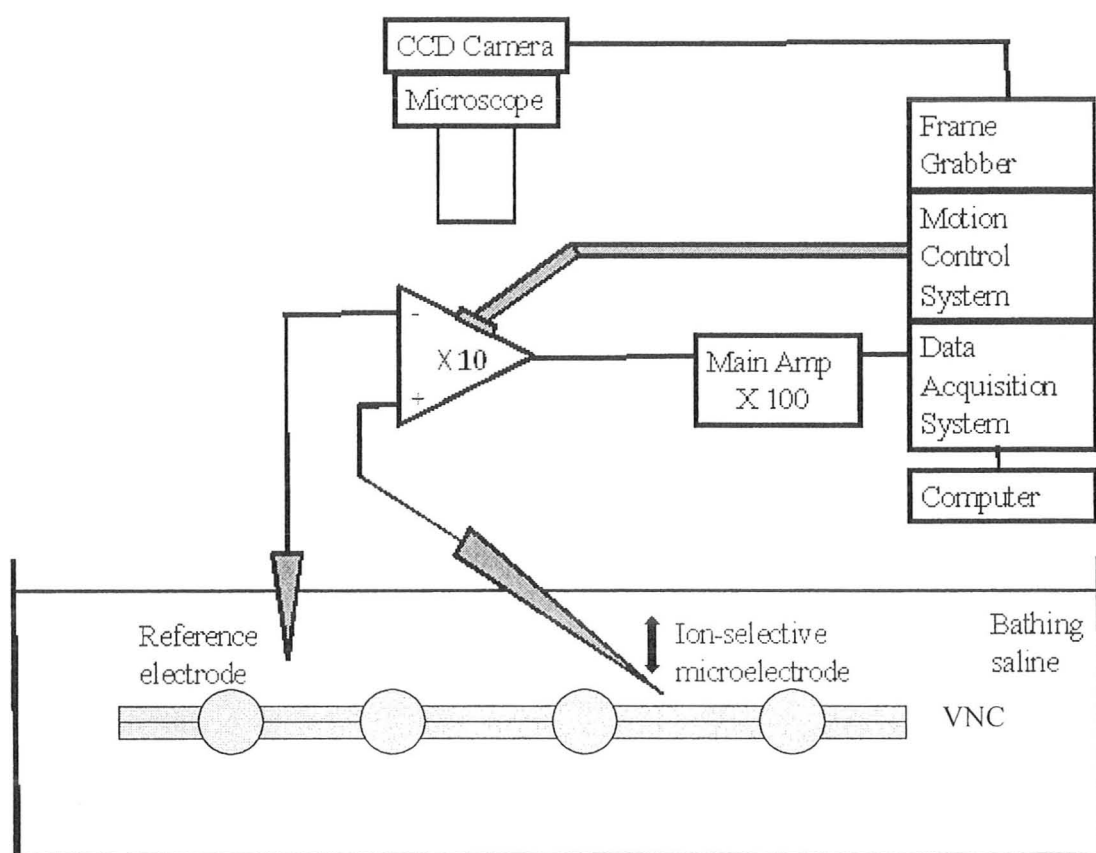


Fig. 2. Schematic diagram of the experimental set-up for the extracellular recording. Spontaneous and evoked action potentials were recorded in control saline. The saline was replaced with saline containing 0.1 mM ouabain, 5 mM Ba^{2+} , or 1 mM CN^{-} and action potentials were recorded again. The experimental saline was replaced once more with control saline and action potentials were recorded.

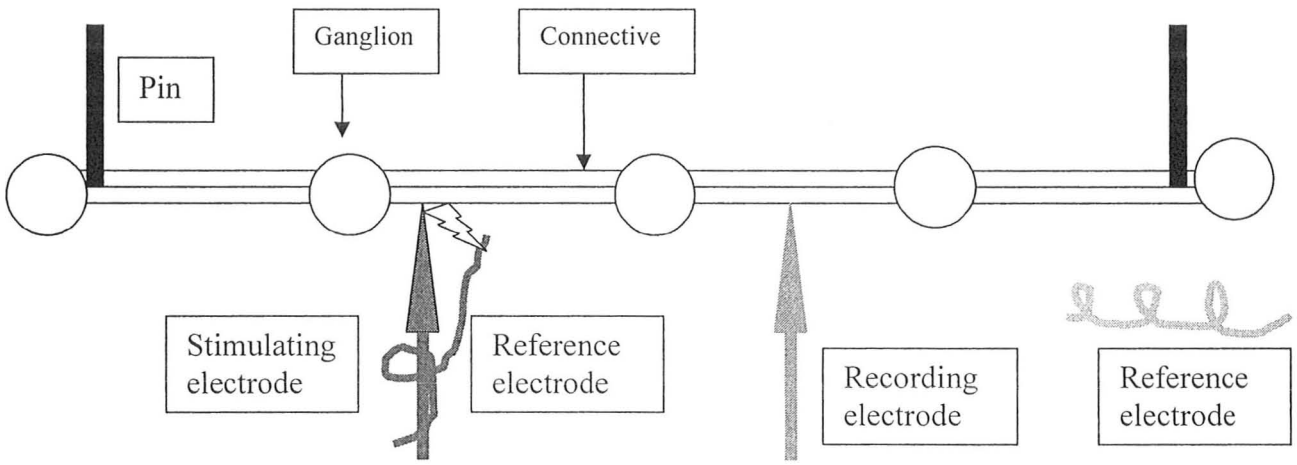


Fig 3. K^+ flux after dissection and scanning of the VNC in 3, 15, or 25 mM K^+ saline at the (A) ganglion and (B) connective (* = $p < 0.05$ compared to 3 mM K^+ saline; $n = 6$ to 9).

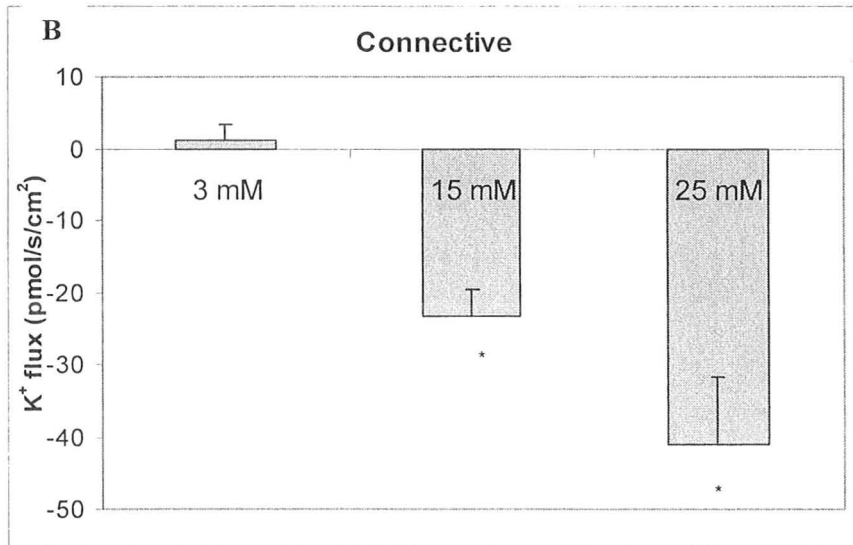
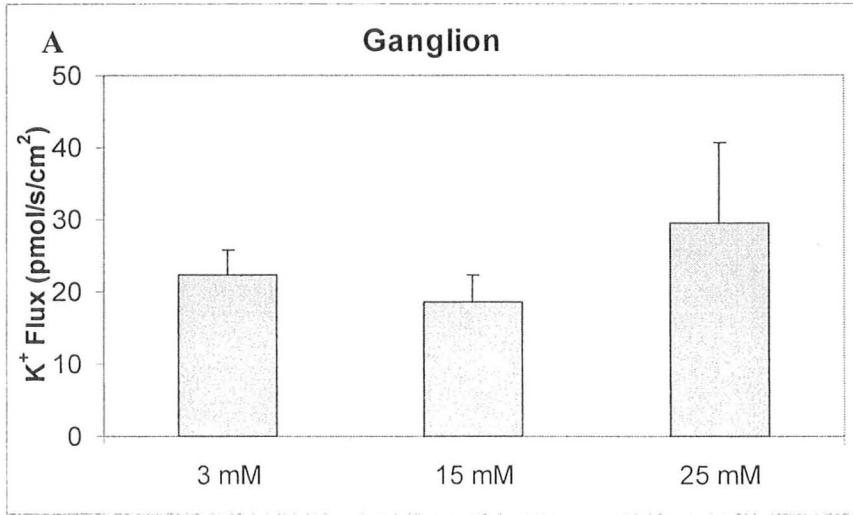


Fig. 4. K^+ flux after the VNC cord was dissected and scanned once in 3 mM K^+ , control saline (Control). (A-D) Control saline or amphotericin B (final concentration 5 μ M in 0.09% DMSO) was added. Two more scans of the same area were performed after the addition of amphotericin B or control saline (Scans 1 and 2). (E-F): The VNC was treated for 15 s with 3 M urea saline then rinsed 4x with control saline and scanned twice more in control saline (Scans 1 and 2) (* = $p < 0.05$ compared to the control scan; $n = 6$ to 8).

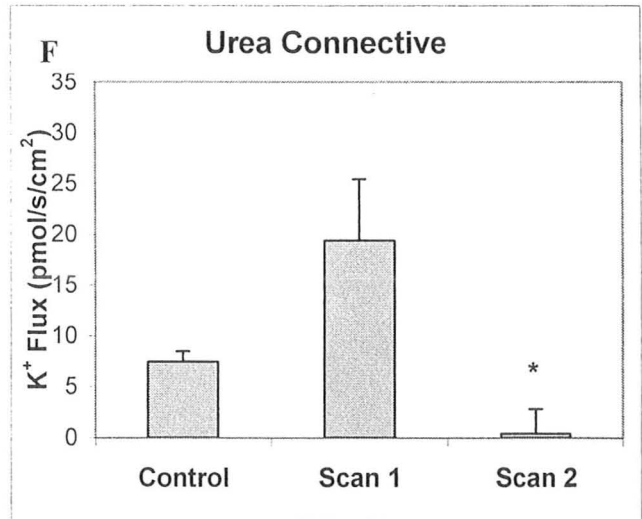
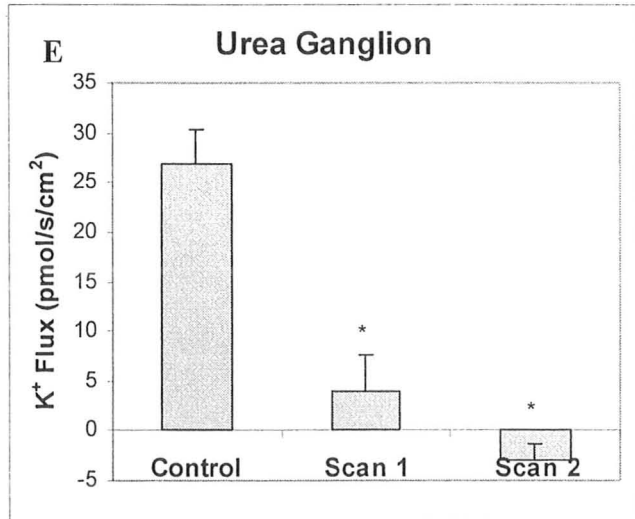
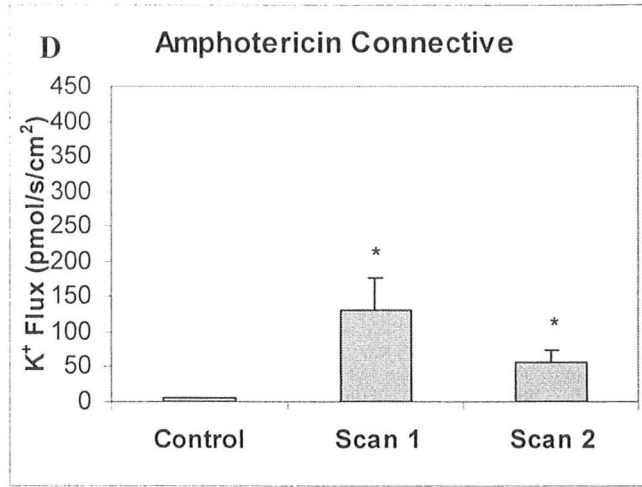
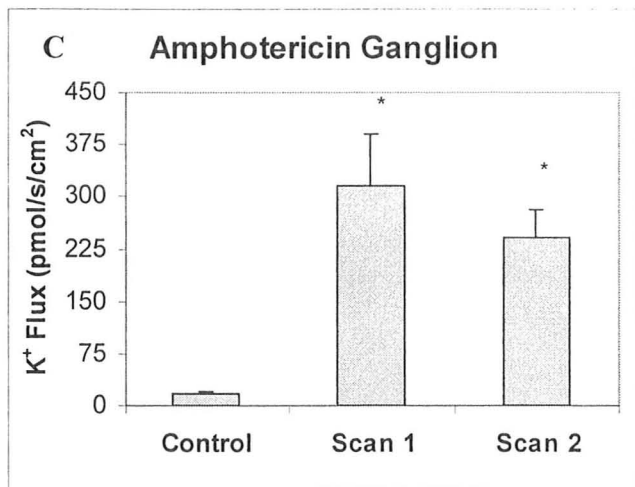
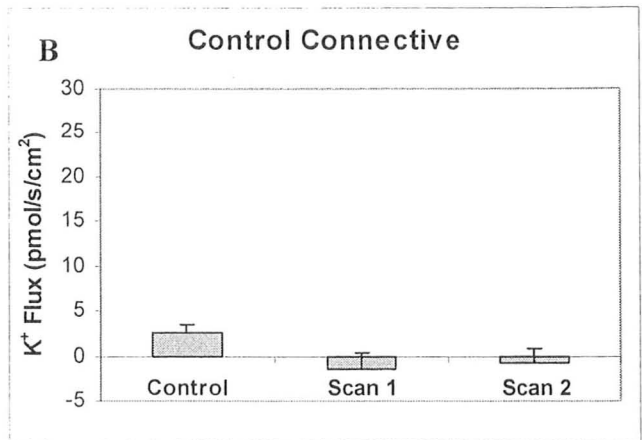
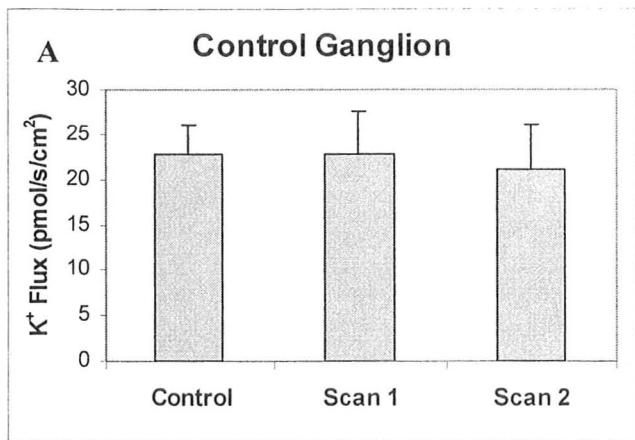


Fig. 5. The effects of the addition of control saline (A and B) or amphotericin B (5 μ M in 0.09% DMSO) (C and D) or 15 s exposure to 3 M urea on K⁺ flux over time (E and F). Each line represents the data from an individual preparation.

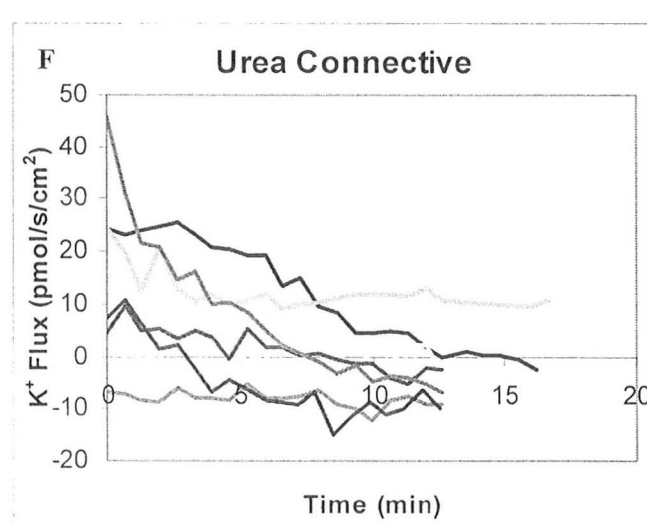
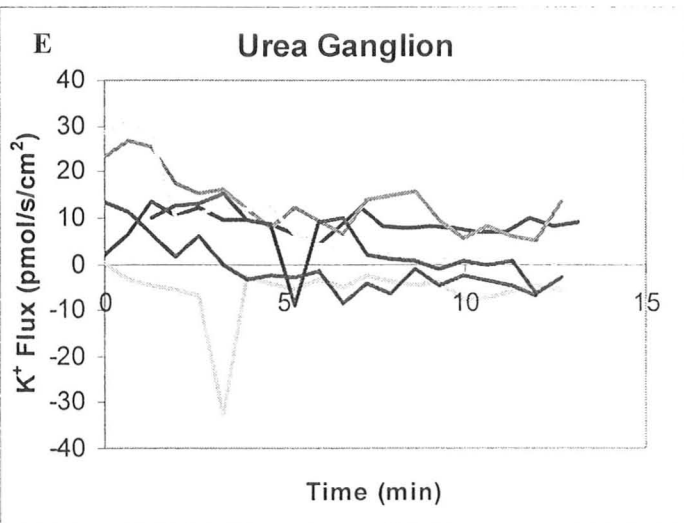
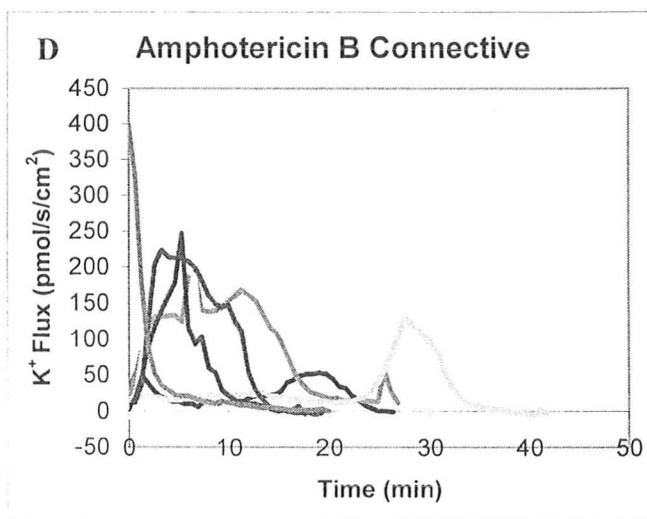
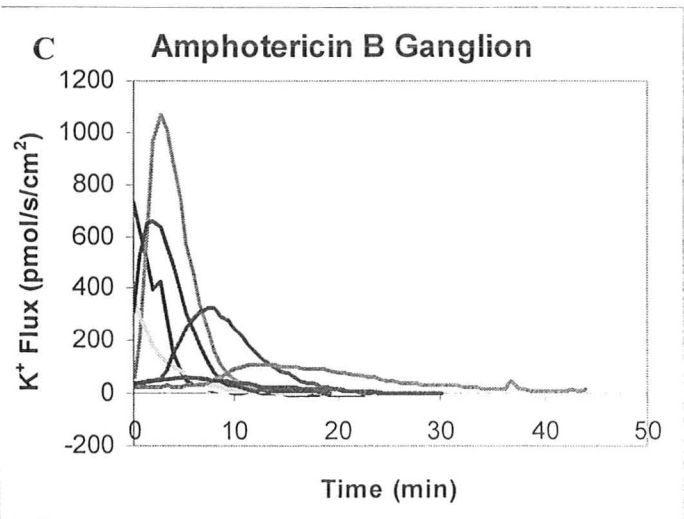
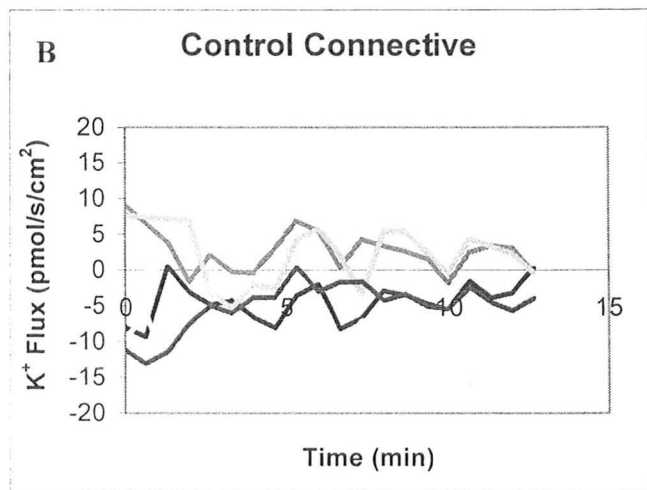
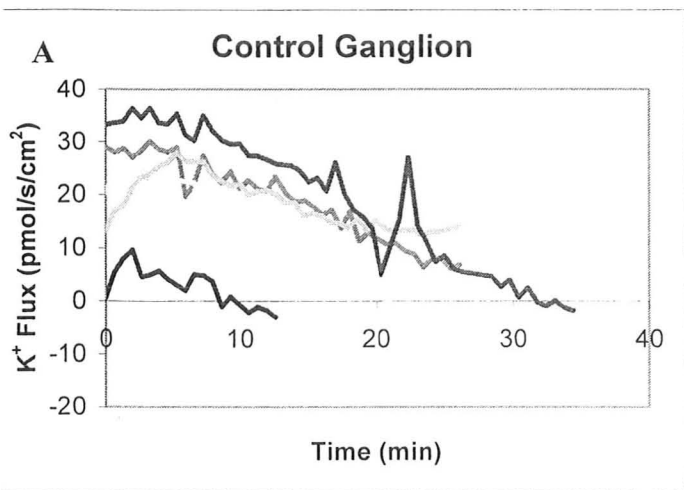


Fig. 6. The effect of CN^- on K^+ flux from the (A) ganglion and (B) connective. K^+ flux in 3 mM K^+ , control saline (Control). The control saline was replaced with saline containing 1 mM CN^- and scanned twice more (Scans 1 and 2) ($* = p < 0.05$ compared to the control scan; $n = 6$).

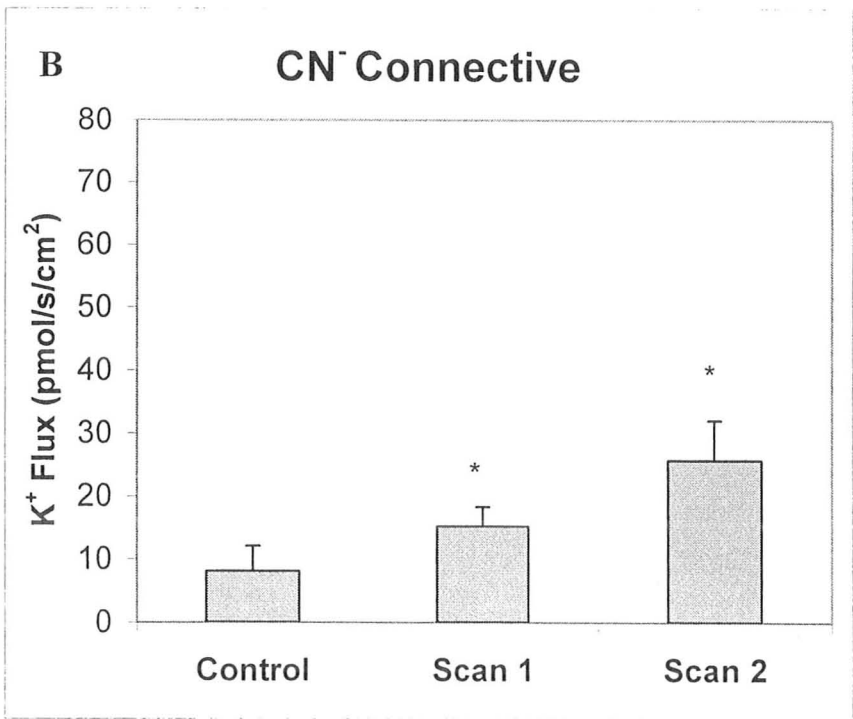
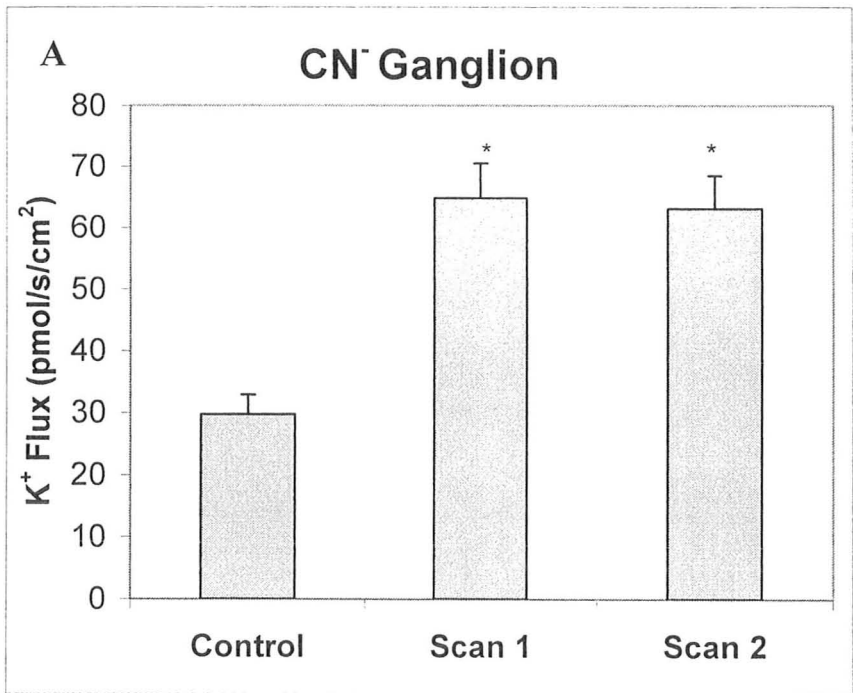
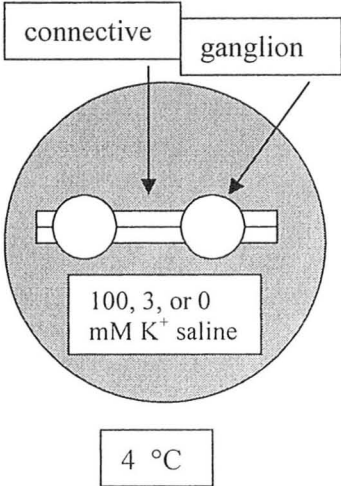


Fig. 7.0. Schematic of incubation in 4 °C K⁺-free, 3 mM K⁺, or 100 mM K⁺ saline for 30 or 60 minutes. The VNC was put in 0, 3, or 100 mM K⁺ saline and incubated at 4 °C for 30 or 60 minutes, then scanned in 3 mM K⁺ saline as it warmed to room temperature (22 °C). Preparations scanned immediately after dissection (at 22 °C) served as controls.

Step 1 -
incubation



Step 2 -
scanning

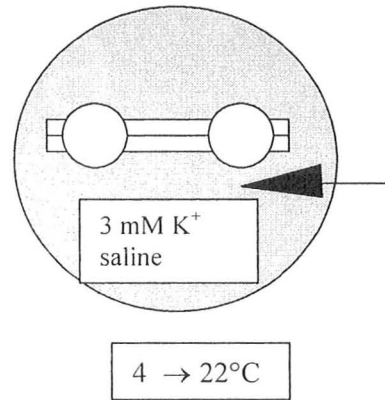
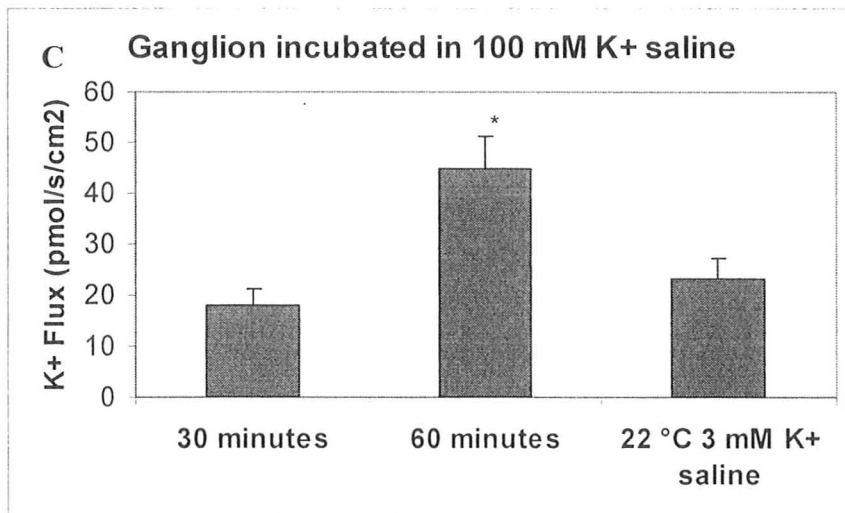
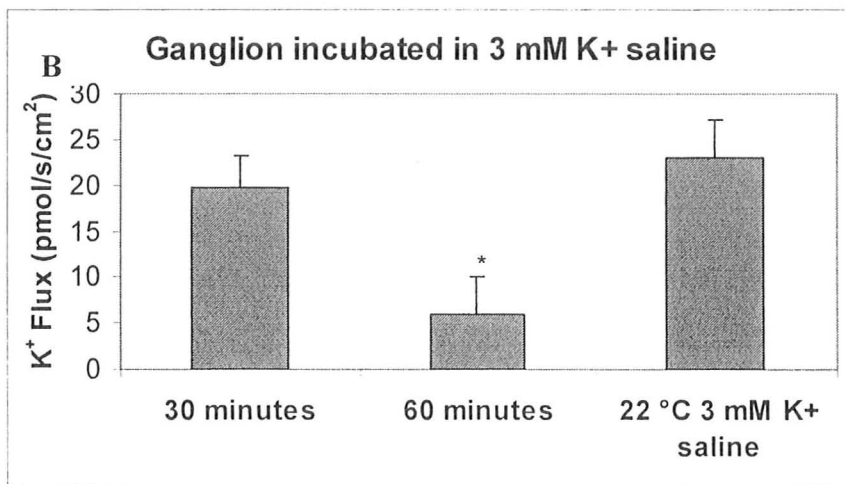
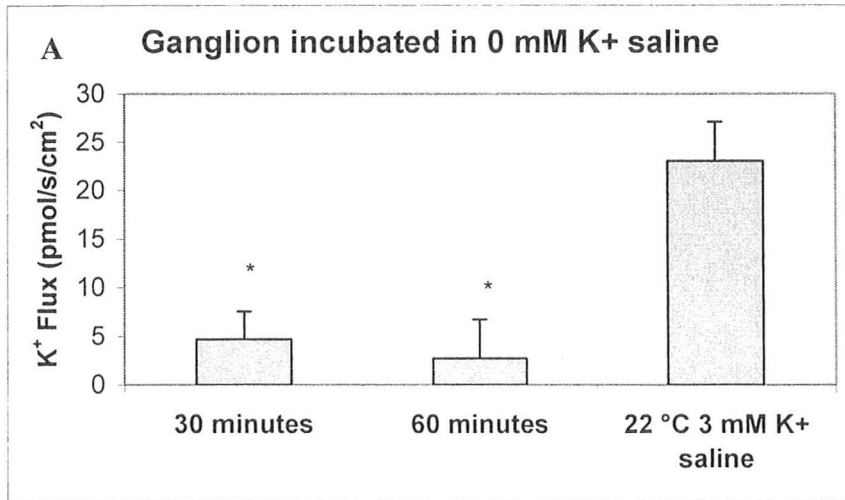


Fig. 7.1. K^+ efflux at the ganglion and the connective after incubation in 4 °C K^+ -free (A and D), 3 mM K^+ (B and E), or 100 mM K^+ (C and F) saline for 30 or 60 minutes (* = $p < 0.05$ compared to the preparations scanned in 22 °C 3 mM K^+ saline immediately after dissection; $n = 6$ to 14).



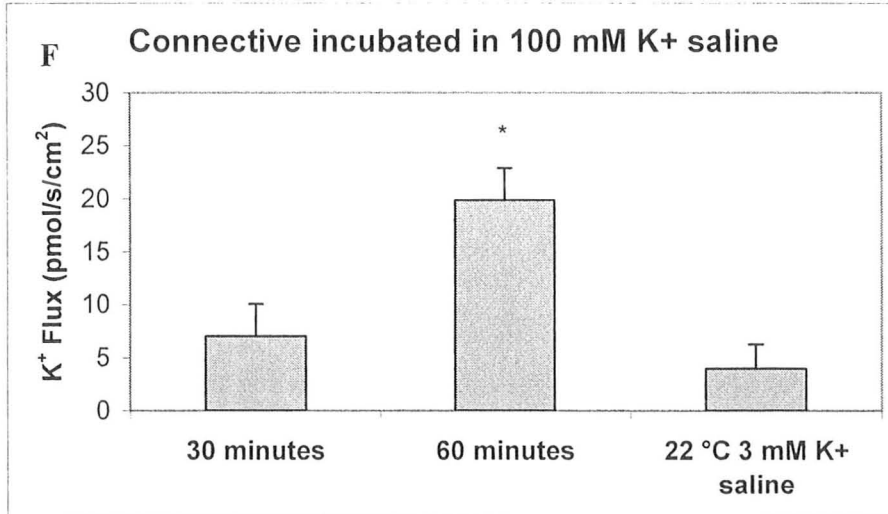
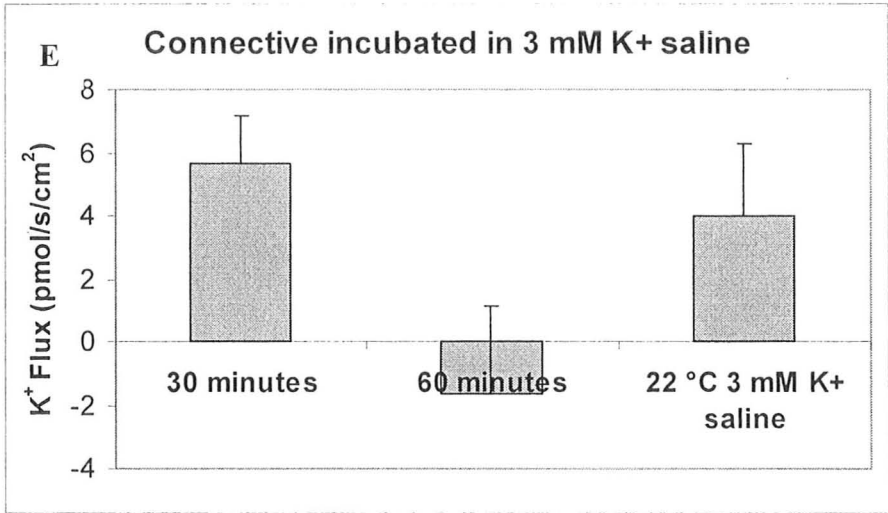
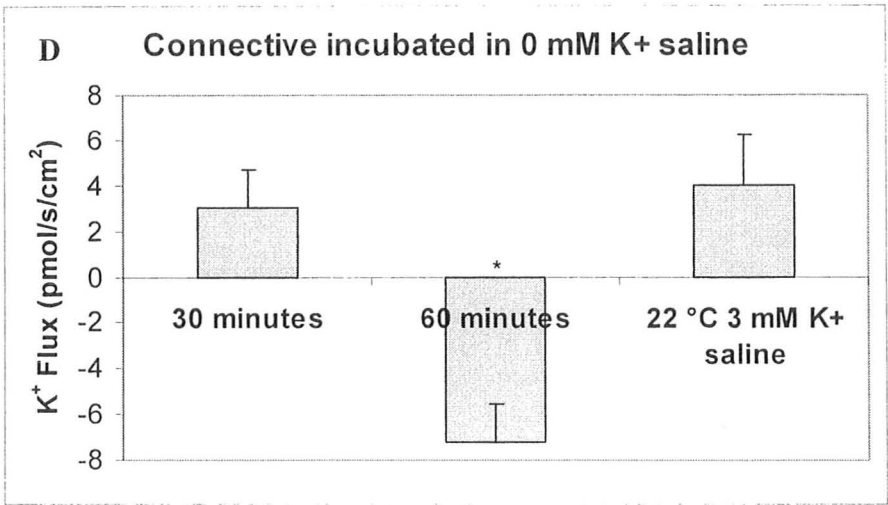
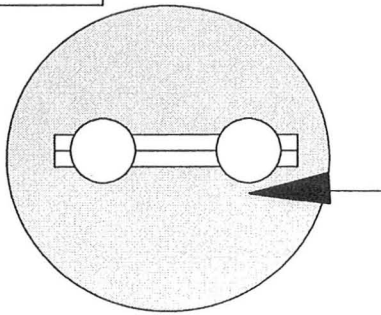


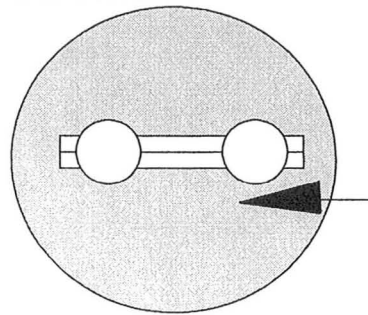
Fig. 8.0: Schematic of removal of Na^+ from the saline. The VNC was put in control saline and scanned (Control). The tissue was rinsed 4x with control saline, 10% Na^+ saline, Na^+ -free saline, or PO_4^- -free/ HCO_3^- -reduced saline and then the preparation was scanned twice more (Scans 1 and 2).

Step 1 -
Control



Control saline

Step 2 -
Scans 1 and 2



Experimental
saline

Fig. 8.1. K^+ flux in Na^+ -free and 10% Na^+ -saline at the ganglion (A) and the connective (B). PO_4^- -free, HCO_3^- -reduced saline served as a control for the Na^+ -free saline (* = $p < 0.05$; compared to the respective control scan; $n = 5$ to 9).

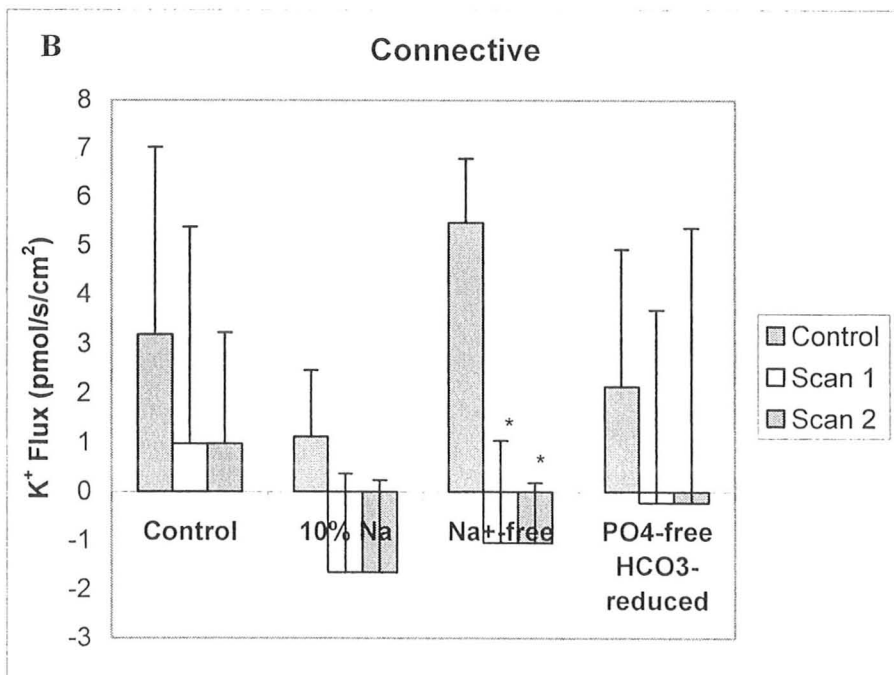
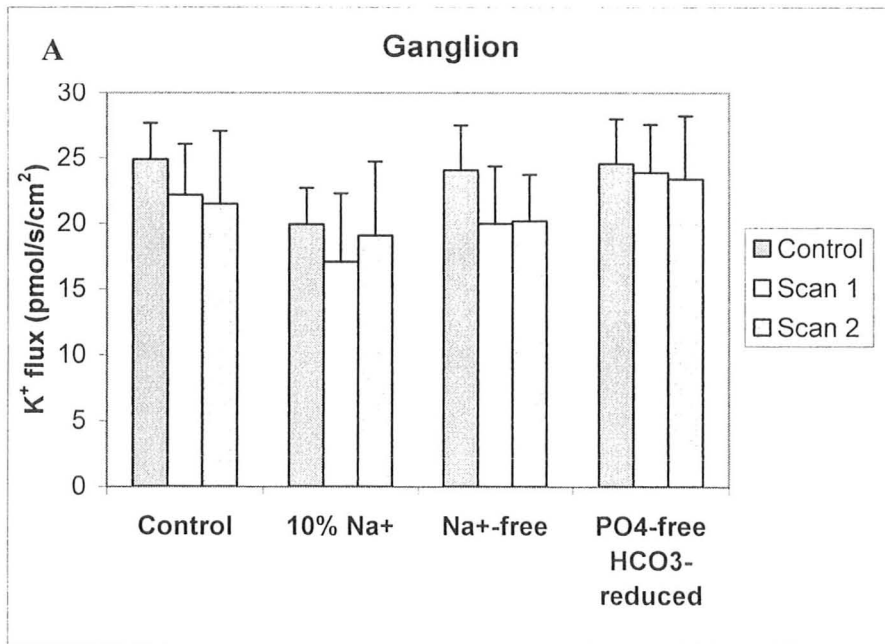
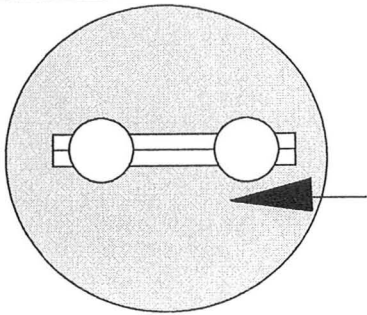


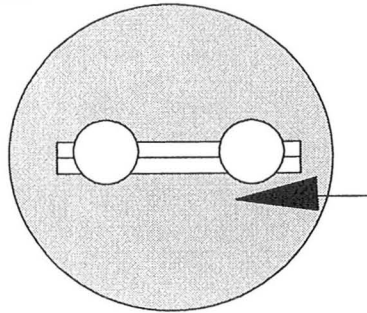
Fig. 9.0. Schematic of exposure to high and low osmolarity saline. The VNC was put in control saline and scanned (Control). The tissue was rinsed 4x with control, high osmolarity, low osmolarity, or normal osmolarity with low Na^+ and Cl^- salines and then scanned twice more (Scans 1 and 2).

Step 1 -
Control



Control saline

Step 2 -
Scans 1 and 2



Experimental
saline

Fig. 9.1. K^+ flux after exposure to saline where the osmolarity had been increased or decreased by ~25% at the ganglion (A) or connective (B). A saline where Na^+ and Cl^- were replaced with sucrose controlled for the removal of Na^+ and Cl^- in the low osmolarity saline. ($* = p < 0.05$, compared to the respective control scan; $n = 5$ to 9).

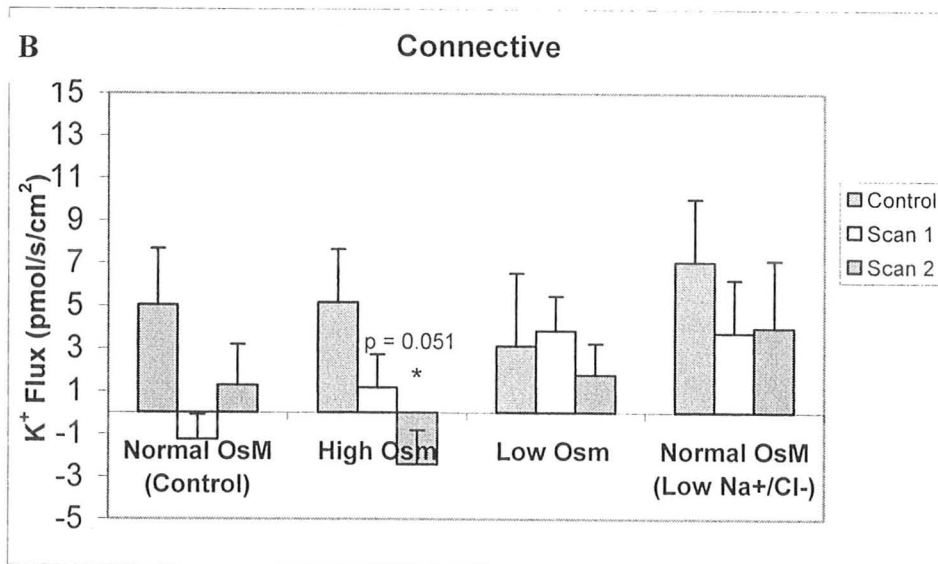
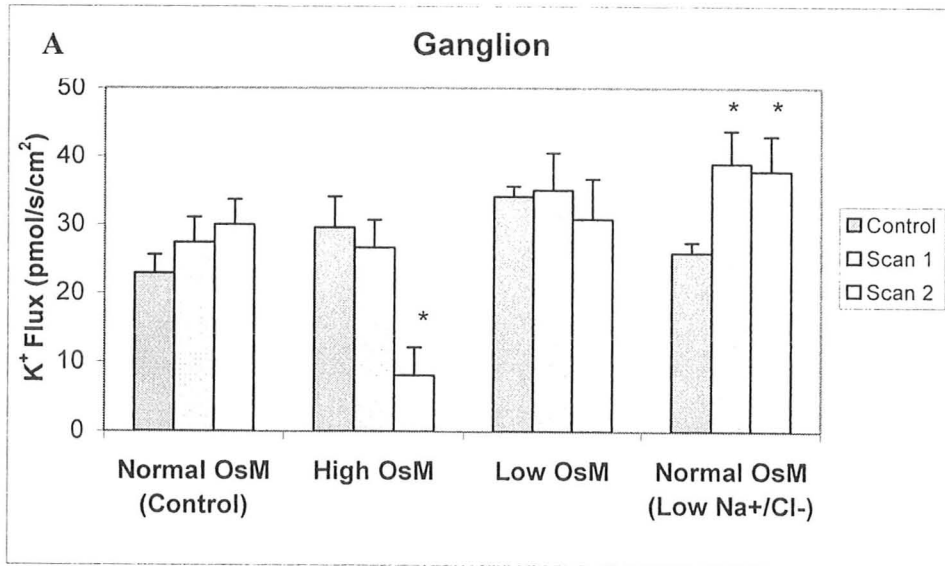
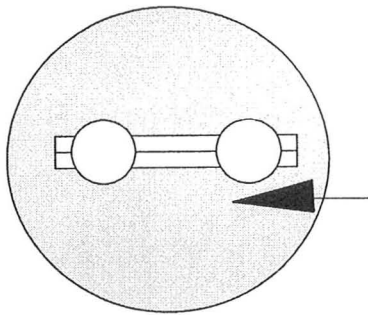


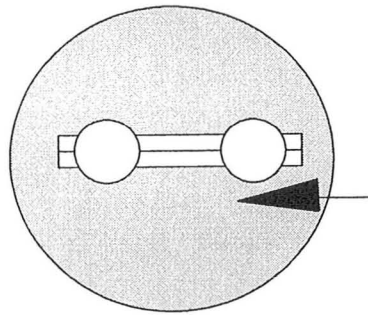
Fig. 10.0. Schematic of changing saline pH. At the ganglion (A) and the connective (B) the VNC was put in pH 7.2 saline containing HEPES as a buffer and scanned (Control). The tissue was rinsed 4x with control or pH adjusted saline and then the preparation was scanned twice more (Scans 1 and 2).

Step 1 -
Control



Control saline

Step 2 -
Scans 1 and 2



Experimental
saline

Fig. 10.1. K^+ flux at the ganglion (A) and connective (B) after exposure to salines with pH ranging from 6.2 to 8.2. HEPES was used as the buffer in salines with $\text{pH} \geq 7.2$ and PIPES was used as the buffer in salines with $\text{pHs} \leq 7.2$. (* = $p < 0.05$ compared to the respective control scan; $n = 6$ to 11).

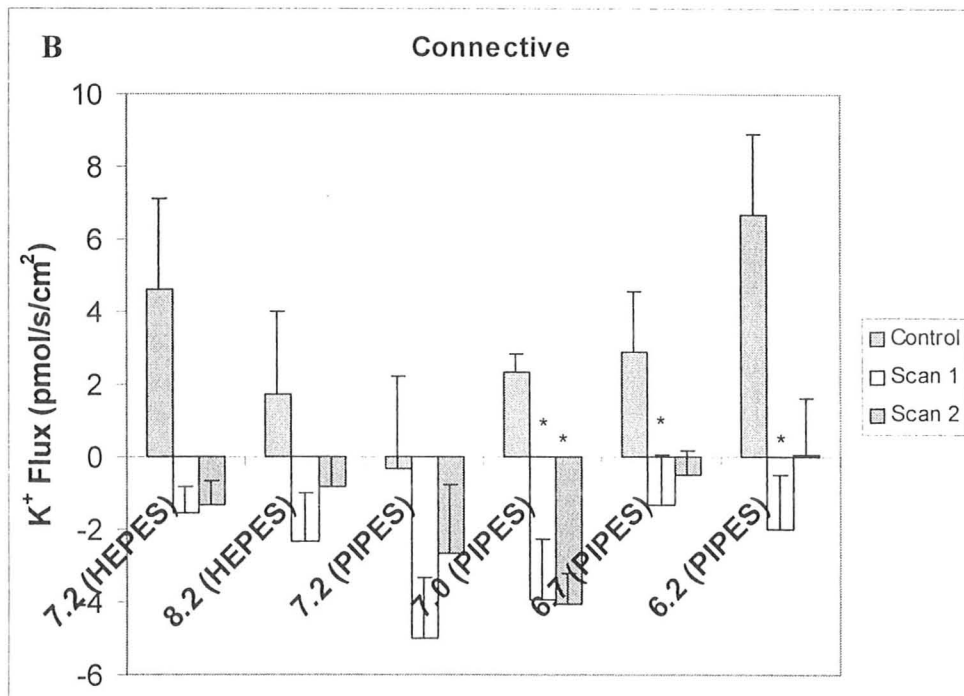
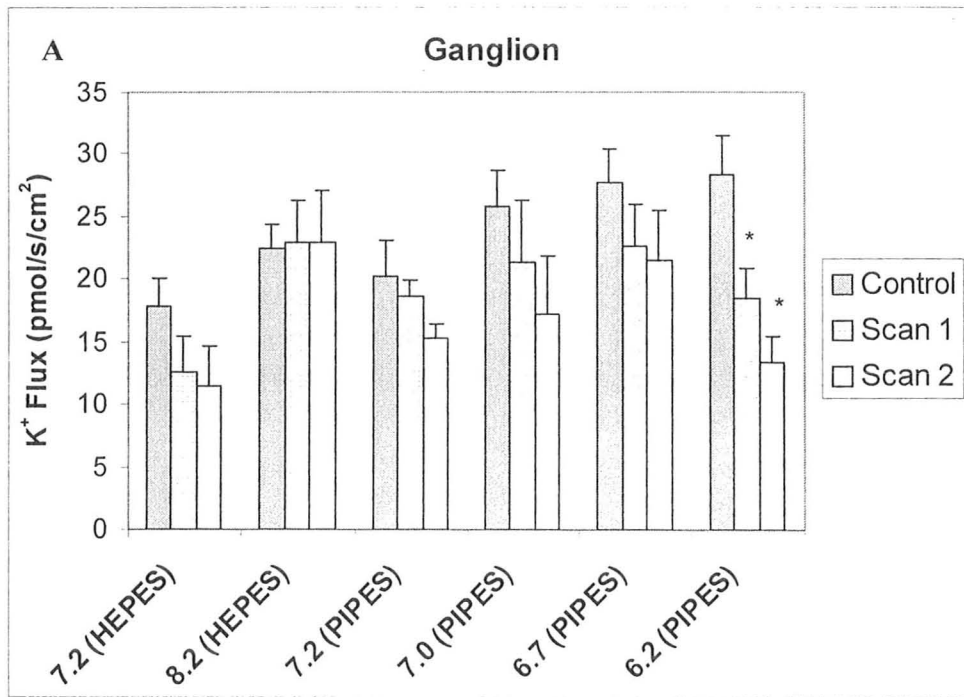
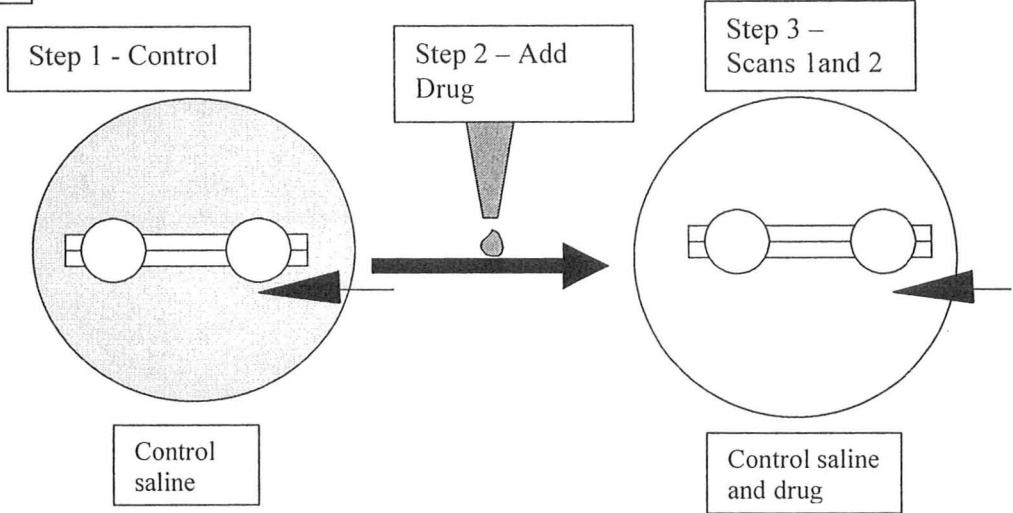


Fig 11.0: Schematic for exposure to ouabain, Baf A₁, TEA⁺, Ba²⁺, or Ca²⁺-free saline. (A) The VNC was put in control saline and scanned (Control). Saline containing the drug was added to provide 0.01 mM Baf A₁ or 0.1 mM ouabain. DMSO (0.1%) served as a vehicle for Baf A₁ and ouabain. The preparation was scanned twice more (Scans 1 and 2). (B) The VNC was put in control saline and scanned (Control). The tissue was rinsed 4x with control saline containing 5 mM Ba²⁺, 20 mM TEA⁺, or Ca²⁺-free saline and the preparation was scanned twice more in the saline containing the drug (Scans 1 and 2). PO₄⁻-free saline served as a control as PO₄⁻ binds with Ba²⁺ and was removed from the Ba²⁺ saline.

A



B

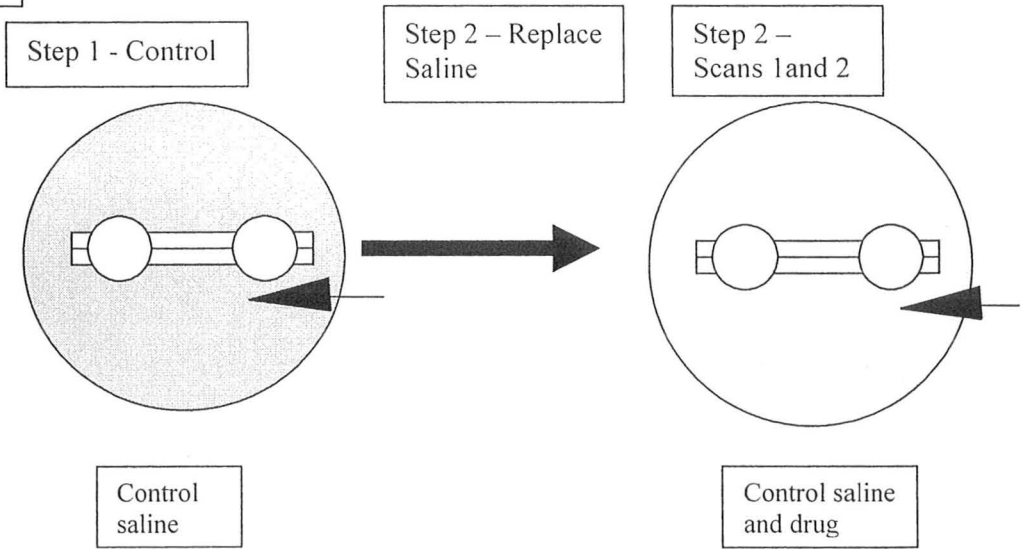
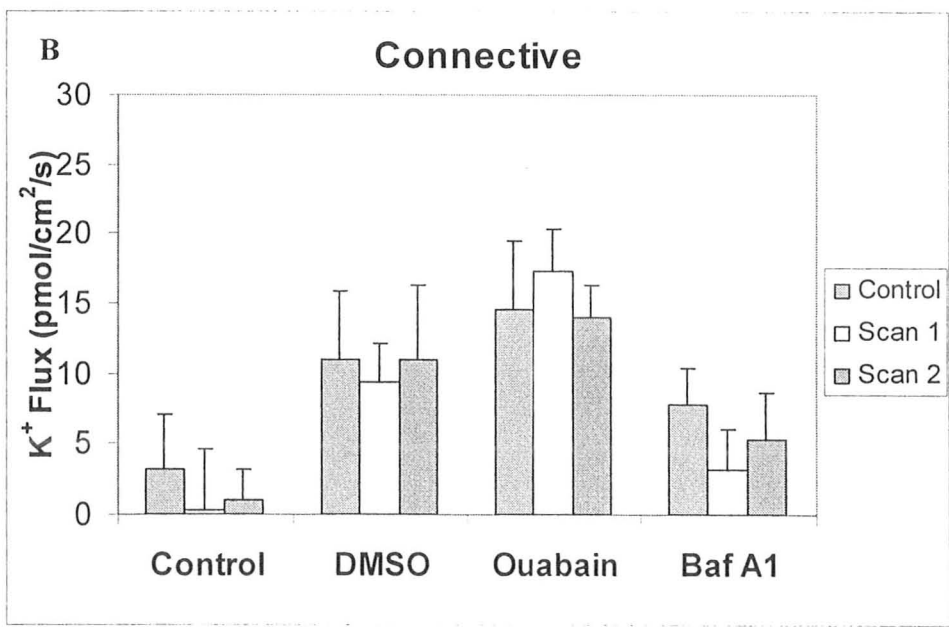
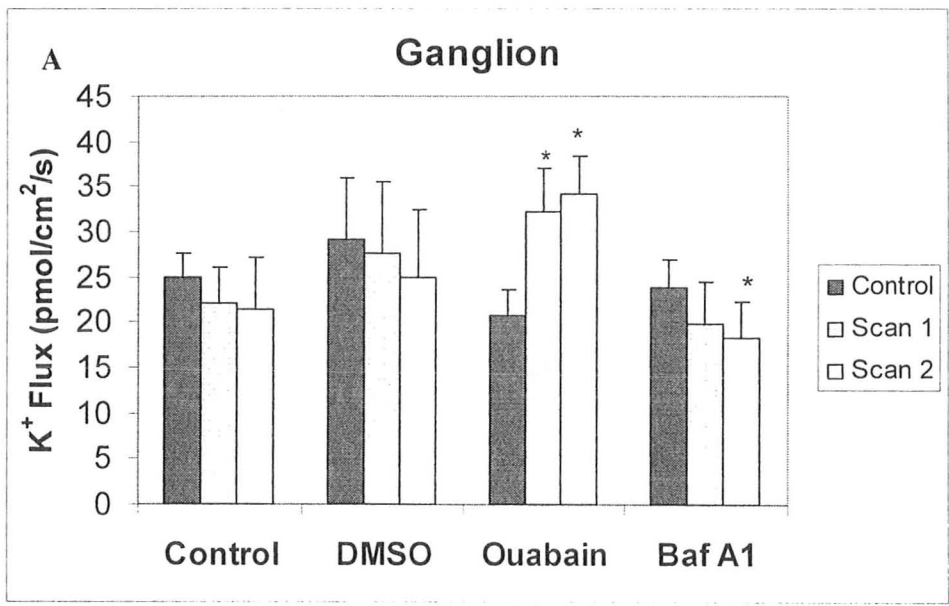


Fig. 11.1. K^+ flux after the addition of the Na^+/K^+ -ATPase inhibitor, ouabain, or the H^+ -ATPase inhibitor, Baf A_1 at the ganglion (A) and connective (B). (* = $p < 0.05$ compared to the control scan; $n = 5$ to 13). K^+ flux after the addition of the K^+ -channel blockers, Ba^{2+} or TEA^+ , or the removal of Ca^{2+} at the ganglion (C) and connective (D) (* = $p < 0.05$ compared to the control scan; $n = 5$ to 13).



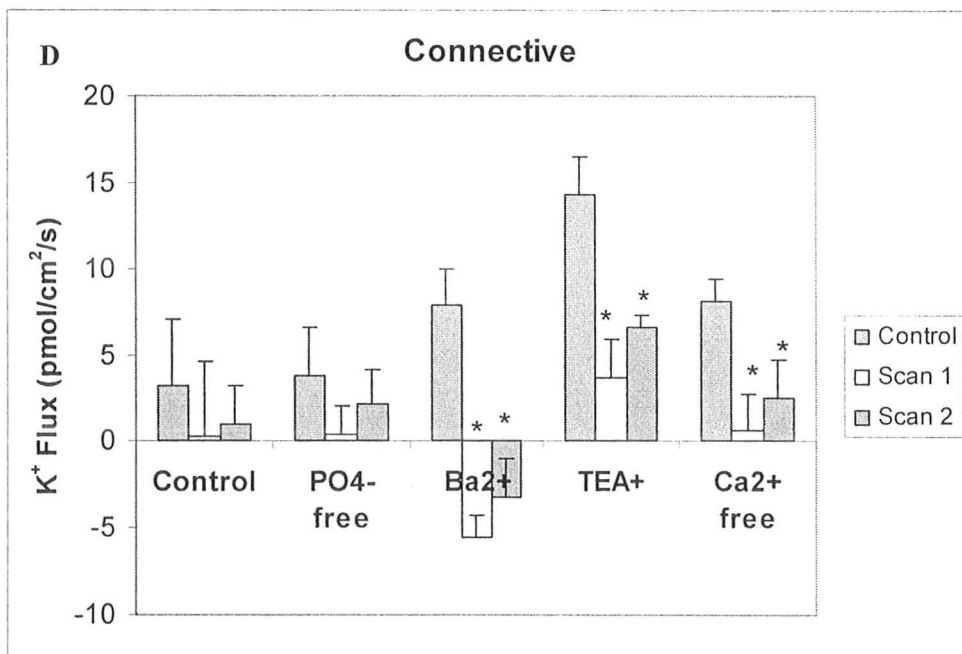
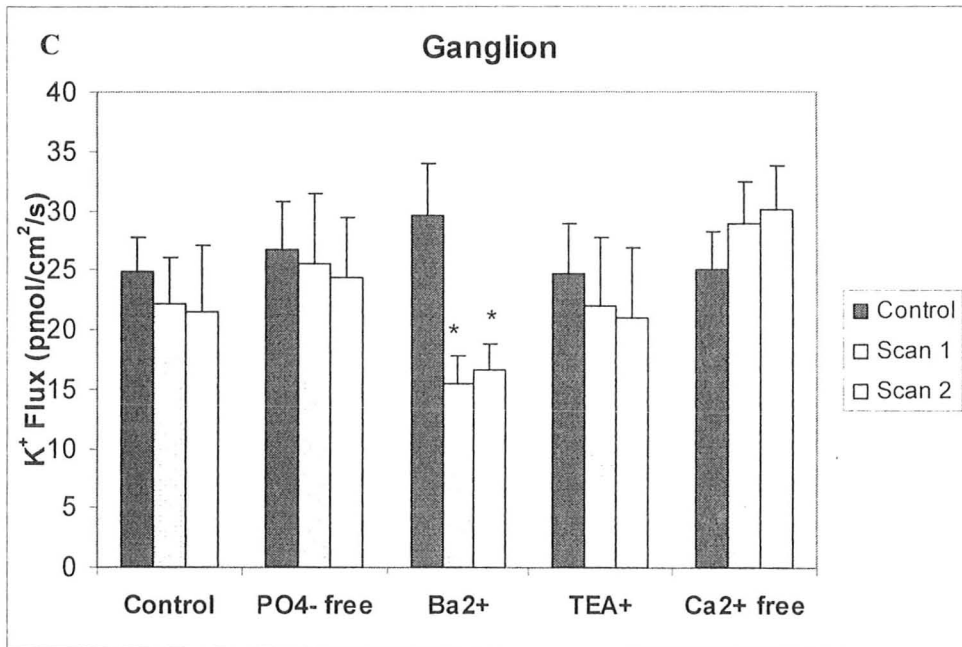
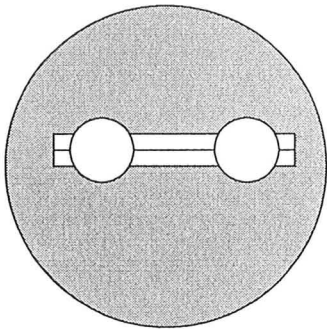


Fig 12.0. The VNC was put in 100 mM K⁺ saline and incubated at 4 °C for 30 minutes with 0.1% DMSO (vehicle), 0.01mM bafilomycin A₁ in vehicle, 0.1 mM ouabain in vehicle, or 5 mM Ba²⁺. The VNC was scanned in 3 mM K⁺ saline with vehicle, 0.01mM bafilomycin A₁, 0.1 mM ouabain, or 5 mM Ba²⁺ at the (A) ganglion or (B) connective.

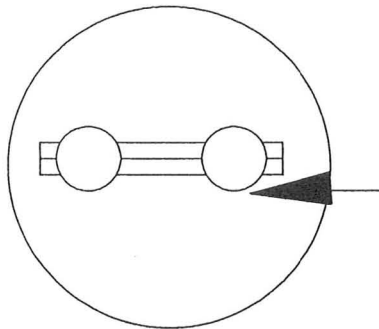
Step 1 -
incubation



100 mM K⁺
saline + Drug

4 °C

Step 2 -
scanning



3 mM K⁺ saline
+ Drug

4 → 22 °C

Fig 12.1. The effects of Baf A₁, ouabain, and Ba²⁺ on K⁺ flux after incubation in 100 mM K⁺ saline at 4 °C for 30 minutes at the ganglion (A) and the connective (B). The Control data was previously presented in Section 3.4 (* = $p < 0.05$ compared to the Control; $n = 6$ to 12).

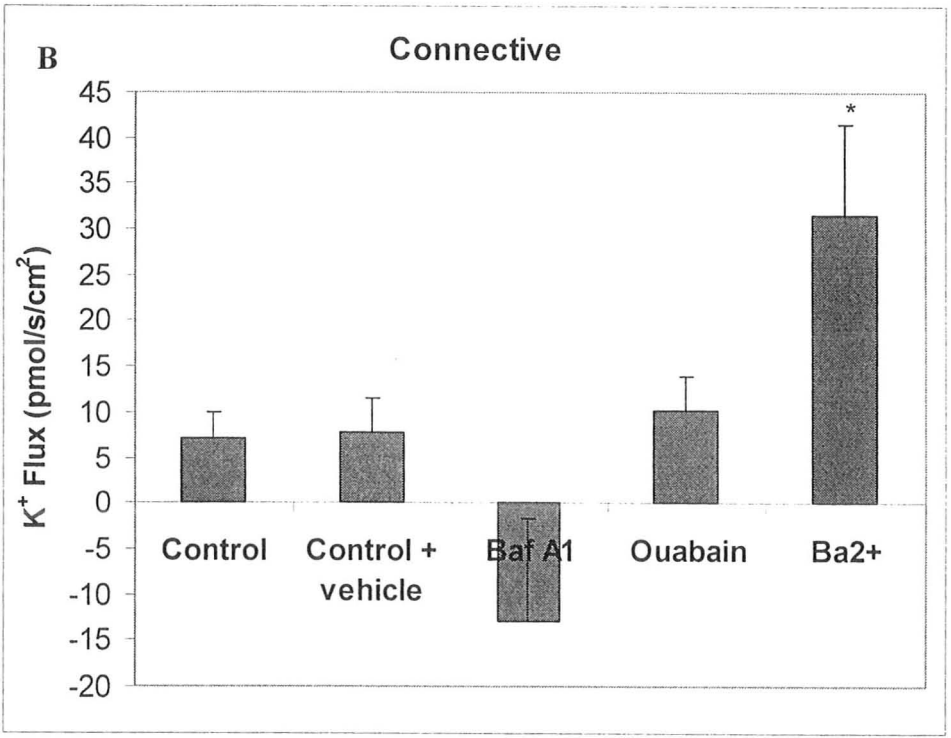
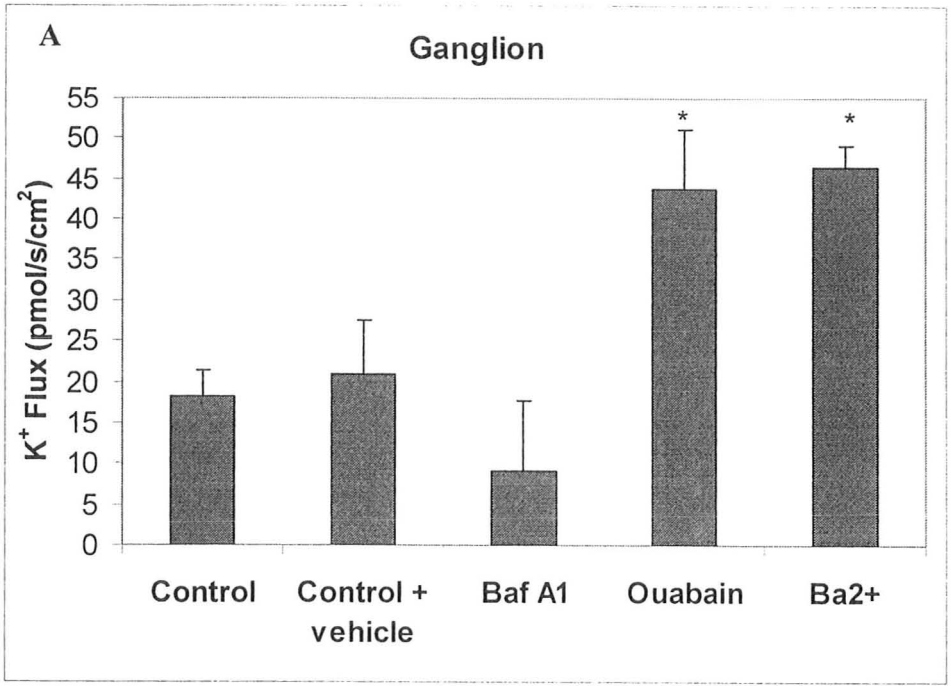


Fig 13. The VNC was put in control saline and scanned (Control) at the ganglion (A) or connective (B). The cerci were touched with the tip of the forceps for approximately 1 minute (~120 times) and the preparation was scanned twice more after stimulation of the cerci (Scans 1 and 2). No significant differences were observed. (n = 4).

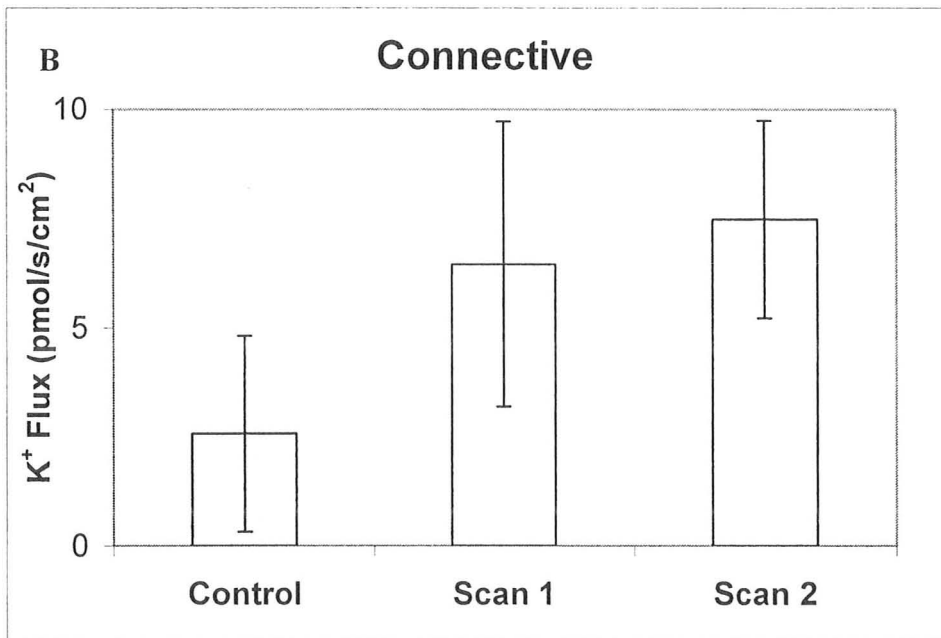
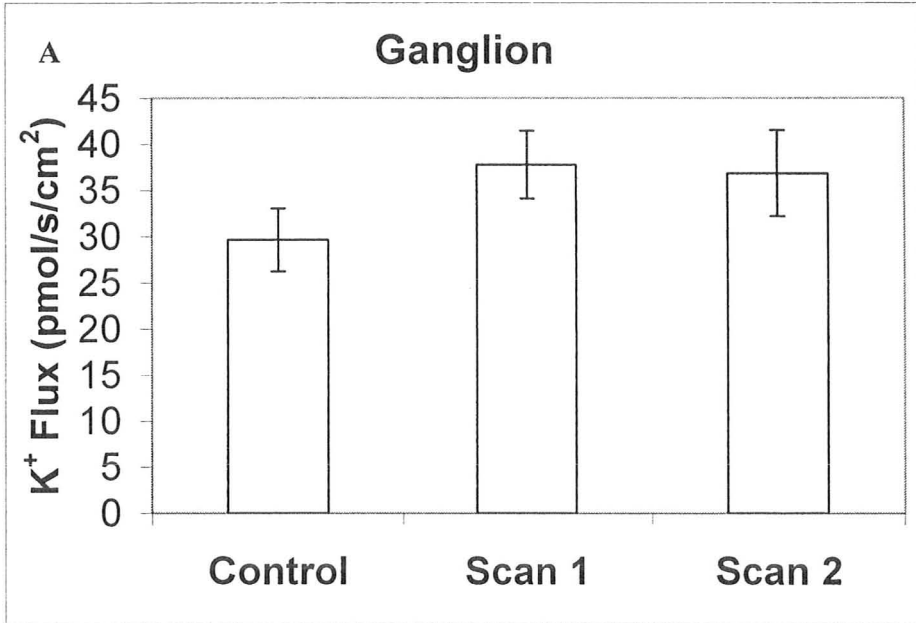
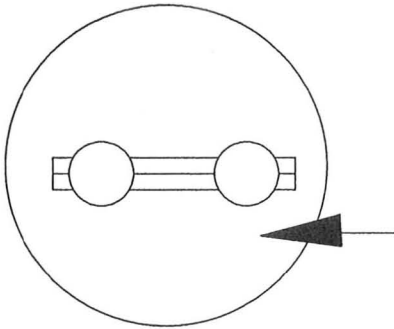


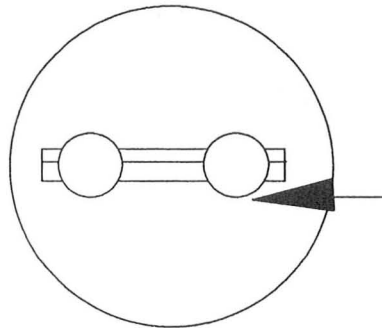
Fig 14.0. The VNC was put in control saline and H^+ flux was measured (Control) at the ganglion (A) and the connective (B). Additional control saline, saline containing DMSO, or saline containing Baf A₁ in DMSO was added to provide final concentrations of 1% DMSO or 10 μ M Baf A₁ in 1% DMSO and the preparation was scanned again (Experimental).

Step 1 -
Control



Control saline

Step 2 -
Experimental



Control saline +
Drug

Fig. 14.1. H^+ flux in control saline and after the addition of the V-type H^+ -ATPase inhibitor, Baf A_1 at the ganglion (A) and the connective (B) (* = $p < 0.05$ compared to the corresponding Control scan; # = $p < 0.05$ control preparation, $n = 5$ to 8).

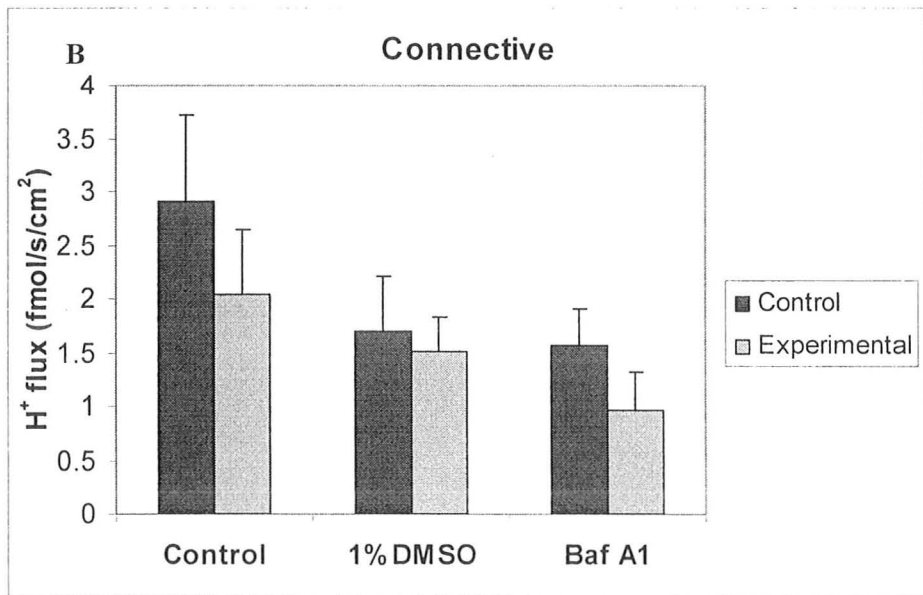
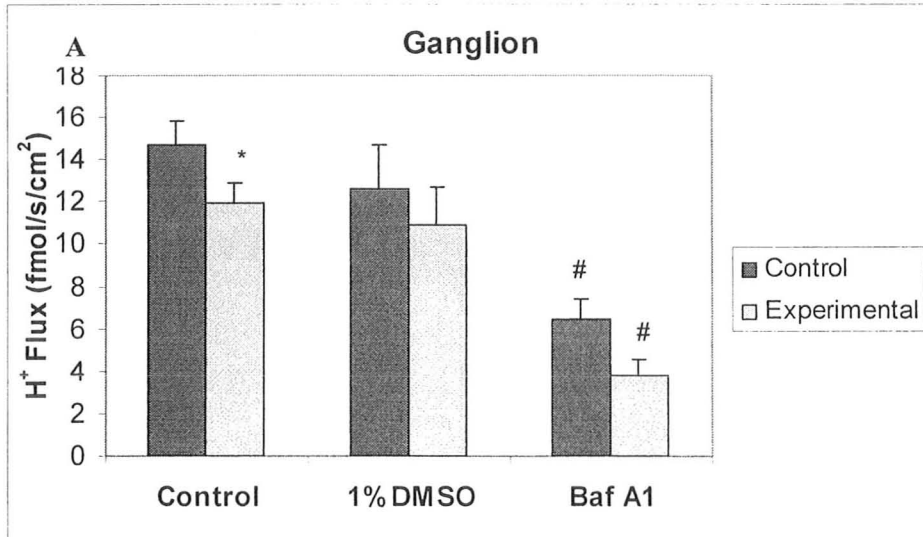
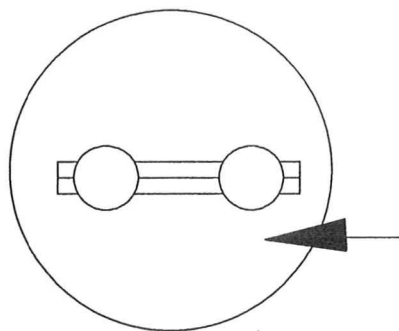
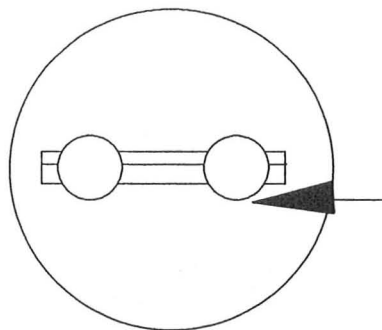


Fig. 14.2. Immediately before scanning 50 μL of either control saline or saline containing Baf A_1 was added to the saline surrounding the preparation. The final Baf A_1 concentration used was 10 μM . A single point was scanned every 40 seconds 35 times.



Control saline

OR



Control saline +
Drug

Fig. 14.3. . H^+ flux over time in control saline and in saline containing the V-type H^+ -ATPase inhibitor, Baf A_1 at the ganglion. There were no significant differences between the efflux in the control and the Baf A_1 treated preparations at any time point. The point to the right of the red line a significantly lower than the original efflux in both the control and Baf A_1 treated preparations ($n = 6$ to 7).

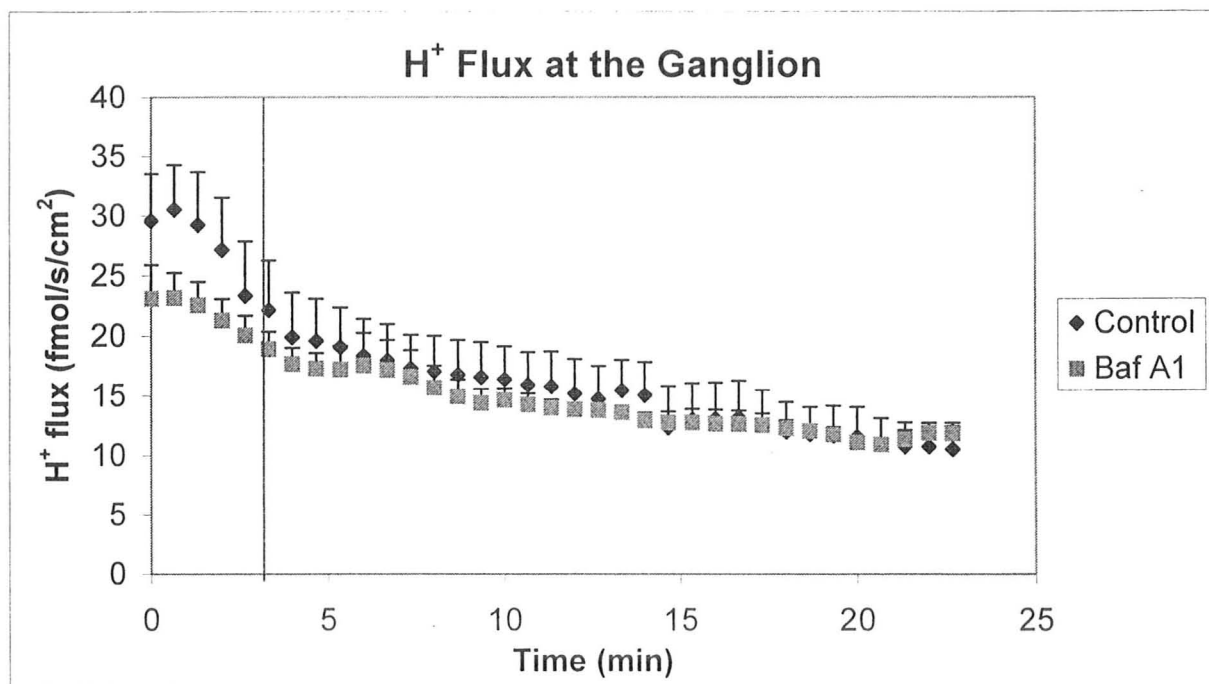


Fig. 15. An example of spontaneous nerve firing observed in control saline. (A) one action potential is contained within the box. (B) shows a close up of two of the action potentials shown in A (in the boxes). Please note the changes in scale.

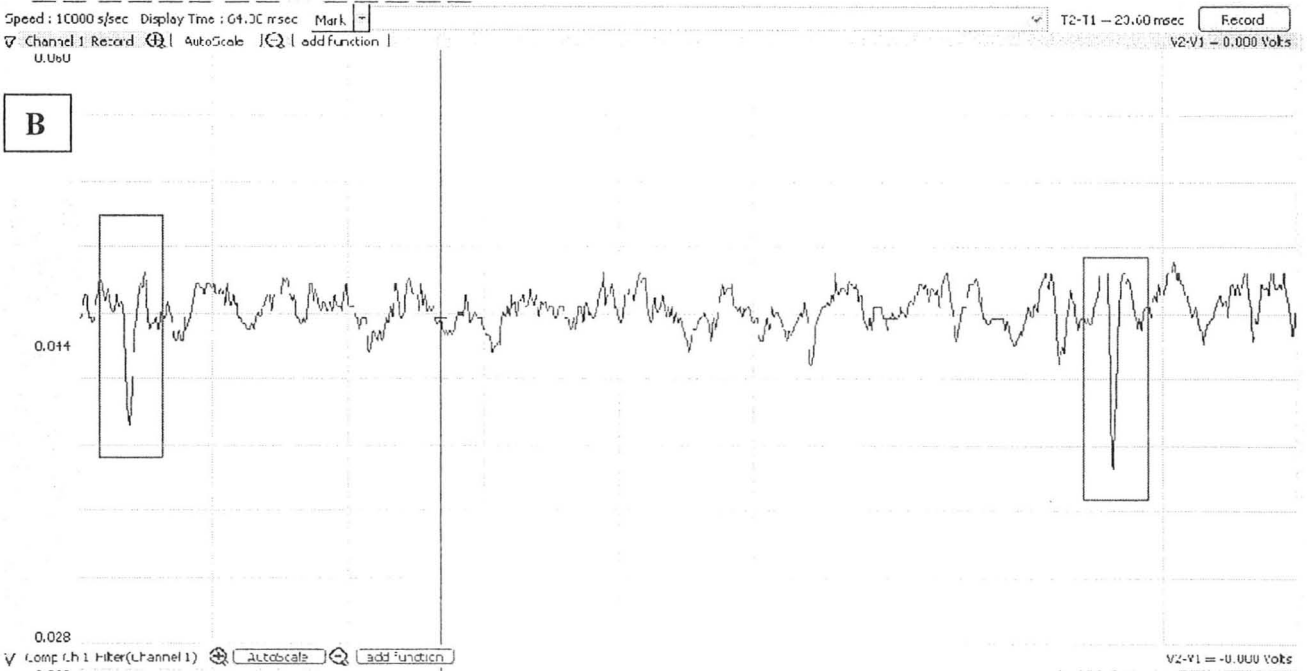
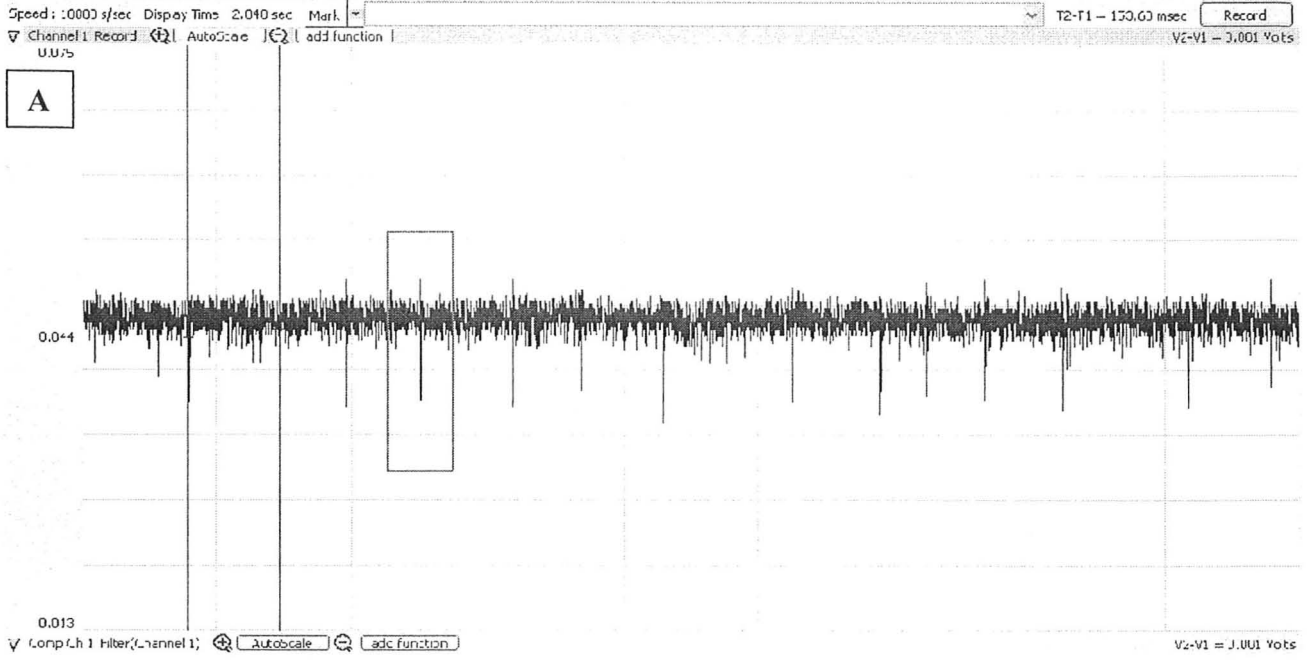


Fig. 16. An example of elicited firing in control saline. The large stimulating pulse is followed by three smaller elicited action potentials. (B) shows a close up of one set of elicited potentials shown in (A). Please note the changes in scale.

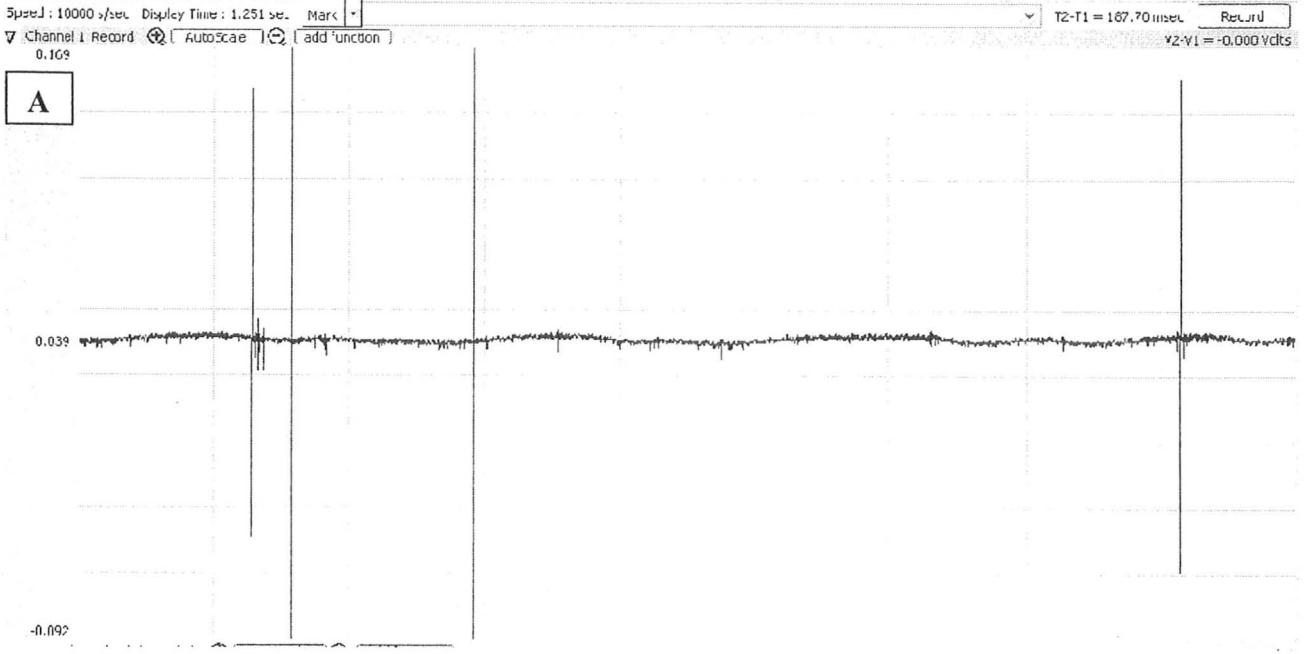


Fig. 17: Working hypothesis for the effects of ouabain at the ganglion. (A) Before the addition of ouabain (B) after the addition of ouabain. A larger overall net efflux is observed after the addition of ouabain since uptake of K^+ by the Na^+/K^+ -ATPase is inhibited. The VNC has been simplified in the figure by showing the BBB as composed of only one layer, instead of multiple cell types. The glial cells surrounding the neurons are not depicted. The transporters are shown in the BBB but may also be in the neuronal membranes as SIET measures the net flux outside the VNC.

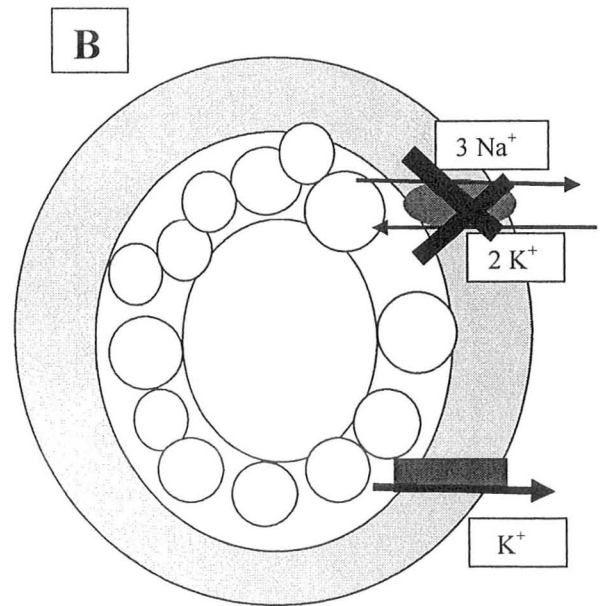
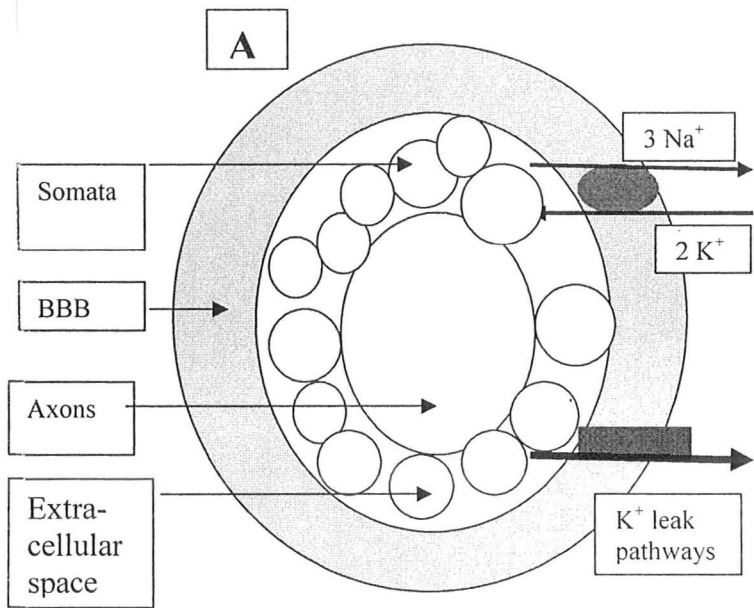


Fig. 18. Working hypothesis for the effects of K^+ channel blockers at the ganglion. A) Before the addition of K^+ channel blockers B) after the addition of K^+ channel blockers. A significant decrease in efflux is observed after the addition of TEA^+ or the removal of Ca^{2+} at the connectives. An influx is observed at the connectives and a reduced efflux is observed at the ganglion after the addition of Ba^{2+} . Evidence indicates K^+ channel blockers also play a role in regulating K^+ flux at the connectives.

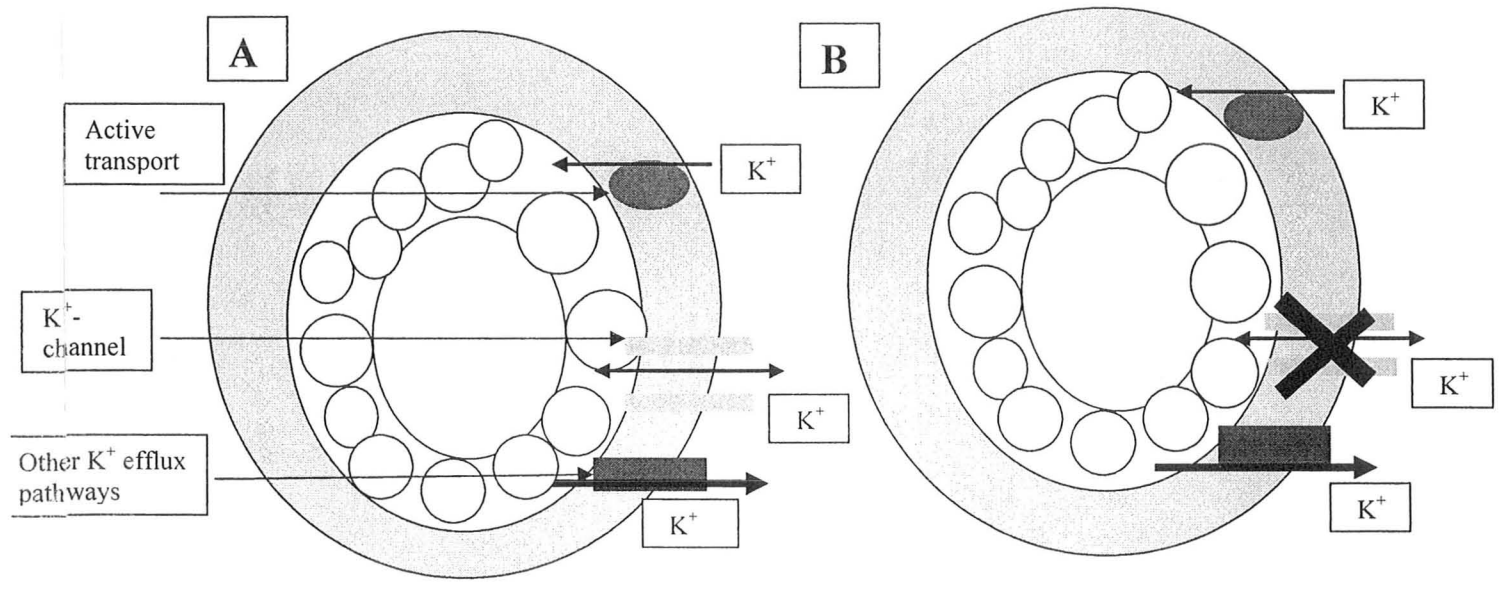
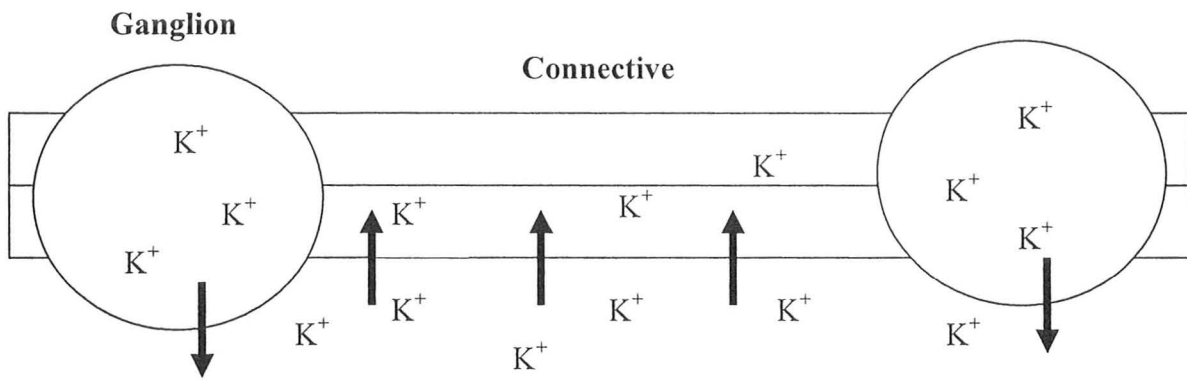


Fig. 19. Cycling of K^+ in 15 and 25 mM K^+ saline. At the connective there is an influx of K^+ . This K^+ is transported to the ganglion within the VNC. An efflux of K^+ is seen at the ganglion.



Appendix A – Saline Composition

Table 1: Composition of 3, 15, and 25 mM K⁺ Salines

Chemical (mM)	3 mM K ⁺ (Control)	15 mM K ⁺	25 mM K ⁺
Glucose	20	20	20
L-Glutamine	10	10	10
Trehalose	5	5	5
HEPES	8.6	8.6	8.6
NaCl	139	127	117
KCl	3	15	25
CaCl ₂	2	2	2
MgCl ₂	2	2	2
NaHCO ₃	10.2	10.2	10.2
NaH ₂ PO ₄	4.3	4.3	4.3

Table 2: Composition of Salines Containing Amphotericin B, Urea, or CN⁻

Chemical (mM)	Control	Amphotericin B	Urea	CN ⁻
Glucose	20	20	20	20
L-Glutamine	10	10	10	10
Trehalose	5	5	5	5
HEPES	8.6	8.6	8.6	8.6
NaCl	139	139	139	138
KCl	3	3	3	3
CaCl ₂	2	2	2	2
MgCl ₂	2	2	2	2
NaHCO ₃	10.2	10.2	10.2	10.2
NaH ₂ PO ₄	4.3	4.3	4.3	4.3
Amphotericin B	-	1	-	-
Urea	-	-	3000	-
NaCN	-	-	-	1

Chemical (mM)	K⁺-free	3 mM K⁺ (Control)	100 mM K⁺
Glucose	20	20	20
L-Glutamine	10	10	10
Trehalose	5	5	5
HEPES	8.6	8.6	8.6
NaCl	142	139	42
KCl	-	3	100
CaCl ₂	2	2	2
MgCl ₂	2	2	2
NaHCO ₃	10.2	10.2	10.2
NaH ₂ PO ₄	4.3	4.3	4.3

Chemical (mM)	Control	10% Na⁺	Na⁺-free	PO₄-free, HCO₃⁻-reduced
Glucose	20	20	20	20
L-Glutamine	10	10	10	10
Trehalose	5	5	5	5
HEPES	8.6	8.6	8.6	8.6
NaCl	139	0.85	-	139
KCl	3	2.7*	-	3
CaCl ₂	2	2	2	2
MgCl ₂	2	2	2	2
NaHCO ₃	10.2	10.2	-	3
KHCO ₃	-	-	2.7*	-
NaH ₂ PO ₄	4.3	4.3	-	-
<i>N</i> -methyl-D-glucamine**	-	138.15	153.5	-

* The addition of *N*-methyl-D-glucamine increased the activity of K⁺. K⁺ levels were adjusted so they would have the same activity as 3 mM K⁺ in saline that didn't contain *N*-methyl-D-glucamine.

** The addition of HCl to lower pH replaced the Cl⁻ from the NaCl.

Table 5: Composition of Salines used in Osmolarity Experiments

Chemical (mM)	Normal Osmolarity (Control)	Normal Osmolarity (low Na ⁺ /Cl)	Low Osmolarity	High Osmolarity
Glucose	20	20	20	20
L-glutamine	10	10	10	10
Trehalose	5	5	5	5
HEPES	8.6	8.6	8.6	8.6
NaCl	139	95	95	139
KCl	3	3	3	3
CaCl ₂	2	2	2	2
MgCl ₂	2	2	2	2
NaHCO ₃	10.2	10.2	10.2	10.2
NaH ₂ PO ₄	4.3	4.3	4.3	4.3
Sucrose	-	89	-	89

Table 6: Composition of Salines used in pH Experiments

Chemical (mM)	HEPES (pH 7.2 and 8.2) (Control)	PIPES (pH 7.2, 7.0, 6.7, and 6.2)
Glucose	20	20
L-glutamine	10	10
Trehalose	5	5
HEPES	8.6	-
PIPES	-	8.6
NaCl	139	139
KCl	3	3
CaCl ₂	2	2
MgCl ₂	2	2
NaHCO ₃	10.2	10.2
NaH ₂ PO ₄	4.3	4.3

Table 7: Composition of 3 mM K⁺ Salines Containing Ba²⁺, Baf A₁, Ouabain, or TEA⁺ and Ca²⁺-free Saline

Chemical (mM)	3 mM K ⁺ (Control)	Ba ²⁺ (5 mM)	Baf A ₁ (0.01 mM)	Ouabain (0.1 mM)	TEA ⁺ (20 mM)	Ca ²⁺ -free
Glucose	20	20	20	20	20	20
L-glutamine	10	10	10	10	10	10
Trehalose	5	5	5	5	5	5
HEPES	8.6	8.6	8.6	8.6	8.6	8.6
NaCl	139	129	139	139	119	141
KCl	3	3	3	3	3	3
CaCl ₂	2	2	2	2	2	-
MgCl ₂	2	2	2	2	2	2
NaHCO ₃	10.2	10.2	10.2	10.2	10.2	10.2
NaH ₂ PO ₄	4.3	-*	4.3	4.3	4.3	4.3
BaCl ₂	-	5	-	-	-	-
Baf A ₁	-	-	0.01	-	-	-
Ouabain	-	-	-	0.1	-	-
DMDS	-	-	-	-	-	-
TEACl	-	-	-	-	20	-
NaCN	-	-	-	-	-	-

* NaH₂PO₄ was not included in salines containing Ba²⁺, as its addition would result in the formation of a precipitate. Removal of PO₄⁻ did not significantly affect K⁺ flux.

Table 8: Composition of 100 mM K⁺ saline containing Baf A₁, ouabain, or Ba²⁺

Chemical (mM)	100 mM K ⁺ (Control)	Baf A ₁ (0.01 mM)	Ouabain (0.1 mM)	Ba ²⁺ (5 mM)
Glucose	20	20	20	20
L-glutamine	10	10	10	10
Trehalose	5	5	5	5
HEPES	8.6	8.6	8.6	8.6
NaCl	42	42	42	32
KCl	100	100	100	100
CaCl ₂	2	2	2	2
MgCl ₂	2	2	2	2
NaHCO ₃	10.2	10.2	10.2	10.2
NaH ₂ PO ₄	4.3	4.3	4.3	-*
Baf A ₁	-	0.01	-	-
Ouabain	-	-	0.1	-
BaCl ₂	-	-	-	5

NaH₂PO₄ was not included in salines containing Ba²⁺, as its addition would result in the formation of a precipitate. Removal of PO₄⁻ did not significantly affect K⁺ flux.

Appendix B – Organic Cation (Tetraethylammonium) Excretion Across the VNC

Introduction

The BBB may also protect the underlying nerves from toxins, including organic cations. The ability of the prototypical organic cation, tetraethylammonium (TEA^+) to cross the BBB was examined using SIET. In addition, regional variations in TEA^+ flux were identified.

Materials and Methods

SIET was used to determine TEA^+ flux. The methods were the same as those described in Section 2.3 with the following exceptions. The TEA^+ -selective microelectrodes were based on Corning ion exchanger (477317) (Fluka, Buchs, Switzerland) and backfilled with 100 mM TEACl. The microelectrodes were stored in 100 mM TEACl once the ionophore had been applied. TEA^+ electrodes were calibrated in solutions containing 10, 1, and 0.1 mM TEA^+ (in saline). TEA^+ electrodes had slopes of 56-63 mV for a ten-fold change in TEA^+ concentration.

During SIET scans a 4 s waiting period was used. The diffusion coefficient for TEA^+ is $0.868 \times 10^{-5} \text{ cm}^2/\text{s}$ (Rheault and O'Donnell, 2004).

The VNCs were pinned in the Sylgard layer of a Petri dish containing 100 mM TEA^+ saline and incubated at 4 or 22 °C for 30 minutes. It was hypothesised that at 4 °C the rate of active transport would be inhibited relative to the rate at 22 °C. This would result in a greater influx of TEA^+ . The preparations were scanned until voltage recorded by SIET became indistinguishable from reference values (30 to 120 minutes). The initial efflux of TEA^+ was calculated as an average of the first 3 scans (approximately 25 minutes) and took place during the first level portion of the sigmoidal curve. Fig. 1 is a schematic of the method.

Statistics

Changes in TEA⁺ flux as a function of time were fitted to curves using GraphPad Prism Project version 3.02. Each point on the graph is the mean of 4 points on the ganglion or connective (\pm standard error of the mean). Each of the 4 individual points are the mean of 3 replicates. The mean slope of the linear portions of the graphs showing TEA⁺ efflux from the ganglion (Figures 3.6A and C) was calculated. Only preparations following a sigmoidal curve with a minimum of three points on the linear portion of the line were included in the calculations. The slope of each individual tissue was calculated and the significant difference between temperature treatments was determined using the two-sample t-test. Differences were considered significant if $p < 0.05$. All statistical calculations were performed using Microsoft Office Excel.

Results

After loading the VNC with TEA⁺ by incubation in 100 mM TEA⁺ saline at 4 or 22 °C efflux from the ganglion follows a sigmoidal pattern while efflux from the connectives follows a linear or exponential pattern (Fig. 2A-D). The initial efflux of TEA⁺ (an average of the first 3 scans) was significantly greater from the ganglia compared to the connectives for both temperatures [11.3 (\pm 2.2) vs. 1.0 (\pm 0.1) and 8.0 (\pm 1.4) vs. 2.0 (\pm 1.1), for 4 and 22°C, respectively]. There were no significant differences in the initial efflux of TEA⁺ between the temperatures at either the ganglion or the connective.

Mean slopes of -0.55 (\pm 0.06) and -0.33 (\pm 0.03) pmol/s/cm²/min were calculated for the linear portions of the 4 or 22°C ganglion curves (not significantly different).

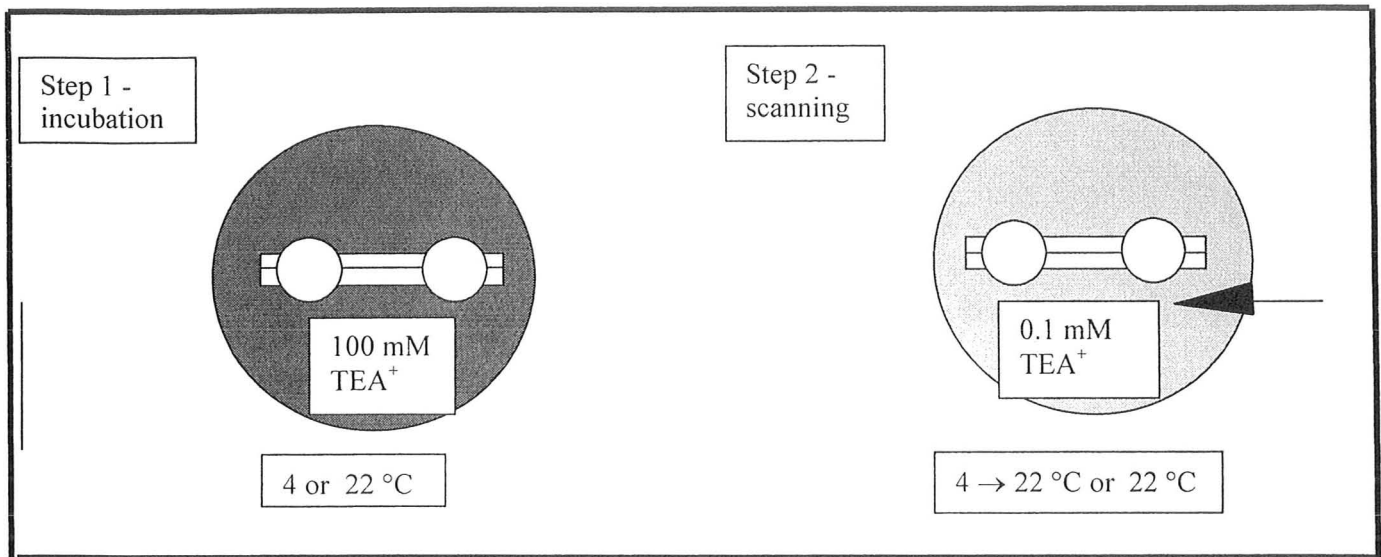


Fig 1: The VNC was incubated in 100 mM TEA⁺ saline at 4 or 22 °C for 30 minutes. The preparation was rinsed 4x with 0.1 mM TEA⁺ saline and scanned in 0.1 mM TEA⁺ saline as it warmed to or was maintained at 22 °C, respectively.

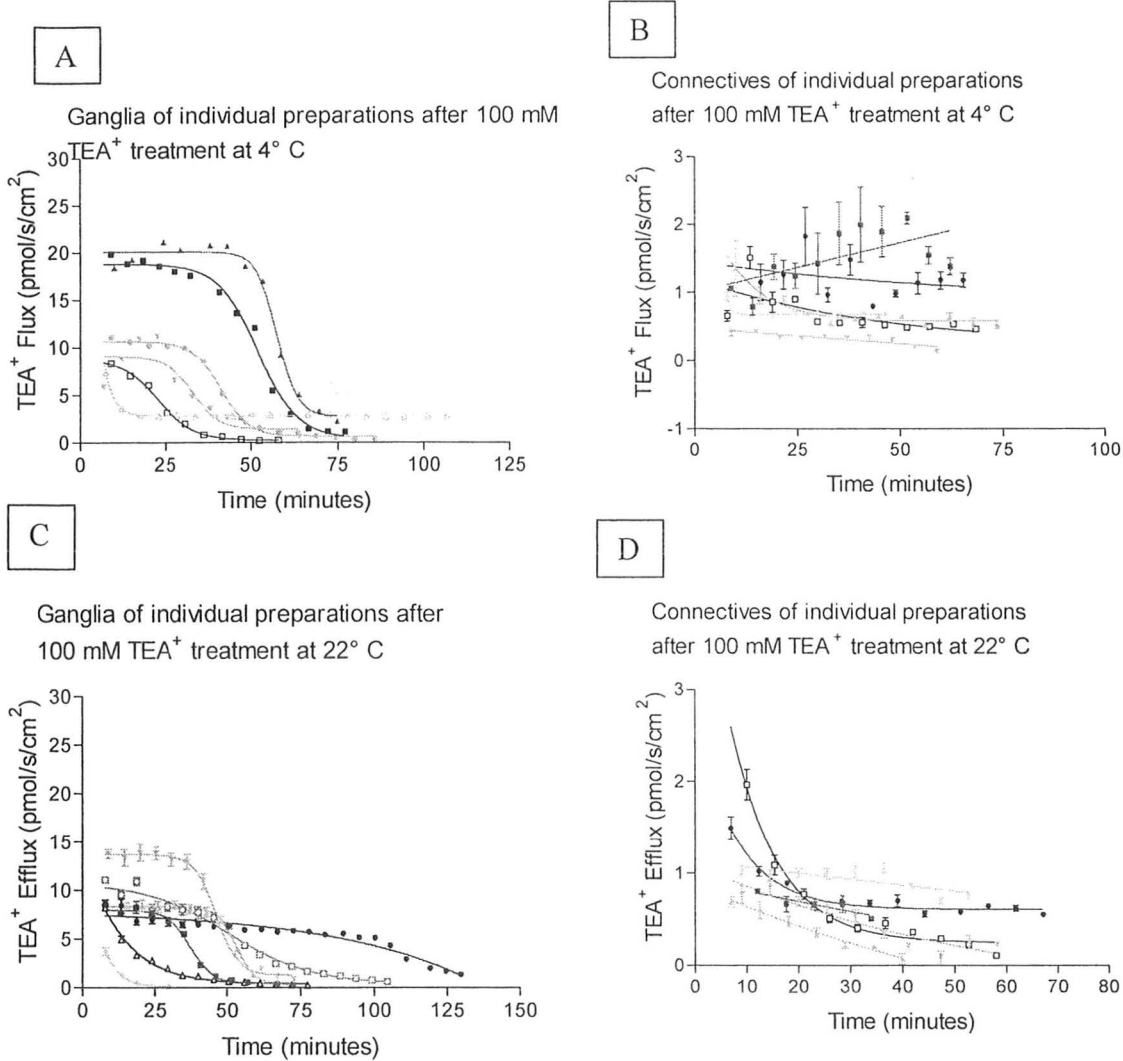


Fig 2: TEA⁺ efflux in 0.1 mM TEA⁺ saline after incubation in 100 mM TEA⁺ saline for 30 minutes at 4 °C from the A) ganglion and B) connective and at 22 °C from the C) ganglion and D) connective. Each line represents an individual preparation.